Experimental treatment of prostate cancer through knocking out *PPARγ* gene

Thesis submitted in accordance with the requirements of the University of Liverpool for the degree of Doctor in Philosophy by:

Bandar Theyab A Alenezi

April, 2022

Dedication

I dedicate this work to the soul of my mother, who passed away 2019. I could not have achieved anything in my life without her love, prayers and support. I still miss you every day.

To my beloved father, brothers, sisters, and my smaller family, for their non-stopping support and love.

Abstract

Prostate cancer is one of the most common male cancers globally. Diagnosis and treatment of prostate cancer remain a continuous burden to health-care systems around the world, and the absence of novel therapeutic targets is a significant concern in prostate cancer research field. In recent years, great effort has been made on the identification and determination of new therapeutic targets. The involvement of PPARγ in the development and growth of prostate cancer has been noticed for some time, and many studies on this subject area have been conducted in the past number of years. At first glance, PPARγ was thought to act as a tumour suppressor in prostate cancer, that have been shown in some studies, revealing that it actually inhibits the growth of prostate cancer cells into a malignant state. However, many other studies have found that suppressing PPARγ activity has an inhibitory effect on the tumorigenicity and metastasis of prostate cancer cells, which is in contrast to other findings. In this PhD project, I have assessed the role of PPARγ in the malignant progression of both androgen-dependant and independent prostate cancer cell lines to establish whether it is a novel therapeutic target. When the effect of PPARγ on malignant progression of the cancer cells was completely examined utilizing the gene-editing technique CRISPR/Cas9 to knockout PPARγ, it was found that the PPARγ-knockout cells exhibited a significant reduction in proliferation, migration, invasion, anchorage-independent growth. The tumour-suppressing effect of *PPAR*γ knockout in prostate cancer cells was also proved *in vivo.* The results in this work suggested that PPARγ is a promoting factor and a therapeutic target for prostate cancer.

Acknowledgements

First all thanks and praise are due to God

I want to convey my heartfelt gratitude and admiration to my supervisor, Professor Youqiang Ke; you've been a fantastic mentor to me. I'd like to thank you for your support and encouragement in my journey, as well as for helping me to progress as a research scientist. You have not been just an academic supervisor, but a true friend, who supported me during my hard times and my good times.

My great appreciation goes to my family, my dear father who always supported and believed in me. To my late mother, I will always make you proud. To my brothers and sisters, to my wife and six children for their unconditional love and support the entire way.

In addition to my supervisors, I would like to thank Dr Asmaa Al-Bayati, Mr. Abdulghani Naeem and Mr. Saud Abdulsamad for their assistance, comments and suggestions throughout my PhD studies, and for being the best of friends.

Last but not least, my greatest appreciation and gratitude goes to my country, Saudi Arabia, for giving me the chance to study at such a prestigious University.

DECLARATION

No portion of the work referred to in this thesis has been submitted in support of an application for another degree or qualification of this or any other university or other institute of learning.

DECLARATION OF ORIGINALITY

This thesis is a product of my own work which has been carried out during my PhD study in the Department of Molecular and Clinical Cancer Medicine (**Pharmacology**), University of Liverpool, between April 2018 and September 2021. All experiments presented in the result chapter were performed by myself under the supervision of my supervisor, Professor Youqiang Ke.

Publications

--**Bandar T. Alenezi,** Mohammed H. Alsubhi, Xi Jin, Gang He, Qiang Wei, and **Youqiang Ke.** Global Development on Causes, Epidemiology, Aetiology, and Risk Factors of Prostate Cancer: An Advanced Study. Highlights on Medicine and Medical Science 2021, 17: 94-117. Published on July 22, 2021.

--Xi Jin, **Bandar A. Alenezi** (Co-First Author), Gang He, Hongwen Ma, Qiang Wei, and **Youqiang Ke**. Peroxisome Proliferator-Activated Receptor Gamma (PPARγ) and Prostate Cancer. OAJOM 2021, 5: 526-531. **DOI:** 10.32474/OAJOM.2021.05.000206.

--Jiacheng Zhang, Gang He, Xi Jin, Qiang Wei, **Bandar T. Alenezi,** Abdulghani A. Naeem, Saud A. Abdulsamad, Mohammed I. Malki, Philip S. Rudland, and **Youqiang Ke.** Molecular mechanisms of the apoptosis-promoting activity of FABP5 inhibitors in prostate cancer cells. Oncology Report 2022; on the process of reviewing**.**

Table of contents

List of abbreviations

Abbreviations	Full name
AR	Androgen receptor
AREs	Androgen response elements
APS	Ammonium persulphate
BPH	Benign prostatic hyperplasia
BRCA1/BRCA2	Breast cancer mutated gene
CK	Cytokeratin
DHT	Dihydrotestosterone
DRE	Digital rectal examination
DMSO	Dimethyl sulphoxide
ERSPC	European Randomized study of Screening for Prostate Cancer
EDTA	Ethylene diamine tetra acetic acid
FABP	Fatty acid binding protein
GS	Gleason score
HCC	Hepatocellular carcinoma
hK3	Human kallikrein 3
IGF-1	insulin-like growth factor-1
IL-6	Interleukin-6
LH	Luteinizing hormone
LUTS	Lower urinary tract symptoms
mpMRI	Multi-parametric MRI
PSA	Prostate-specific-antigen
PZ	Peripheral zone

PAP	Prostatic acid phosphatase
PIN	Prostatic Intraepithelial Neoplasia
PCA3	Prostate cancer antigen 3
PPAR	Peroxisome proliferator-activated receptor
PVDF	PolyVinylidene DiFluoride
SPSS	Statistical Package for Social Sciences
TURP	Transurethral resection of the prostate
TRUS	Trans-rectal ultrasound
TZ	Transition zone
PETP	Positron emission tomography
AS	Active surveillance
WW	Watchful waiting
ADT	Androgen Deprivation Therapy
OS	Overall survival
CRPC	Castration-resistant prostate cancer

CHAPTER ONE

INTRODUCTION

1. INTRODUCTION

1.1 Epidemiology of cancer

1.1.1 Cancer incidence

Cancer is considered and continues to be a significant global health problem. As reported in GLOBOCAN, the number of newly diagnosed cancer cases in both males and females exceeded 19 million worldwide in 2020 which includes 10.1 million in men and 9.2 million in women [1]. Breast (11.7%), lung (11.4%), colorectum (10%), and prostate (7.3%) cancers are the most prevalent forms[2]. (Figure 1.1).

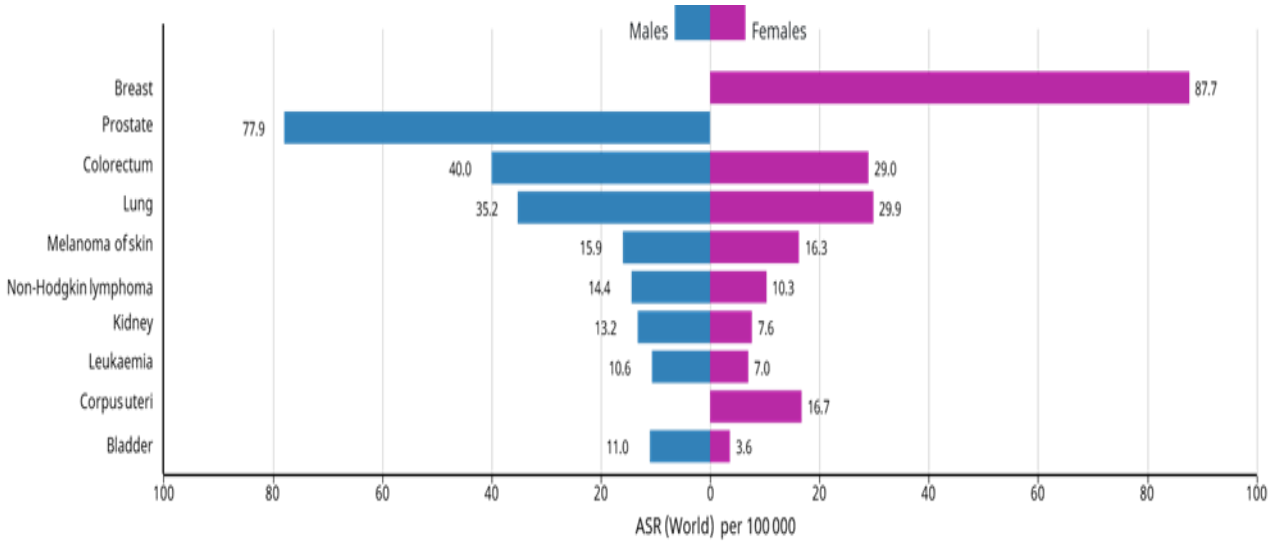

Figure 1.1. Age-Standardised Rate (ASR) of ten most common cancers in the world in 2020 (Globocan, 2021).

Based on the age of patients, the oldest patient group has the largest number of instances. The number of instances diagnosed in the group of people aged up to 24 years old accounted for just 1.1% cancer patients. Meanwhile, the number of new cancer cases diagnosed among those aged 65 and older accounts for more than 65% of all cancer cases[2]. (Fig 1.2). While black and white males had greater rates of cancer than Asian males, white females are found to have a higher incidence of cancer than Asian and black females [3].

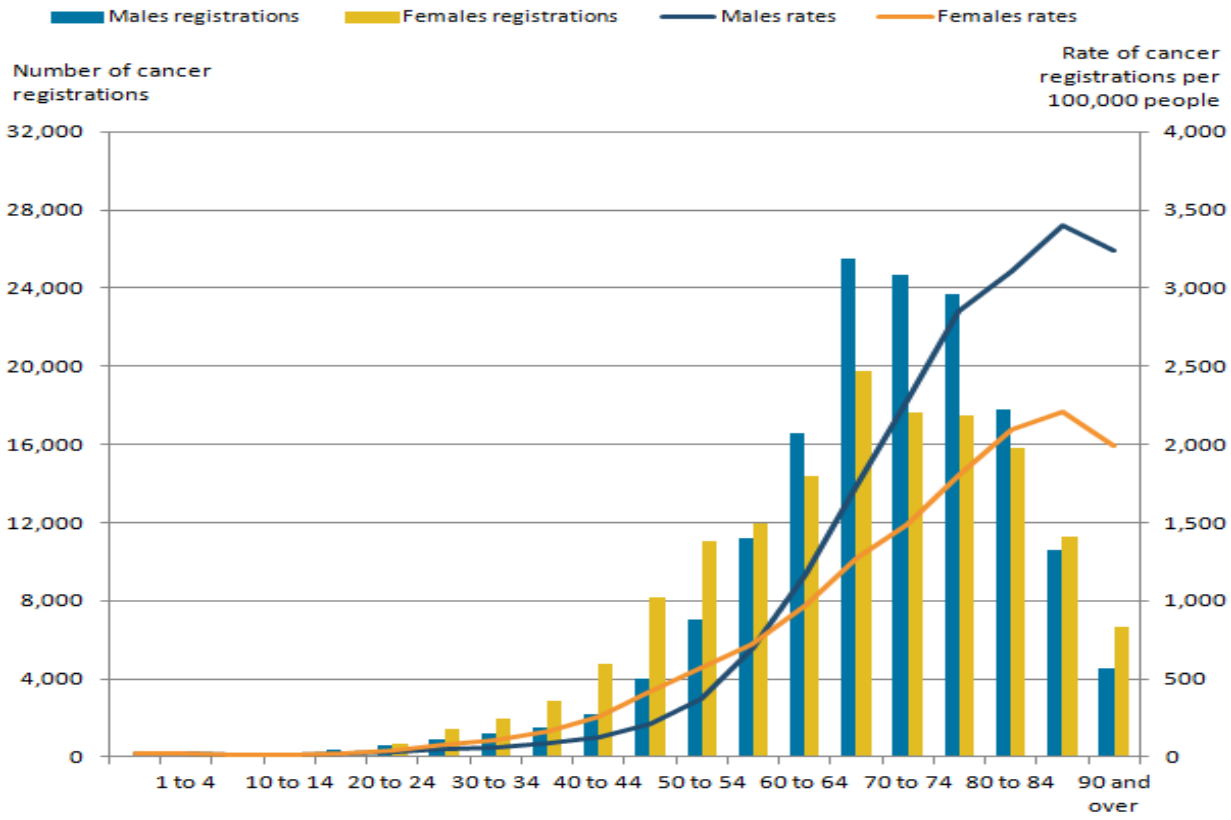

Figure 1.2. Cancer registrations and age-specific mortality rates (per 100,000 individuals) in the United Kingdom in 2015 [2].

1.2 Epidemiology of prostate cancer

1.2.1 Prostate cancer incidence

Prostate cancer is the most often diagnosed kind of cancer in male and the second most frequently diagnosed type of cancer in the developed countries [1, 4]. Prostate cancer incidence rate has recently grown around the globe. The incidence of prostate cancer is highest in North America, Australia, France, and Sweden, moderate in Denmark, England, Italy and Spain, and extremely low in Singapore, Japan, India, and China, correspondingly [5, 6]. Each year, around 417,000 more prostate cancer patients are identified in Europe [7]; and, similarly in the UK, it is prevalent in male with the greatest incidence rate, which ranks the 17th among European nations [6]. Between 2013 and 2015, around 47,700 more incidents were reported in the UK. Prostate cancer incidence has grown by around 6% in male in the last decade in the UK (figure 1.3), and is anticipated to grow by another 12% between 2014 and 2035 [4].

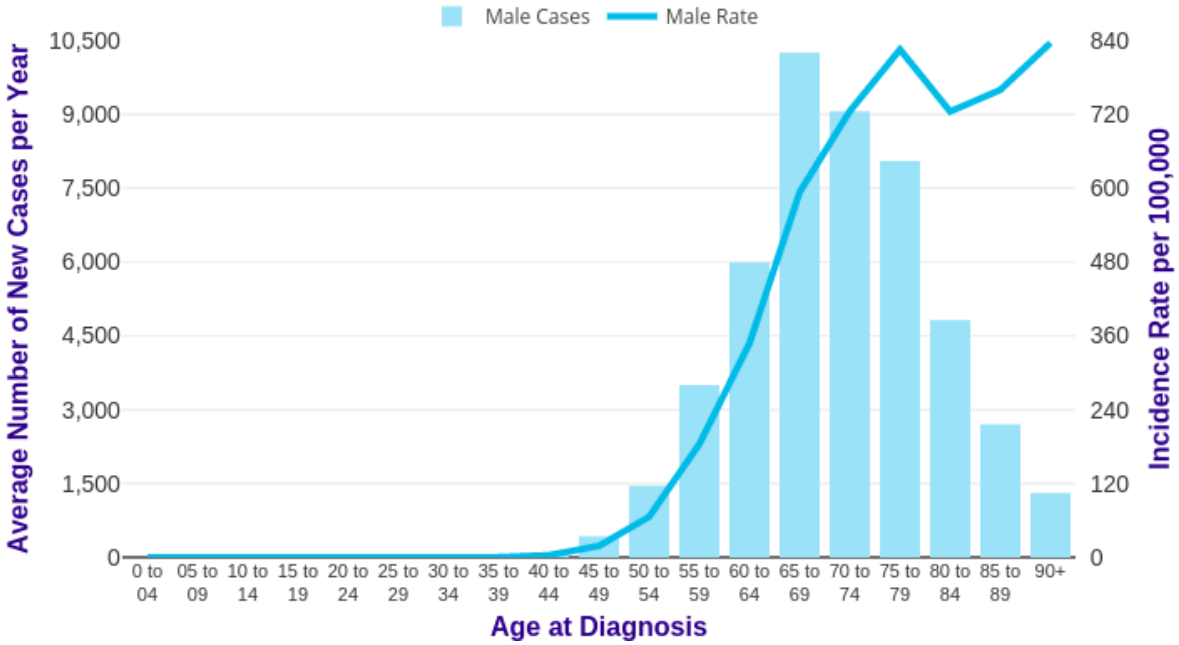

Figure 1.3. Age-based prostate cancer incidence in the United Kingdom, 2013-2015 [8].

1.2.2 Prostate cancer mortality

Prostate cancer is the fifth leading cause of male cancer death worldwide. Comparing with the developed countries, the number of deaths caused by prostate cancer increased at a faster rate in emerging economic power nations, which include countries from some parts of South America, Asia, sub-Saharan Africa, and the Caribbean nations [1, 5, 6]. Prostate cancer is considered to be the sixth leading cause of cancer death in Europe, while the UK ranks the 15th in terms of death rate [7]. Prostate cancer is the second leading cause of cancer death in the United Kingdom. Prostate cancer claimed around 11,600 (13% of the patients) lives in the United Kingdom in 2016 [9]. Increased age was associated with the increased risk of prostate

cancer [8, 9]. In the duration between 2014 and 2016, roughly 74% of prostate cancer death in the United Kingdom was in men aged 75 or older. The age-specific mortality rate began to rise as early as 55-59 and reached its peak in 90 or older [9] (Fig 1.4).

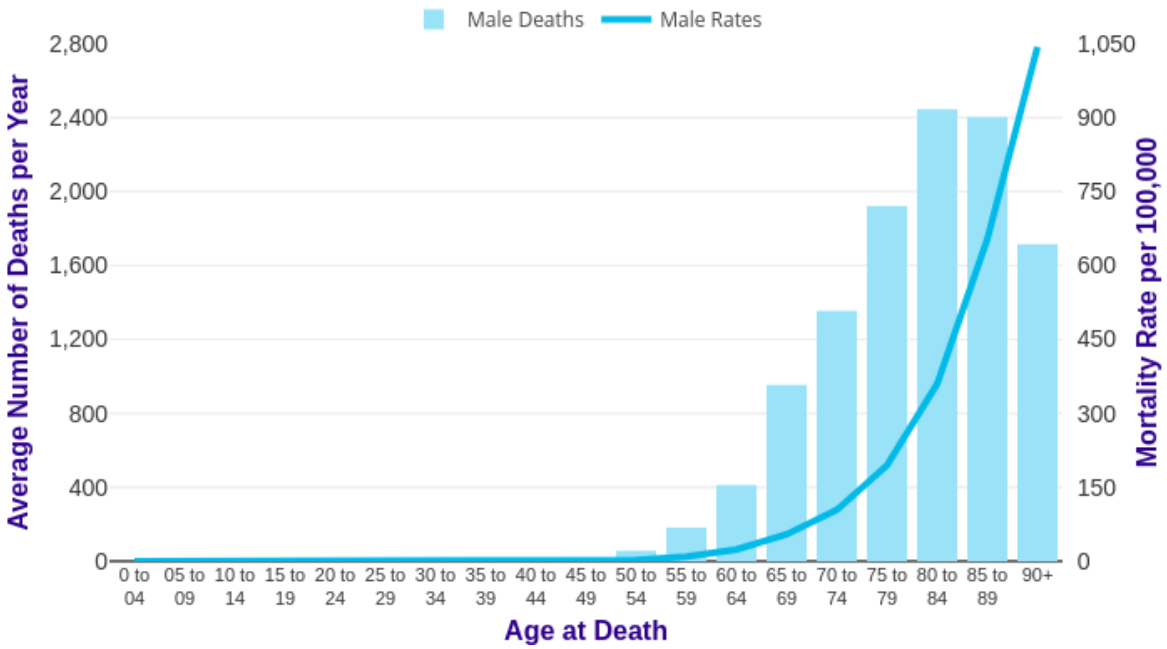

Figure 1.4. Annual averages of prostate cancer deaths and age-specific mortality rates in the United Kingdom from 2014 to 2016. [9].

1.2.3 Prostate cancer survival

In 2010, it was estimated that 84 percent of prostate cancer patients would survive ten years. Since 1970, the ten-year survival rate for this malignancy has risen, as indicated in Figure 5. Between 1971 and 2010, the 10-year survival rate increased by 59%. Nowadays, in England, more than 8 in 10 men are projected to live at least ten years after receiving an initial prostate

cancer diagnosis. This may be due to early diagnosis testing such as prostate-specific antigen (PSA) detection or transurethral prostate resection diagnosis (TURP) [10, 11]. When the twenty most often occurring malignancies in the United Kingdom are compared, prostate cancer ranks third in terms of ten-year survival [10].

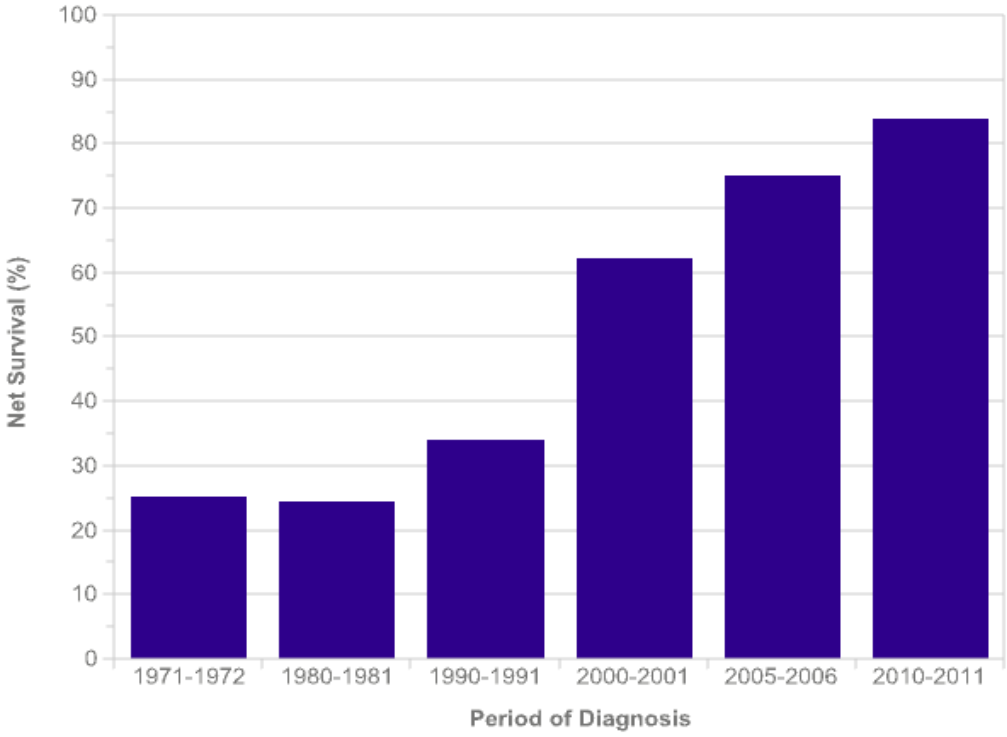

Figure 1.5 Prostate cancer ten-year survival rate [10]. The bar charts illustrate the ten-year survival rate for UK prostate cancer patients aged 15 to 99 years.

1.2.4 Risk factors of prostate cancer

1.2.4.1 Age

Prostate cancer is uncommon in men under the age of 40, but the incidence increases dramatically with the increasing age [5]. Thirteen-point seven percent (13.7%) of the incidences were in the age group of 60-79, 2.2% in the age group of 40-59, and far less than 0.005% in the group less than 39-year-old [11]. However, it was revealed during autopsies of deceased subjects that the rate of prostate cancer was significantly higher in men aged between 50 and 60 (roughly 20%) and in men aged between 70 and 80 (50%) [12].

1.2.4.2 Ethnicity

It was observed that the incidence and fatality rates of prostate cancer vary by race [13]. African American men had the highest risk of prostate cancer, with 275.3 cases per 100,000; while white Caucasian men had a rate of 172.9 cases per 100,000, a 37.2 percent drop [14]. Asian men had the least risk of prostate cancer with a rate of 10 cases per 100,000, but it was observed that the rate of Asian men developing prostate cancer has been fast growing in recent years [15].

1.2.4.3 Family history

It was established that familial history was a significant prostate cancer risk factor in men [16]. Those having a family history of prostate cancer are predicted to develop prostate cancer six years earlier than men lacking a family history [17]. Inherited factors were expected to be present in 5-10% of confirmed cases, with 40% of diagnosed individuals being under the age of 55. As a result, there was a high correlation between family history of prostate cancer and individual risk of prostate cancer in men [18]. Nonetheless, the clinical presentation of this disease in conjunction with a family history did not imply an early onset of cancer, and there was no indication of any difference in the severity of malignancies between hereditary-related and non-hereditary instances [19-21]. Additionally, it was believed that if one or more family members had a history of breast cancer, additional male members of the family would have a greatly increased chance of developing prostate cancer [22]. Inherited mutations in certain genes, such as BRCA1, BRCA2, and HOXB13, contribute for some incidences of hereditary prostate cancer. Men with mutations in these genes have a significant risk of acquiring prostate cancer and, in some situations, other cancers throughout their lifetimes. Men who have BRCA2 or HOXB13 gene variants may also be at a greater risk of developing life-threatening forms of prostate cancer [23].

1.2.4.4 Diet

Numerous studies were conducted in an attempt to elucidate the function of fat consumption in prostate cancer. Foods high in fat and red meat intake were related to the development of prostate cancer. The researchers hypothesised a link between prostate cancer and animal fat consumption. A prior research found that men who took linoleic acid (found in vegetable oils, nuts, seeds, meats, and eggs) had a fivefold increased chance of developing prostate cancer. An anticipated explanation for increased prostate cancer risk associated with excessive fat diet was that fatty acids affect serum sex hormone levels, which in turn increases the incidence of prostate cancer [24, 25].

Japanese immigrants residing in the United States of America may provide insight into the impact of diet and environmental variables, as it was previously believed that these men maintained a low risk of prostate cancer. However, they shifted to a high-risk category, and this risk was found to correlate with the duration of time they resided in a new country. A research comparing the total fat consumption of African Americans and Asian Americans with the risk of prostate cancer indicated a 15% increase in the incidence of prostate cancer [26-30]. Red meat consumption may be associated with prostate cancer, however further research this is necessary.

Another mechanism by which a high-fat diet might influence the development of prostate cancer is by the activation of insulin-like growth factor-1 (IGF-1), which is released by the liver and elevated by a high-fat diet. IGF-1 was shown to promote proliferation and inhibit

apoptosis in cohort studies, where men with a higher IGF-1 concentration had a 4.3-fold increased chance of developing prostate cancer [31, 32].

1.2.4.5 Other factors

Some factors, such as cigarette smoking, alcohol intake, socioeconomic position, occupation, vasectomy, prostate gland inflammation, and sexually transmitted infection, were found to be associated with an increased risk of prostate cancer, according to the statistical evidence [33].

1.3 The pathology of prostate cancer

1.3.1 Prostate gland anatomy

The prostate is a male reproductive gland composed of fibromuscular tissue that surrounds male urethra. It is encased in a thin sheath that forms the actual capsule. Outside of this is a pseudo-capsule formed by three covering layers that enclose the gland from the frontal, posterior, and side directions. Areas above the gland run parallel to the bladder neck, as illustrated in figure 1.6. Prostate gland is composed of ducts and a basement membrane that are surrounded by stroma; the channels are lined with columnar and secretory cells. The

primary purpose of the prostate gland is to supply proteins and electrolytes necessary for the secretion of prostatic fluid, which aids in sperm transmission [34, 35].

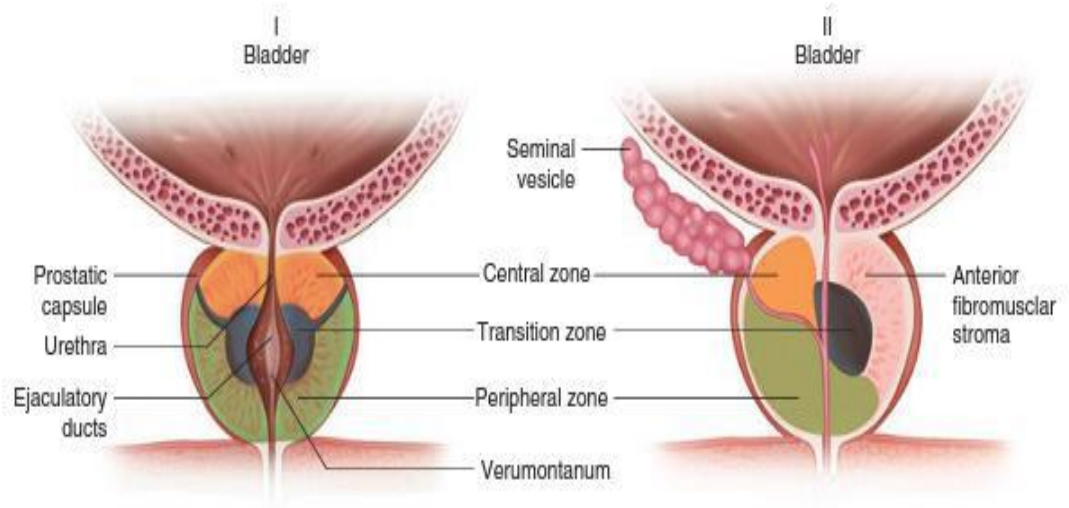

Figure 1.6: Prostate anatomy illustrating the prostate's three zones and their connections to urinary bladder [34].

The prostate gland is divided into three zones: the transitional zone, the central zone, and the peripheral zone. The majority of the prostate is glandular tissue (70%) with the remaining 30% being fibromuscular stroma tissue. The central zone is surrounded by ejaculatory ducts. Twenty-five percent of the core zone is made up of glandular tissue. Prostatic adenocarcinoma is extremely uncommon in this region (only around 1-5%). On the other hand, the peripheral zone, where the majority of prostate adenocarcinomas occur (70%), contains 70% glandular tissue, and it is located in the lateral and posterior regions of the prostate. The prostate's central zone is shaped like a triangle, with its base connected to the seminal vesicles (Figure 1.6) and its apex at the verumontanum [34, 36-38].

1.3.2 Physiology of prostate

The prostate, often known as a male sex accessory organ, is important in the reproductive process. Prostate gland secretes a fluid that, when combined with sperm cells and fluids secreted by the seminal vesicle, bulbourethral gland, and other glands, forms semen. The fluid produced by the prostate, which contains fructose, glucose, enzymes, and PSA, serves as nutrition for sperm as it travels through the female body during fertilization. Prostate fluid contains acidic minerals like zinc and citrate, but other fluids in sperm made by seminal vesicles are alkaline and can neutralise the acidic vaginal fluids, allowing sperm to survive [39, 40].

1.3.3 Normal prostate cells

The prostate gland is composed of epithelial and stromal cells. Prostate epithelial cells are classified into three types: luminal cells, basal cells, and neuroendocrine cells [41]. The most common type of prostatic epithelial cell is a luminous cell. They are a component of the prostate's exocrine compartment, secreting proteins including PSA and prostatic acid phosphatase (PAP) to the glandular lumina [42]. Luminal cells are androgen-dependent cells with an elevated level of androgen receptor (AR) expression. They also express the cell surface markers cytokeratin (CK) 8, CK18, and CD 57 [43].

In the prostate gland, basal cells are second biggest epithelial cells. They are found above the basement membrane, are generally undifferentiated, and have little secretory capacity. Basal cells are thought to be the major compartment of proliferation in the prostate gland. Basal cells are androgen-independent cells that may not express AR and so do not respond to androgen

ablation therapy [44]. These cells have elevated CK5 and CK14 levels, along with CD44. Furthermore, they express autocrine factors such as Bcl-2 and p63, which defend the cells against DNA damage [45].

Neuroendocrine cells are found in prostate gland between the luminal and basal cells. They are not androgen-responsive and can be distinguished by the expression of serotonin, a thyroid stimulating hormone, and chromogranin A. The precise role of neuroendocrine cells is unknown; however, evidence suggests that they may aid the growth of luminal cells and the progression of prostate cancer to an advanced phase [46, 47]. It is to be noted that citrate play a major role in prostatic fluid formation, as citrate is used by prostatic cells as an energy source (Krebs cycle oxidation) or as a source of cytosolic acetyl CoA for fatty acid synthesis [48].

1.3.4 Prostate cancer initiation

1.3.4.1 Benign prostate hyperplasia (BPH)

Benign prostatic hyperplasia develops (BPH) when prostatic epithelial cells surround the urethra expand and overgrow. BPH is a non-malignant disorder in which the prostate gland enlarges and both stromal and glandular structures proliferate. Its prevalence rises with age. The causes of BPH are unknown; however, it was once considered to be caused by hormonal or growth factor stimulation. Clinically, people with BPH have urine irregularities such as frequent urination, urgency, and so on. BPH was discovered to begin in the transitional zone, notably in the submucosal layer. Because this region surrounds the urethra, compression will cause lower urinary tract discomfort [34, 49, 50].

1.3.4.1 Prostatic Intraepithelial Neoplasia

Prostatic Intraepithelial Neoplasia (PIN) is a cancer precursor or a substage of cellular change from a normal condition to a cancerous prostatic epithelium. PIN implies abnormal epithelial cell growth without penetration into the adjacent stroma [51]. PIN can be diagnosed by a range of architectural and cytological features, resulting in minimal differences that may make it indistinguishable from malignancy [52]. PIN is divided into two grades: low grade and high grade. Low grade PIN is a well differentiated early invasive tumour composed primarily of basal cells [53]. PIN of high grade is a poorly differentiated tumour with a secretory luminal cell population [44, 54]. Tufting (the most prevalent variety), cribriform, micropapillary, and flat are the four basic types of high-grade PIN [55]. It has been demonstrated that high grade PIN is a significant marker and the sole known precursor of prostatic cancer [56].

1.3.4.2 Gleason score

In 1966, Doctor David Gleason developed a histological grading method (Gleason score, GS) to assess the severity of prostate cancer. Gleason grades vary from Gleason score 1 to 5. It is a prostate cancer assessment instrument that measures the degree of loss of normal glandular tissue architecture and is based on subjective microscopic interpretation. Grade 1 is the least aggressive pattern, while Grade 5 is the most aggressive pattern [57] (Figure 1.7).

Due to the histological diversity of various lesions inside each tumour, each case received two grades (primary and secondary). They can vary from Gleason grade 2 to 10 by combining the two grade patterns to generate the so-called Gleason scores (GS) or combined GS [58]. GS is a composite of primary grade, which is greater than 50% of the overall pattern seen and represents the majority of tumour, and secondary grade, which is between 5% and 50% of the total pattern and represents the minority of tumour. This approach categorises the scores into

three categories: well differentiated (GS2-6), moderately differentiated (GS7), and poorly differentiated (GS8-10) [59-61]. Recently some pathologists further divide the GS7 carcinomas into 2 categories: 4+3 and 3+4. The 4+3 cases have much worse outcomes than 3+4 cases [61].

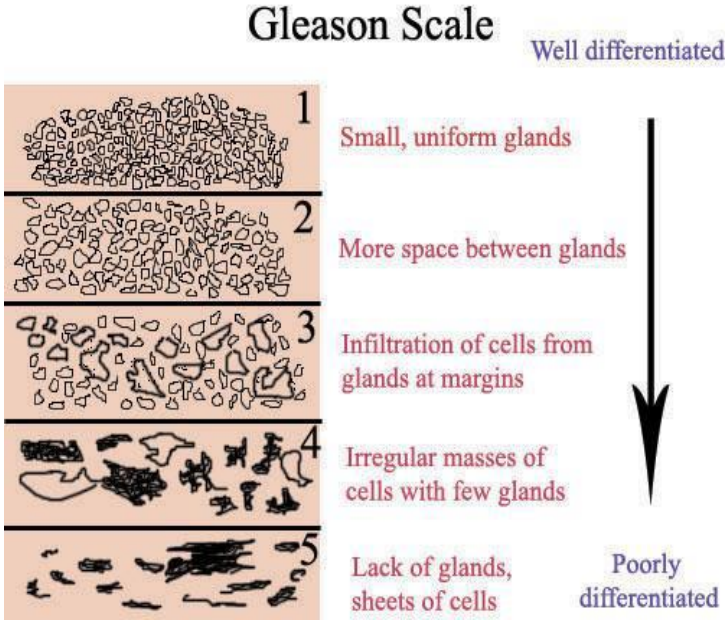

Figure 1.7. Gleason score grading system.

1.3.4.3 Prostate cancer diagnosis

A biopsy is frequently performed on men with a PSA of more than 10 ng/ml and/or a positive DRE to confirm the diagnosis of prostate cancer. Prostatic tissue is removed for microscopic inspection during a biopsy. Most patients in the UK will have a trans-rectal ultrasound guided (TRUS) biopsy, which involves inserting an ultrasound probe through the rectum to assess the prostate and guide needle sample of prostatic tissue. The treatment is performed using a local anaesthetic. A trans-perineal biopsy, in which a needle is inserted into the perineum to reach the prostate, is another approach. This surgery is often performed under a general anaesthetic. A multi-parametric MRI (mpMRI) scan can be performed before either treatment to determine

which parts of the prostate are likely to be affected by cancer tissue. The MRI scan allows for a more exact biopsy, which minimises the volume of samples required. Pain in the rectum and penile area, short-term bleeding, infections in the urinary tract, acute urine retention, sepsis, and transient erectile dysfunction are all possible side effects of a biopsy [62]. Other popular screening tools include a CT scan (which examines for cancer spread to adjacent lymph nodes and bones), X-rays, a bone scan, and a PET scan (positron emission tomography) [63].

1.4 Prostate cancer treatments

A risk evaluation method is utilised to help provide proper treatment to prostate cancer patients. The National Institute for Health and Clinical Excellence (https://www.nice.org.uk/guidance/ng131) and the European Association of Urology [64] have produced clinical guidelines for prostate cancer assessment and therapy that divide localised prostate cancer into three categories: low, intermediate, and high-risk groups depending on the risk of biochemical relapse after surgery or external beam radiotherapy.

1.4.1 Localised prostate cancer treatments

Patients with localised prostate cancer may have numerous therapy choices, including active surveillance (AS), watchful waiting (WW), as well as several drastic therapies. A radical prostatectomy is a surgical procedure used to eliminate prostate cancer. It is still believed to be the most efficient treatment and outperforms WW and AS [65-67]. Because prostate cancer

frequently grows slowly, some patients may not require active therapy, and medications may even produce adverse effects and reduce quality of life. AS, which uses a routine programme of constant observation with digital rectal examination, periodic biopsy, serial PSA testing, and consultations, is frequently used to track the cancer more thoroughly in low risk patients who do not require active therapies [64].

1.4.2 Locally advanced prostate cancer treatments

Locally advanced prostate cancer has clinically disseminated outside the prostatic capsule, with penetration of the pericapsular tissue, bladder neck, or seminal vesicles, without lymph node association or distant metastases. External beam radiotherapy with ADT, which is androgen deprivation by medicinal, surgical castration, anti-androgens, and combination androgen blockade, (and possibly high dose-rate brachytherapy) is a treatment option for patients with locally advanced prostate cancer, as is radical prostatectomy (typically followed by ADT and radiotherapy), ADT alone, and WW [64]. There are various forms of ADT that seek to limit the effect of androgen. The most common types of ADT are surgical castration, which removes the testicles, luteinizing hormone releasing hormone agonists (e.g. Goserelin) and GnRH antagonists (e.g. degarelix), which decrease the amount of androgen, anti-androgens (e.g. Flutamide, Enzalutamide, and Bicalutamide), which compete with androgen to lessen androgen

binding to AR, and CYP17 inhibitor (e.g. Aberaterone) that blocks the formation of androgen [68].

1.4.3 Metastatic, recurrent, and progressive diseases treatments

ADT is an effective treatment for prostate cancer because prostate epithelial cells and practically all prostate cancer cells require testosterone to proliferate. Consideration should be directed to cancer restaging and treatment with additional local radical therapy (radiotherapy or surgery) in the case of local recurrence or progression following radical treatment, knowing that ADT is the mainstay of care for metastatic disease [69]. Three large clinical trials comparing ADT alone to ADT plus chemotherapy (docetaxel) in metastatic prostate cancer patients within three months after ADT beginning have been completed in recent years [70-72]. In all three trials, ADT with docetaxel resulted in a superior overall survival (OS). As a result of these findings, docetaxel in combination with ADT is now regarded the new standard of care for men with metastases at first presentation, provided they are physically adequate to receive the medicine [69].

Although ADT is initially beneficial in the majority of patients, resistance always develops. Castration-resistant prostate cancer (CRPC) is a term that refers to a condition that has progressed, either radiographically or biochemically, in the presence of a castration level

of circulating testosterone (<50ng/dl) [73]. Notably, CRPC is not completely hormone resistant, since alternative types of ADT can be useful as second line hormone therapy [74].

CRPC seems to be an incurable stage of prostate cancer, with a poor prognosis for the majority of patients developing metastases [75]. Prior to the discovery of docetaxel, treatment for CRPC was extremely limited with few survival benefits. Two pioneering phase III trials indicated improved OS and pain relief in patients with metastatic CRPC (mCRPC) treated with docetaxel [76, 77]. Docetaxel was later approved as a first-line chemotherapeutic drug by the US Food and Drug Administration (FDA) in 2004 and has since been a cornerstone of therapy for patients with mCRPC. At the moment, patients with mCRPC have a limited number of therapeutic options, including ADT with abiraterone and enzalutamide [78, 79], immunotherapy with sipuleucel-T, which utilises activated patient-derived antigen-presenting cells to act as an immune modulator or vaccine [80], and alpha emitter Ra 223 [81]. Numerous CPRC patients have benefit from these treatments, which have resulted in increased survival. Unfortunately, not all patients benefit from the prescribed therapy. For example, only around 50% of patients respond to docetaxel as a first line therapy [76, 78].

1.5 Prostate cancer cell lines

Researchers in prostate cancer introduced numerous cell models to contribute in the study of molecular pathogenesis, proliferation, apoptosis, tumorigenicity, and metastasis. PNT2,

LNCaP, 22Rv1, DU-145, PC3 and PC3-M are the most commonly utilised prostate cancer cell lines in laboratories.

1.5.1 PNT2

PNT2 cell line is considered to be a normal human prostate cell line that was generated from prostate epithelial cells of a 33-year-old male by immortalization via transfection using a plasmid encoding the genome of simian virus 40 (SV40) with a faulty replication origin [82]. T proteins and markers of differentiated luminal cells of the glandular prostate (cytokeratin 8, 18, and 19) are widely expressed in immortalised cells. PNT2 cells, in addition, express PSA and PAP but not CK14 (an epithelial basal cell marker) [83].

1.5.2 LNCaP

LNCaP cells were isolated in 1977 from a needle aspiration biopsy of a lymph node metastatic lesion in a 50-year old patient with prostate cancer [84]. LNCaP cells are known to be androgen sensitive; they have a high affinity nuclear androgen receptor (AR), which responds to androgens by up-regulating cell proliferation. In vivo experiments revealed that tumours grew from the injection site were visualized and detected earlier in male mice than in female mice, indicating an androgen-sensitive feature. CK8 and 18 are expressed in LNCaP, as well as the wild type of TP5 [85]. LNCaP cells are considered to be both AR-responsive or AR-

independent depending on the culture condition. AR-Independent LnCap cells are generated through continuously culturing LnCap AR-responsive cells in the absence of androgen [86].

1.5.3 22Rv1

The 22Rv1 cell is produced from a human prostate cancer xenograft (spread in mice following castration-induced regression and relapse of the parental, androgen-responsive CWR22 xenograft) [87]. The 22Rv1 cell line is known to be a moderately malignant androgen-sensitive prostate epithelial cell line. When compared to other prostate cell lines, 22Rv1 expresses high levels of PSA and AR, and has a distinct genotype and phenotype [87, 88].

1.5.4 DU-145

The first well-established prostate cancer cell line was DU-145. It was extracted from a moderately differentiated brain metastasis in a 69-year-old Caucasian male [84]. DU-145 cell line is known to express extremely low level of prostatic acid phosphatase (PAP), does not express AR and PSA [84]. DU145 cells also express intermediate filament proteins, as well as CK7, 8, 9, and 19, but not CK5 or 14. [89, 90]. *In vivo* tests revealed that when DU-145 was injected into the SCID mice, metastases were identified in organs including liver, lung, spleen, adrenals, kidneys, and lymph nodes [89].

1.5.5 PC3 and PC3-M

PC3 cells were recovered from a bone marrow metastases of a GS4 prostatic adenocarcinoma in a 62-year-old male [91]. PC3 cells are known to be androgen-independent and do not express PSA or AR. PC3-M is considered to be a PC3 metastatic subline. It was derived from a liver metastasis in a nude mouse caused by an intrasplenic injection of PC3 cells, and it shares some characteristics with PC3 but is more malignant and aggressive [92].

1.6 Prostate cancer biomarkers

Biomarkers are molecules that, when measured or examined, can reveal useful illness information prior to the completion of standard clinical exams. They can be determined from a variety of sources, including tissue biopsy, blood samples, and urine samples [93]. Some of the biomarkers that have been investigated and used in prostate cancer detection are described below.

1.6.1 4k score

Kallikreins are a collection of 15 serine proteases that are involved in altering cell regulation, increasing extracellular matrix alteration, and increasing invasiveness and angiogenesis in cancer cells [94].

This assessment is based on plasma analysis of four prostate-derived kallikrein proteins, along with other clinical characteristics, to determine the risk of a high-grade Gleason score upon biopsy [93]. The OPKO medical firm developed this test by combining four kallikrein molecules (tPSA, fPSA, intact PSA, and kallikrein-related peptide 2 (hK2). The test result is correlated with clinical variables such as age and previously negative specimens to determine the stage of disease development [95]. This test was commonly used to detect patients in the early stages of disease who had not yet manifested clinical symptoms. This test is intended to detect patients who are at an increased risk of developing high-grade cancer. Due to the fact that biopsies can be limited to high-risk instances, the 4K score test may lead to a decrease in the frequency of biopsies [96]. Current guidelines consider the 4K score to be a diagnostic/prognostic test for detecting aggressive prostate cancer risk [97].

The 4K score results in an 8% reduction in needless biopsies in newly screened cases [93]. As shown in a retrospective Swedish research, the 4K test outperformed the combined PSA and age criteria in accurately predicting the outcomes of the prostate cancer patients [95, 98]. According to European retrospective research, the 4K score is highly predictive of aggressive cancer [99]. Additionally, this score is cost-effective, since its adoption can result in a 48-56% reduction in biopsies [95, 100].

Based on the NCCN guidelines, the 4K score may be beneficial in men who have never had a biopsy or who have had a negative biopsy. However, they cautioned against using it as a first-line screening method. Additionally, the FDA had not authorized the application [95]. This test

is unfavourable in males within 96 hours of DRE, those on 5α-reductase inhibitors, and those who have received medical or surgical therapy for BPH, limiting its applicability to a broad population [93].

1.6.2 PCA3 assay

The Hologic Company developed this assay named the Progensa assay [194]. It is based on the detection of Prostate Cancer Gene 3 (PCA3) and PSA RNA in male urine samples and the calculation of the ratio of PCA3 RNA to PSA RNA. The PCA3 level is associated with the level of prostate cancer malignancy in this assay [93].

FDA authorised this test in 2012 for biopsy-negative individuals (prostate cancer patients who have shown a negative result in past prostate biopsy). Due to widespread dispute over the precise PCA3 cut-off level and its genuine prognostic value, it had not been approved for use as a screening test in men with elevated PSA levels, although it was agreed to be used to men who had previously been examined with biopsy. PCA3 is more selective than PSA since it is unaffected by infection or inflammation of the prostate [93, 101].

PCA3 is more predictive of patient outcome than other diagnostic assays. Sensitivity and specificity fell between 53% to 69% and 71% to 83%, respectively [93]. While some research [70, 102] indicated a relationship between the PCA3 score and very malignant prostate cancer, others [103, 104] indicated a lack of linkage between this score with disease severity.

Furthermore, whether the PCA3 assay correlates with the overall Gleason scores is yet to be established [93, 96].

1.6.3 TMPRSS2 and ERG.

The combination of transmembrane protease, serine 2 (TMPRSS2) and erythroblast transformation-specifically related gene (ERG) resulted in a gene dysregulation that was initially identified in 2005 in blood-derived tumours and thereafter in solid tumours, including prostate carcinomas. In men, the concentration of this fusion protein can be determined in collected urine samples following prostate massage [96, 105].

According to the information in prostate cancer genome atlas, the most prevalent kind of this derangement is E26 ETS, which was detected in 58% of tumours [96, 106]. It was hypothesized that TMPRSS2:ERG is prostate cancer-specific and has a 94% predictive value [107]. According to the European Randomized Study of Prostate Cancer Screening (ERSPC), combining PCA3 and TMPRSS2: ERG enhanced the predictive value for detecting high-risk prostate cancer cases [67]. On the other side, several researchers discovered that this fusion gene was lacking in patients with aggressive carcinomas [95, 108].

1.6.4 Michigan prostate score (MiPS)

This composition was created in 2013. It determines the amounts of PCA3 in the blood, PCA3 in the urine, and TMPRSS2 in the urine: ERG. This score was developed primarily for men who had a high blood PSA level before undergoing a biopsy test, as well as those who had previously received a negative biopsy screening test [93].

Salami et al. [109] found that by integrating three diagnostic assays, the Michigan score can significantly improve the capacity to diagnose prostate cancer when compared to each test alone. Leyten et al. [101] observed a 35% reduction in unnecessary biopsies for men at risk of prostate cancer when the MiPS score is assessed in advance. However, the latest work by Gopalan et. al. indicates that there is no substantial link between the TMPRSS2: ERG gene fusion and patient outcome. Additionally, the assay cut-off value would still be a point of debate [93, 110].

1.6.5 IL-6

IL-6 is a member of the cytokine family and is regarded as a potent proinflammatory cytokine with a variety of functions. IL-6 plays a role in inflammatory response and modulates cell signalling. It plays a role in cell proliferation and distant metastasis. It has been linked to lung, breast, head and neck, and, most intriguingly, prostate cancer [111-115]. Numerous cells, including fibroblasts, keratinocytes, mast cells, macrophages, T and B cells, are involved in the

synthesis of IL-6. This cytokine plays a role in monocyte differentiation and dendritic cell maturation regulation [116, 117].

Autopsies and analysis of prostate cancer patients, analyses of three prostate cancer cell lines (PC3, DU145, and LNCaP), and assessments of blood samples from prostate cancer patients who were resistant to treatment all showed an elevated IL-6 level. Although IL-6 expression was detected in CRPC, its relationship to patient survival remains unknown [95, 115].

According to Nguyen and colleagues, elevated IL-6 level enhanced prostate cancer cell growth and facilitated distant dissemination through altering cellular proliferation, invasiveness, and epithelial to mesenchymal transition (EMT). Anti-IL-6 antibody, on the other hand, had the opposite effect, reducing the proliferation of prostate cancer cell lines by inhibiting the action of IL-6. It has been demonstrated that IL-6 promotes prostate cancer invasiveness via EMT. As a result of EMT activation, fibroblasts release matrix metalloproteinases (MMPs) in response to IL-6 stimulation, resulting in an increased invasiveness of prostate cancer cells [113, 115, 118].

In the future, IL-6 may be utilised to predict chemotherapy response. Mahon et al. found that docetaxel treatment altered the levels of IL-6 and six other cytokines. After one round of docetaxel treatment, those with an elevated IL-6 expression level had a poor prognosis [95, 119].

1.6.6 CTCs

Circulating tumour cells (CTCs) are cancer cells that have the ability to enter blood vessels and circulate. CTCs have the potential to establish a metastatic site. Blood tests have revealed these cells in a number of cancer patients. The typical blood cell to CTC ratio was assumed to be 10^6-10^9:1. As a result, detecting these cells needs a highly sensitive laboratory technique [96, 120]. CellSearch® is a kit manufactured by (Menarini Silicon Biosystems Inc., USA) and used to quantify these tumour cells in blood samples. The approach is based on enriching cells immunomagnetically, labelling them with fluorescent dyes, and then counting them under fluorescence-based microscopy [36].

The percentage of these cells was found to increase in more advanced prostate cancer disease. According to one study, these cells exhibited heterogeneous traits. Apart from their rarity [96, 121], it was postulated that this heterogeneity might be associated with the treatment resistance, and hence CTCs may be utilised to monitor prostate cancer treatment management [122].

Although one study found a link between CTCs and overall survival in patients with prostate cancer, additional clinical trials are needed to analyse these cells before they can be established as a biomarker. Due to the sensitivity required to detect CTCs, only CellSearch®, an FDA-approved technology, is now available to perform this test [96, 123]. This again has an effect on the test's limits.

Circulating free nucleic acid concentrations can be affected by tumour size, location, and vascularity, and they may also be derived in part via CTC lysis. However, mutation analysis of

circulating free nucleic acids, specifically DNA, has shown much higher sensitivity than CTCs, establishing circulating free tumour DNA (cftDNA) as the best source for molecular investigation. This type of analysis can be repeated as many times as necessary without causing the patient any discomfort [124].

1.6.7 Immune checkpoints and regulators PD-1 and PD-L1

The programmed cell death receptor 1 (PD-1) is a 288-amino acid transmembrane glycoprotein belonging to the immunoglobulin family. It is thought to be an immune system inhibitory receptor that is expressed on a variety of immune cells, most notably cytotoxic T-cells. T-cells, B cells, and macrophages express PD-L1 as a PD-1 ligand. When PD-L1 binds to PD-1 in normal tissues, this conjugation stabilises the immune system and regulates the immune response during infection or inflammation [125, 126]. Numerous tumour cells, including breast carcinoma, lung carcinoma, and melanoma, were shown to express PD-L1 [127].

Taube et al. found that the interaction of PD-1 and PD-L1 in the tumour microenvironment can block cytotoxic T cells, which may lead to malignant cells evading immune detection and eradication. However, when the connection between PD-1 and PD-L1 is inhibited, tumour cells may be destroyed by cytotoxic T cells. Thus, developing drugs that inhibit the interaction of PD-1 and PD-L1 may be a future option for treatment of cancer [125].

James Allison and Tasuku Honjo made a breakthrough in the field of immunology when they discovered a way to stimulate the immune system to eradicate cancer. This discovery resulted in the introduction of numerous immune checkpoint inhibitors that showed promising results in the treatment of melanoma, kidney, and lung cancers [128, 129].

Ipilimumab was the first immunological check point inhibitor explored in prostate cancer, and it was evaluated in two clinical trials in individuals with CRPC. However, the trials did not result in an increase in patient survival. Pembrolizumab, another PD-1 inhibitor, was evaluated in patients with prostate cancer in a phase 2 trial, and the trial showed that 4 out of 20 patients had a substantial PSA response [130]. In 2018, the largest study to date was undertaken to determine the status of PD-1 expression in 539 primary prostate carcinoma cases and 57 CRPC cases. PD-1 expression was found in 8% of primary prostate carcinomas and 32% of CRPC [129, 131].

Additional immune checkpoint member is B7-H3 (CD276), it was discovered to have a poor prognosis in prostate cancer, and was associated with more aggressive illness and a poorer patient outcome. B7-H3 levels were shown to be higher in cancer patients treated with hormone therapy following prostatectomy [95].

Additional research is required to completely understand the mechanisms by which immune regulators work and to improve immunotherapy for prostate cancer using immune checkpoint inhibitors.

1.6.8 Prostate-specific Membrane Antigen (PSMA)

PSMA is a type II membrane protein that functions as a glutamate-releasing carboxypeptidase [132]. Even though it is expressed in all forms of prostate tissue, it has also been detected in other types of tumours, such as those of the kidney, bladder, testis, and breast [133]. Despite the fact that it is elevated in prostate cancer relative to benign prostate disease [134], its usefulness as a biomarker in prostate cancer has been underutilised until recently. Earlier research established that its expression in the serum of individuals with benign against malignant illness was not substantially different [135].

1.6.9 Ion channels

Ion channels and transporters (ICT) are a new type of membrane protein that is overexpressed in a variety of human malignancies. ICT can now represent novel cancer biomarkers in addition to controlling several aspects of cancer cell behaviour.

The role of calcium channels in PCa has been known among ICTs for over 30 years, with the first finding that calcium channel blockers impact cancer progression towards a more aggressive phase. Later study discovered additional kinds of channel proteins that play a key regulatory role in cancer transformation. VGCC (mostly L-type) expression has been found in androgen-responsive LNCaP cells. Androgens trigger Ca2+ currents in these cells, which mediate the effects of androgens [136].

Ca2+ influx occurs through TRPCs as well, promoting either cell growth or death depending on the TRPC subtype. TRPM8 is particularly intriguing because the gene contains ten putative androgen responsive regions, implying that androgens influence the protein's production and subcellular distribution. TRPM8 also promotes androgen independence and increases the metastatic potential of PCa. TRPM8 may be a valuable marker for prostate cancer outcome in general, as loss of TRPM8 expression appears to be associated with androgen independence and a bad prognosis. TRPC1 has similar characteristics, with expression levels decreasing as PCa progresses from androgen-dependent to androgen-independent [136].

M.B. Djamgoz and colleagues' work clearly demonstrated that the expression of VGSC, particularly SCN9A, in PCa is associated with a high metastatic potential, and that its activity promotes cell migration, which is essential for the metastatic cascade [136].

1.7 Androgens and prostate cancer

1.7.1 Androgens and prostate

Male androgens, also known as testoids, play a critical role in regulating the formation, size, and function of the prostate gland, as well as in maintaining male traits, through their binding to AR [137]. The primary androgen of men (more than 90%) is testosterone, which is largely generated in the testes. Androgen is required for the development of the prostate's basic function [138]. The hypothalamus regulates androgen secretion in men. As the level of

androgen (primarily testosterone) in the peripheral circulation decreases, the hypothalamus releases a pulse of luteinizing hormone-releasing hormone (LHRH). This pulse of LHRH can bind to a specific receptor in the pituitary gland, triggering the release of luteinizing hormone (LH) [138]. The released LH in peripheral blood promotes the leydig cells to initiate steroidogenesis [139]. Testosterone is converted to a more effective metabolite called dihydrotestosterone (DHT) in the prostate gland as a result of 5-α—reductase enzyme stimulation. DHT binds to AR, a nuclear hormone superfamily transcription factor that is ligand-dependent. DHT-AR bind to and activate androgen response elements (AREs) in the promoter regions of the downstream genes in the nucleus, which may govern prostate cell growth, survival, and differentiation [102, 138-144].

In localised prostate cancer, radical prostatectomy and external radiation therapy are frequently used therapeutic procedures [145]. Suppression of androgen signalling is critical for patients diagnosed with advanced or metastatic prostate cancer, and therefore androgen deprivation therapy (ADT) by medicinal, surgical castration, anti-androgens, and combination androgen blockade becomes a popular therapy [146]. ADT, as the primary successful treatment, is capable of inducing an initial response in approximately 80-90% of patients. Nonetheless, after 14–20 months, patients develop progression to androgen-independent prostate cancer, which is no longer responsive to ADT [147].

1.7.2 Androgen-independent prostate cancer

Androgen-independent prostate cancer had been previously referred to as Castration Resistant Prostate Cancer (CRPC) [139]. CRPC is a stage of prostate cancer that is resistant to castration and the patients have a poor prognosis and a shorter survival time from the time of progression [139]. The identification of molecular pathways behind prostate cancer cells' transition from androgen-dependent to androgen-independent state is a critical topic for prostate cancer research and is a requirement for the development of novel CRPC therapy strategies [148-150].

1.8 Progression to castration-resistance prostate cancer

The molecular mechanism by which androgen-dependent prostate cancer advances to CRPC is a significant scientific subject that has been addressed by numerous laboratories. At the moment, ADT is the primary treatment option for prostate cancer [151]. Nonetheless, the majority of patients treated with ADT will eventually relapse and become CRPC. Certain CRPC cells express AR, whereas others do not. While AR-negative CRPC cells do not respond to ADT, AR-positive CRPC cells are predominantly androgen sensitive and express AR. However, their continuous development and expansion are no longer dependent on androgen stimulation, and hence ADT treatment for CRPC is no longer effective [150, 152]. The precise mechanism by which prostate cancer cells differentiate into CRPC cells from androgen-dependent cells is unknown. Numerous hypotheses have been presented to explain the process

underlying this critical change [153]. Each explanation can only answer a fragment of the topic, and at the moment, no individual hypothesis can adequately explain this transition.

1.8.1 AR-dependent signalling pathway in CRPC

AR is a ligand-dependent transcription factor that is a member of the steroid hormone receptor family. It is composed of four functional domains: (1) the ligand-binding domain (LBD); (2) the DNA-binding domain (DBD); (3) the hinge region; and (4) the large N-terminal domain (NTD) [154]. The continuous activation of AR has been reported to be a crucial mechanism of CRPC development [155]. Although ADT decreases the level of androgen in peripheral blood, it has no effect on the level of DHT. Thus, DHT can be used to sustain the stimulation of AR [156]. Numerous molecular and cellular alterations have been suggested to be associated with the development of CRPC, particularly AR amplifications, AR mutations, AR-ligand signalling, aberrant AR co-regulating factors, as well as AR splice- Biomarkers [157, 158].

While AR is present at both the mRNA and protein levels, and can occur in plasma membrane, in all individuals with prostate cancer, its possible sensitivity amplification in CRPC may be a result of long-term androgen deprivation. There is an increase in AR expression at both the mRNA and protein levels, which is a result of the gene's amplification [159]. Chen 2004 revealed the overexpression of AR in prostate cancer xenografts and their transition from androgen-dependent to androgen-independent growth. Additionally, these authors discovered that overexpression of the AR can convert the AR antagonist to agonist [160]. Amplification

of the AR gene has been observed in 30% of CRPC patients, whereas copy number gain has been observed in 80% of CRPC cases [159, 161, 162]. Amplification was seen infrequently in untreated cases [9]. Additionally, high levels of AR amplification were found in 38–63% of circulating tumour cells from individuals with CRPC who developed metastases [155, 163]. Although AR sensitivity amplification is currently a major theory to explain how the cancer cells become castration resistant, the difficulty to use this theory to explain this pathological process is that in a large number of metastatic cases, AR is not expressed at all. Thus more studies are needed to understand the true molecular mechanisms underlying the malignant progression process leading to CRPC.

1.8.2 Other pathways

Numerous investigations identified additional mechanisms involved in the evolution of CRPC. These include the following: inhibition of apoptosis via activation of the anti-apoptotic Bcl-2 gene, which can result in androgen independence [164, 165]; it was noted that activation of receptor tyrosine kinases can induce the PI3K/AKT or mitogen activated protein kinase (MAPK) pathway, which results in phosphorylation of AR, resulting in the production of a ligand independent AR [166, 167]. Several pathways contribute to prostate cancer cells' survival in the lack of androgens. Apart from the primary idea that substantiated the AR sensitivity-amplification hypothesis, several other concepts had been proposed in recent years. One of the most significant novel theories was the FABP5-related signalling pathway theory,

which postulated that this pathway, rather than the AR-related pathway, was critical for CRPC cell malignancy progression [168].

1.9 Fatty acid binding proteins

1.9.1 Fatty acid binding proteins family

Fatty acids are formed by the hydrolysis of ester bonds in oil or fat and play a variety of roles in the human body's cell metabolism. Fatty acids are a component of a cell and hence serve as an energy source [169]. Previous studies had established that fatty acids act as signalling molecules that play critical roles in intracellular signalling transduction in a variety of cell metabolic activities, including cell proliferation, gene regulation, and apoptosis [170, 171]. After fatty acids were generated in adipocytes, they can easily penetrate the cell membrane and enter the cytoplasm. Free fatty acids can be transported to neighbouring cells by passive diffusion or protein transporters. Both the fatty acids in cytoplasm and the intracellular fatty acids can either join metabolic processes and act as sources of nourishment, or bind to intracellular fatty acid-binding proteins, which transport them into cells and organelles [172].

Fatty acid binding proteins (FABP's), also referred to as intracellular lipid chaperones, are members of the super lipid-binding protein (LBP) family [173]. Since 1972, twelve FABPs have been discovered, amongst them, two are specific to fish [174, 175]. Since FABP family members were discovered or were frequently found in various organs, they were labelled after those organs. But FABPs are not exclusively expressed in the specified organs or cells. For

instance, FABP1 (liver FABP or lFABP) is expressed predominantly in liver cells, but it is also expressed in other organs and tissues such as the pancreas, intestine, lung, stomach, and kidney; FABP5 (epidermal FABP) is abundantly expressed in skin, brain, adipocyte, tongue, intestine, macrophage, lung, liver, kidney, heart, mammary gland, skeletal muscle, retina, testis, and spleen [170, 175]. Fatty acids are ubiquitous in nature, acting as basic elements for lipid biosynthesis and retention. Increased FABP production is typically associated with an increase in the inflow of fatty acids entering cells [176].

1.9.2 General functions of FABPs

FABPs possessed a plethora of characteristics. FABPs can actively bind and deliver lipids to specific sites or organelles inside a cell in their capacity as a lipid chaperone. Such organelles or specific sites include lipid droplets that are used for lipid storage, while the endoplasmic reticulum is used for signal transduction, transport, and membrane construction [177]. Fatty acids can be delivered to a variety of locations within a cell: to the mitochondria or peroxisomes for oxidation; to cytosolic or other enzymes for activity modulation; and to the nucleus for transcriptional regulation of lipids [177]. Fatty acids can be delivered to extracellular signalling via an autocrine or paracrine route [178] (Figure 1.8). FABP can reach the nucleus in order to transfer fatty acids to transcriptional regulators, such as peroxisome proliferator-activated receptor (PPARs) family members to perform their biological functions [179-181]. FABPs were shown to be able to transport fatty acids from cytoplasm to their nuclear receptor PPAR

[177]. It was observed that FABP expression is concentrated in the cytoplasm and nucleus of cancerous tissues [180, 182]. These studies suggested that FABPs participate in distinct signalling pathways in nucleus that regulate gene expression. An illustration of fatty acid transportation and metabolism route inside a cell is shown in Figure 1.8.

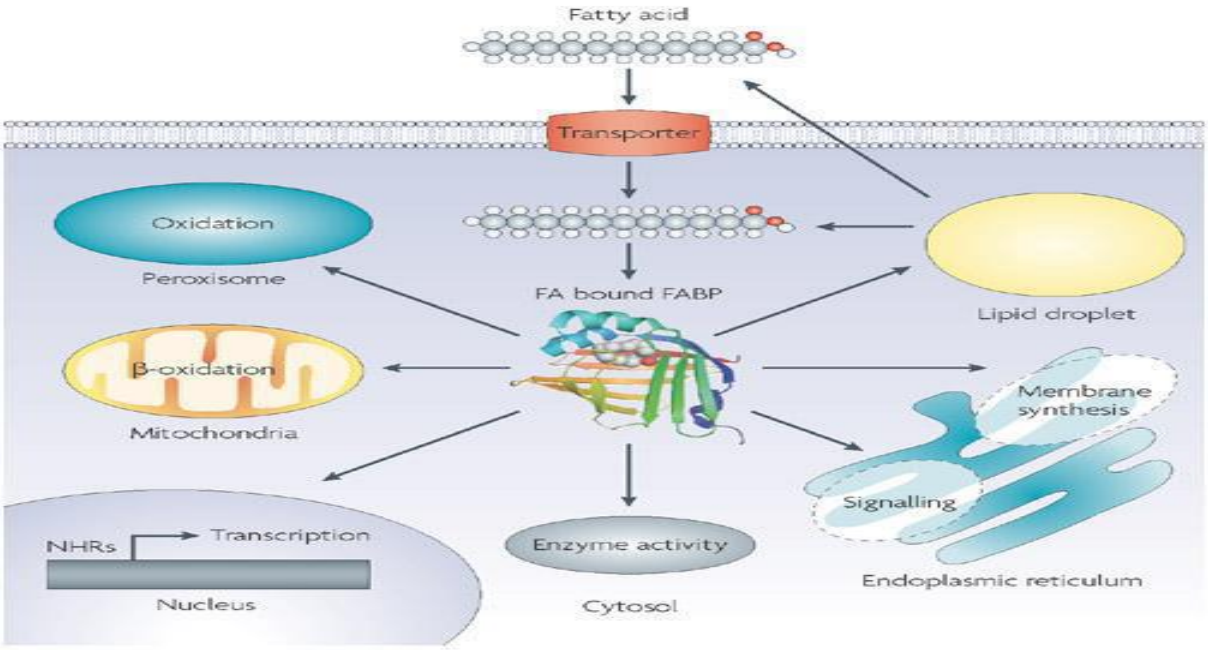

Figure 1.8 Roles of FABP's in the cells. Fatty acids are transported into cells via membrane diffusion and the assistance of receptors such as the G-protein. FABPs act as a chaperone, regulating all lipid transport and storage functions in the cell. FABPs transport lipids within cells to the endoplasmic reticulum (ER) for signalling; to the mitochondria for oxidative processing; and to the nucleus for transcription activity [170].

1.9.3 The role of FABP5 in cancer

FABP5 or E-FABP is highly expressed in cancer cells, contributing to their aggressive characteristics by boosting proliferation, invasion, tumorigenicity, and metastatic potential. FABP5 expression was also associated with therapeutic resistance and poor prognosis in a variety of malignancies, including gastric cancer [183, 184], melanoma [185], cervical cancer [186], breast cancer [187], prostate cancer [188-190], cholangiocarcinoma [191], and oral cancer [192]. Across all cancer types, the significance of FABP5 in driving prostate cancer has received the greatest attention. Numerous studies established that FABP5 facilitated tumour invasion in both *in vitro* and *in vivo* [193].

FABP5 expression was detected in triple negative breast cancer, illustrated in a cohort study; a high level of FABP5 was related with aggressive disease and poor survival. The authors suspected that FABP5 acted by modifying the extracellular matrix, allowing tumour cells to invade neighbouring organs [187].

Since 2000, our molecular pathology group in Liverpool has been investigating FABP5. We analysed and quantified the relative levels of FABP5 in benign and malignant prostate and breast cancer cell lines after identifying it as a differentially expressed gene. When compared to benign analogues, FABP5 expression levels were 6.5-fold and 5-17-fold higher in breast and prostate malignancies, respectively [194, 195].

Morgan et al. identified considerably elevated FABP5 levels in prostate cancer cells and tissues. Increased FABP5 expression was found to be strongly linked with decreased patient

survival time. When the level of FABP5 in prostate cancer cells was reduced using RNAi, their tumorigenicity and metastatic capacity were significantly reduced both in vitro and in vivo [194]. During comprehensive research on the molecular processes behind FABP5's malignancy-promoting activity, a novel signal transduction pathway was revealed that was launched by the activation of fatty acids carried by FABP5. This signal transduction pathway is outlined as follows: Increased FABP5 transports a substantial proportion of fatty acids into the cytoplasm, where the majority of the fatty acids are used as fresh sources of energy for the cells, while some are sent to their nuclear receptor PPARγ. The active PPARγ can initiate a number of molecular events or a chain of molecular processes, including up-regulation of some cancer-promoting genes, such as VEGF, and down-regulation of some putative tumour suppressor genes, to facilitate or to inhibit the malignant progression of the cancer cells [194]. Therefore, it was recently established that fatty acids activate PPARγ via the FABP5-PPARγ-VEGF signalling pathway (Fig.1.9), making it a critical therapeutic target for CRPC angiogenesis inhibition [195].

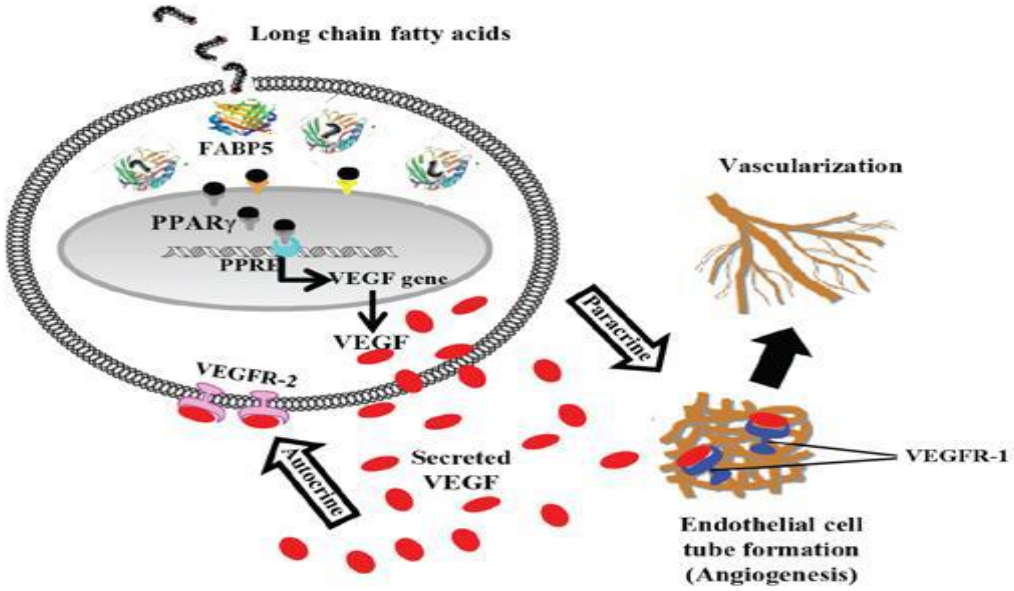

Figure.1.9: Schematic illustrations of FABP5-PPARγ-VEGF pathway [195]. Fatty acids transported by FABP5 can activate PPARγ, which in turn increases VEGF expression. VEGF is a potent antigenic factor that, when bound to its receptor VEGFR1, promotes the formation of vessel networks that are required for cancer cell growth and expansion. Additionally, VEGF can directly promote cancer cell malignancy via an autocrine mechanism by simulating the receptor that is highly expressed on the surface of prostate cancer cells (VEGFR-2).

1.9.4 Targeting FABP5 for prostate cancer treatment

To examine the feasibility of targeting FABP5 as a therapeutic method for prostate cancer, FABP5 gene was knocked down in highly malignant PC3-M cells using RNA interference to establish a subline (Si-clone-2) expressing a dramatically lower quantity of FABP5 [194]. When Si-clone-2 was orthotopically transplanted into the prostate gland of mice, it resulted in a 63-fold reduction in average tumour size, a 7-fold reduction in tumour incidence, and a 100%

reduction in metastasis [194]. This finding demonstrated that the short FABP5 siRNA produced from within cancer cells is extremely effective at reducing the malignant progression of a mouse-derived tumour. However, due to their instability and short half-life at body temperature, siRNA molecules are rapidly degraded when administered externally as reagents. As a result, siRNA cannot be utilised directly as prostate cancer treatment. Even when siRNA against FABP5 was solubilized in a stabilising agent (named Atolecollagen, derived from bovine skin extracts) and injected directly into a defined prostate cancer tumour in the experimental nude mice, these siRNA molecules were only able to slow and stabilise tumour growth, but not to reverse cancerous progression or decrease tumour sizes [196].

Our group have recently tested a potent FABP5 inhibitor, SB-FI-26, that was an active component of a Chinese herbal medication (Incarvillea sinensis) and was used to treat rheumatism and pain in traditional medicine [196, 197]. SB-FI-26 strongly inhibited the proliferation, migration, invasiveness, and colony formation of PC3-M cells in vitro, as demonstrated in our study. Orthotopically implanted the PC3-M cells into the prostate gland of the male nude mice and then administrating this inhibitor demonstrated that the FABP5 inhibitor SB-FI-26 produced a 9-fold reduction in the average size of primary tumours, a 50% reduction in metastasis [198]. Therefore, due to these findings, it has been postulated that SB-FI-26 may act as a competitive inhibitor of fatty acids for FABP5 and thus limit the transport of intra- and extracellular fatty acids into the cytoplasm [198]. When SB-FI-26 lowers fatty acid absorption, it may result in a decrease or discontinuation of fatty acid-induced PPARγ

activation. Thus, PPARγ may lose its ability to upregulate downstream cancer-promoting genes, such as VEGF, and to inhibit apoptotic genes [196].

In addition to our prior work, our lab has successfully treated CRPC in nude mice using the new bio-inhibitor dmrFABP5 by inhibiting FABP5's biological activity. dmrFABP5 was developed by modifying the structure of the fatty acid-binding motif. To create a cDNA coding for a doubly-mutated FABP5, site-directed mutagenesis was used to alter two of the three amino acids in the fatty acid-binding motif [190]. The mutant protein dmrFABP5 has a structure that is quite similar to that of wtrFABP5, however it is nearly incapable of binding to fatty acids. We have demonstrated that dmrFABP5 has a dominating negative effect on FABP5 biological activity, and hence on PC3-M cells' tumorigenicity and metastatic capacity. Thus, in vitro, dmrFABP5 suppressed PC3-M proliferation, invasiveness, migration, and colony formation. Furthermore, dmrFABP5 was highly effective in inhibiting both the primary prostate gland tumour and the subcutaneous tumour in the flank when tested in naked mice. Thus, dmrFABP5 reduced the mass of prostate gland tumours by an average of 13-fold and subcutaneous tumours by 3-fold. Notably, dmrFABP5 completely inhibited metastases in animals implanted with CRPC cells in the prostate gland [198].

1.10 Peroxisome Proliferator-Activated Receptor Gamma (PPARγ)

1.10.1 PPARγ

PPARγ is a ligand-dependent transcription factor that belongs to the superfamily of nuclear hormone receptors [199]. PPARγ is grouped into two isoforms, PPARγ1 and PPARγ2, with the latter containing thirty additional amino acids (Figure 1.10) [199].These two isoforms are produced due to the alternative mRNA splicing of the PPARγ gene [200]. PPARγ activation is mediated by both synthesized and endogenous ligands [199]. When activated, PPARγ catalyses its transfer through into nucleus and creates a heterodimer dimer with the retinoid X receptor (RXR), where it acts as a transcription factor by binding to DNA [201].

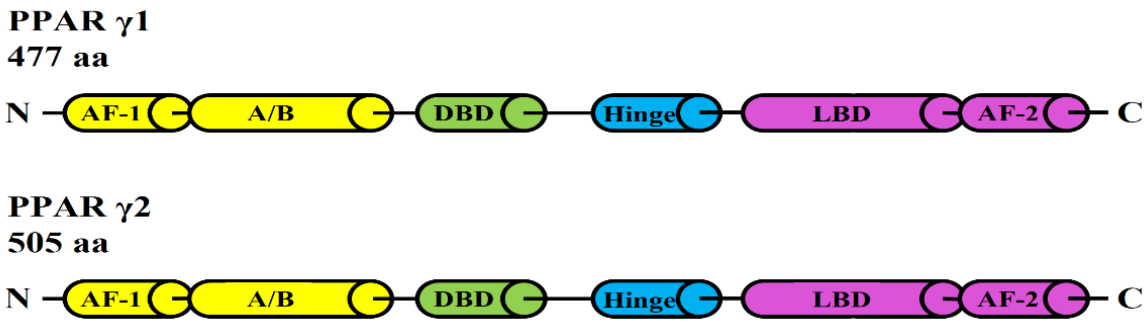

Figure 1.10: PPARγ1 and PPARγ2 structures. At protein level, PPARγ consists of an activation function 1 (AF-1) region, a variable or Hinge (A/B) region, a DNA-binding domain (DBD), a ligand-binding domain (LBD), and an activation function 2 (AF-2) region. PPARγ2 has an extra of 30 Amino acids. Adapted [199].

It is widely recognised that PPARγ is required for adipocyte differentiation, the inflammatory processes, and glucose uptake consumption in the peripheral body parts, and that PPARγ agonists are often used to treat type II diabetes [199]. Diabetes type II is considered to be the most common endocrine-metabolic disorder globally, defined by insulin resistance and impaired insulin secretion [202]. To sensitise tissues to insulin action, PPARγ agonists have been used (adipose tissue, muscle, and liver). However, these medications have been linked to serious adverse events such as weight gain, oedema, heart failure, and an elevated chance of myocardial infarction [202].

Initially, it was hypothesized that PPARγ acted as a tumour suppressor in prostate cells since agonist ligands inhibited the generation of prostate cancer cells; however, further research revealed that PPARγ agonists inhibit cell growth in a mechanism independent of PPARγ [203-207].

Moreover, PPARγ expression is associated with increased cancer grade/stage [208-210]. This implies that PPARγ activity is not a tumour suppressor, but rather may contribute to the development and/or progression of prostate cancer, as tumour suppressor protein expression often decreases during the malignant progression. PPARγ expression appears to be highly associated with advanced stages and grades of prostate cancer, insinuating that it is an oncogene. For instance, in around 200 samples, researchers discovered that PPARγ expression was significantly higher and more intense in prostate cancer and prostatic intraepithelial neoplasia (PIN) tissues than that in benign prostatic hyperplasia (BPH) and normal prostate

tissues [210]. Likewise, other research showed that advanced prostate cancer tissues had significantly higher PPARγ expression than low-risk prostate cancer and BPH samples ($P<0.001$) [209]. Moreover, two studies discovered that in comparison with the benign tissues, malignant tissues expressed more PPARγ [211, 212]. Taking these data into account, they strongly suggest that PPARγ is not a tumour suppressor and that its stimulation may be involved in promoting the development of prostate cancer.

1.10.2 Role of PPARγ in prostate cancer

Ahmad et al. recognized PPARγ as a novel gene that induces prostate carcinogenesis using a Sleeping Beauty screen in prostate-specific Pten/ mice [208]. Sleeping beauty screening is a synthetic DNA transposon developed to insert precisely defined DNA sequences into vertebrate animal chromosomes in order to introduce new features and uncover new genes and their functions [206]. When compared to littermate controls, mice with insertions upstream of the PPARγ gene that elevated PPAR protein expression had a reduced survival time and an increased incidence of lung and lymph node metastases [208]. Enhanced PPARγ expression in these animals was associated with increased PPARγ expression in target genes FASN, ATP citrate lyase (ACYL), and acetylCoA carboxylase (ACC) [208]. In three prostate cancer cell lines, DU145, PC3, and PC3M, overexpression of PPARγ enhanced cell proliferation and migration, however siRNA suppression of PPARγ had the inverse result [208].

Ahmad et al. identified a substantial association between PPARγ levels and the grade of prostate cancer, as well as a relationship between reduced pTEN expression and inferior disease-specific survival in individuals with low PTEN expression [208]. Moreover, Ahmad et al. analysed data from the cBioportal (www.cbioportal.org) and determined that the PPARγ gene was elevated in 26% of advanced cancers and that the enzyme 15lipoxygenase 2 (ALOX15B), which reconstructs 15S hydroxyeicosatetraenoic acid, an endogenous PPARγ ligand, was upregulated in an additional 17% of cases [208]. Furthermore more than half of all sequenced cancers expressed one or more of the PPARγ target genes FASN, ACC, or ACLY, strongly suggesting that PPARγ activation plays a promotive role in the development and progression of prostate cancer [208].

One of the earliest studies to investigate the role of PPARγ in prostate cancer was driven by the observation that diets high in omega-3 fatty acids appear to be related with a lower incidence of prostate cancer than diets high in omega-6 fatty acids. One of these fatty acid metabolites, 15-Deoxy-12,14-prostaglandin J2 (15dPGJ2), is a specific PPARγ activator and has been shown to have anticancer potential [213]. Butler et al. [214] next investigated if the anticancer properties were due to PPARγ activation. They found that whereas 15dPGJ2 and other PPARγ activators such as ciglitazone induced cell death in three prostate cancer cell lines, PPARα and PPARβ ligands did not. This original result stimulated more investigations into the use of PPARγ activating ligands in prostate cancer, which revealed that PPARγ agonists decreased AR levels and activity while reducing prostate cancer cell proliferation [109, 215,

216]. Additional mechanistic investigations established conclusively that these drugs had an effect independent of PPARγ (Figure 1.11). One study noticed, PPARγ agonists inhibited cell proliferation by increasing proteasomal degradation of transcription factor specificity protein 1 (SP1) [204]. Other studies have suggested different methods by which PPARγ agonists hinder prostate cancer cell growth in a PPARγ-independent manner, including inhibition of BclxL/Bcl2 functions [205], inhibition of the CXC chemokine receptor type 4/CXC motif chemokine 12 (CXCR4/CXCL12) axis [206], and inhibition of the AKT signalling pathway [217]. A further work demonstrated that PPARγ agonists increased AR signalling in C42 prostate cancer cells in a PPARγ-dependent manner [218]. As a result, whereas PPARγ agonists are likely to promote AR signalling, their actions on SP1 or other pathways in some cell types result in indirect AR repression and decreased prostate cancer cell proliferation.

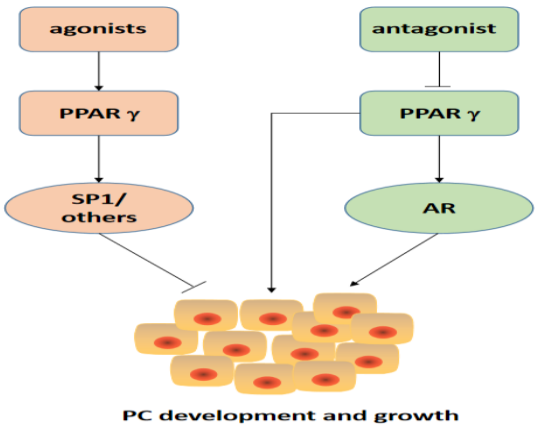

Figure 1.11: The role of PPARγ and ligands in prostate cancer growth, adapted [203], although PPARγ agonists have been proven to decrease prostate cancer cell growth, this has been demonstrated to occur via PPARγ-independent pathways. Recent research revealed that PPARγ had an oncogenic role in the

development and progression of prostate cancer, both AR-dependent and AR-independent. PPARγ antagonisit agents may be beneficial in the treatment of advanced prostate cancers and in preventing the development of prostate cancer. PPARγ: peroxisome proliferator-activated receptor gamma; SP1: specificity protein 1; AR: androgen receptor; PC: prostate cancer.

Previous investigation in our laboratory showed that the increased FABP5 levels contribute considerably to malignant development in CRPC model cell systems by binding to and transporting the increased quantities of fatty acids into cells and delivers the fatty acids to their nuclear receptor PPARγ and activate it [219]. Our work demonstrated that the treatment with PC3-M cells with the PPARγ antagonist GW9662 inhibits tumour development in a manner similar to that obtained by the treatment with FABP5 inhibitor dmrFABP5. This result suggests that dmrFABP5 inhibits the FABP5-PPARγ-VEGF signalling pathway, although it did not reduce the uptake of excellular cell fatty acids [195]. These results suggested that the amount of fatty acid uptake increased as the increasing malignancy of the cancer cells. While most of the fatty acids may be used as new energy sources, the exassive amounts of fatty acids may be used as signaling molecules to stimulate and thus to activate PPARγ [190]. Previous studies demonstrated that a chemical FABP5 inhibitor SB-FI-26 strongly inhibited fatty acid uptake by the prostate cancer cells. So, SB-FI-26 may function as a competitive inhibitor of fatty acids for FABP5 and thus impede the transportation of intra- and extracellular fatty acids through into cytoplasm [198]. SB-FI-26 inhibits fatty acid uptake, which may result in a decrease or cessation of fatty acid-induced PPARγ activation. As a result, PPARγ may lose its strength to

continue promoting the downstream cancer-promoting genes, such as VEGF, or suppressing tumour-suppressing gene [195]. Our earlier research established that the FABP5-PPARγ-VEGF signalling axis, rather than the androgen receptor-initiated route, is the primary channel for malignant signal transduction in CRPC cells [195]. As a result, PPARγ appears to play a key rrole in this axis.

1.10.3 Role of PPARγ isoforms in prostate cancer

Due to the fact that PPARγ agonists inhibit AR activity and prostate cancer cell proliferation, it was previously hypothesised that they functioned as a tumour suppressor in prostate cells [109, 214-216]. However, PPARγ agonists have been demonstrated to inhibit cell proliferation and AR activity in a manner independent of PPAR activity [204-206]. Based on the experimental observation that PPARγ expression increased with the increament of the grade/stage of prostate cancer [208-210], it was suggested that PPARγ was an oncogene. Further clarrification is needed on the exact role of PPARγ in the malignant progression of the cancer cells.

To investigate whehter PPARγ can be used as a potential therapeutic target in prostate cancer treatment, it is critical to bear in mind that PPARγ exists in two isoforms. PPARγ2 is identical to PPARγ1, except that it has an additional 30 amino acids at the amino terminus. PPARγ1 is expressed in a variety of organs, whereas PPARγ2 is mostly expressed in adipocytes and governs their differentiation [220, 221]. However, a recent research by Strand et al [222]

showed a substantial heterogeneity between the two PPARγ isoforms. In this study, PPARγ gene in mouse prostate epithelial cells was first knocked out, and then the individual PPARγ1 and 2 transcripts were reinstated, respectively, to establish two different sublines expressing PPARγ-1 and PPARγ-γ, respectively. When these modified cells were used in a reconstitution assay of the prostate, it was observed that restoring PPARγ1 led to the development of adenocarcinoma, wheras restoring PPARγ2 resulted in the development of benign glands.

According to a recent study, both PPARγ isoforms are expressed in human tissue in the majority, but not all, of local and metastatic cancers, with PPARγ1 being the most abundant. Using IHC and RNA in situ hybridization, the researchers demonstrate that both PPARγ1 and PPARγ2 are expressed in epithelial cells from isolated benign prostate glands. These findings suggested that PPARγ1 may play a larger role in the development of prostate cancer than PPARγ2. Indeed, both these functional studies and the results by Strand et al [222] seem to suggest that PPARγ1 has oncogenic potential in prostate cells, whereas PPARγ2 has tumour suppressive characteristics [190]. Strand et al. demonstrated in a mouse prostate reconstitution experiment that expression of PPARγ1 alone in benign mouse prostate epithelial cells results in the development of an adenocarcinoma-like tissue, whereas expression of PPARγ2 alone results in a highly differentiated phenotype [222]. PPARγ1, but not PPARγ2, increased BPH1 cell proliferation in the soft agar colony formation experiment [190]. Moreover, blocking PPARγ1 decreased the growth of PC cell lines expressing PPARγ1 endogenously or constitutively [190]. This is consistent with the notion that PPARγ1 is a tumour promotor gene.

The treatment with PPARγ2 suppressed the proliferation of LNCaP cells, indicating PPARγ2's role as a tumour suppressor [190].

1.11 Aims and scope:

To further clarrify and to establish or to eleminate whether PPARγ plays a promotive role in prostate cancer development, and to test whether PPARγ can be used as a treatment target for prostate cancer, I plan, in this work, to:

1- Utilize the state of art techinque, crispr/cas9, to completely knockout the PPARγ gene from androgen-dependent prostate cancer cell 22rv1, and androgen-independent prostate cancer cell Du145, in order to establish two cell lines whose PPARγ expression is completely abrogated.

2- Confirm the knock out effect by western blot and sanger sequence analysis on both cell lines.

3- Perform the standard bio-assays in-vitro to assess the effect of PPARγ knock out on the malignant characteristics of the two prostate cancer cell lines. These bio-assays include the following:

- Proliferation assay.
- Cell mobility (wound healing) assay.
- Invasion assay and
- The anchorage-independent growth assay.

4- Fnially, in-vivo work will be performed in nude mouse model to compare the tumourigenicity between the PPARγ-knock-out cells and their parental control cells.

5- I will use statistical analysis to analyse my results and to assess and to confirm whether PPARγ is , or is not, a cancer-promoting gene; and to conclude whether PPARγ is a treatment target for prostate cancer.

CHAPTER TWO

MATERIALS AND METHODS

2.1 Cells and cell culture

Four benign and malignant prostate epithelial cell lines were used in this study. PNT2 is a cell line was established from normal prostate epithelial cells by immortalisation with SV40 transfection, they are linked cell lines that have an epithelial appearance [223]. The 22Rv-1 cell line is a human prostate cancer epithelial cell line that was derived from a CWR22 xenograft that had been castrated and relapsed in mice prior to getting serially reproduced in mice. The cell line expresses prostate specific antigen (PSA) [223]. Prostate cancer cell lines DU145 and PC3M are all highly malignant cell lines which do not express AR [223]. DU145 and PC-3M cell lines were established from metastatic prostate cancer lesions in the brain, bone, and lymph nodes, respectively. The varying tumour microenvironments and origins of numerous cell lines have resulted in these cells possessing a range of features. DU145 expresses prostate-specific antigen, while PC-3M does not [223]. The cell culture experiments were conducted under a tissue culture hood (LabGard, USA) in accordance with university safety protocols. All cells were cultured in RPMI 1640 media supplemented with 10% (vol/vol) foetal calf serum, 100 U/ml penicillin (Bioser, East Sussex, UK), 100ug/ml streptomycin (Bioser, East Sussex, UK), and L glutamine (20mM) (Invitrogen). In addition to the aforesaid supplements Monolayer cultures of cells were produced and maintained in a humidifier incubator (Borolabs, UK) at 37oC with 5% CO2.

Prostate cell line	Source	PSA Expression
PNT2	Normal epithelial cell	-
22Rv1	Primary tumour	+
Du145	Brain lesions	+
PC3m	Bone and lymph nodes	-

Table2.1: Source and PSA expression of utilised prostate cancer cells.

2.1.1 Cells thawing

Cell vials kept on various racks in a liquid nitrogen tank were removed from the tank and immersed in a 37 ºC water bath to gently thaw. The cells were then diluted with 20ml of new media to eliminate the impact of the DMSO, followed by 3 minutes at 91xg centrifugation. The supernatant was removed, and the pelleted cells were resuspended in new media. The number of cells was determined using a haemocytometer and cultivated in a 25-cm^2 flask. Cells were observed and the medium was replaced every three days to ensure adequate supplementation.

2.1.2 Cells subculture

The medium containing the cells was placed into a flask and observed daily under a microscope. When the cells reached around 70%–80% confluence, they were subcultured in an aseptic tissue culture hood. The medium was withdrawn from the flask, the cells were rinsed

with phosphate buffer saline (PBS), and then incubated for 3 minutes with trypsin in versine (2.5 %: 97.5 %, v/v). Following that, cells were examined under a microscope to verify they were properly rounded and detached. To inhibit trypsin activity, a twofold volume of fresh medium containing 10% FBS was added and centrifuged at 91xg for 3 minutes. The pellet was resuspended in RPMI medium and divided evenly into three fresh flasks.

2.1.3 Cells cryopreservation

Cells were stored at a cool temperature. The cells were prepared for frozen storage by removing the media, washing with PBS, treated with trypsin, and resuspended in fresh medium. Cells were then transferred to a Universal tube and counted using a hemocytometer. The pellet was centrifuged for 3 minutes at 91xg before being resuspended in freezing media made by adding DMSO to RPMI at a ratio of 7.5 %. To avoid explosions when exposed to liquid nitrogen, special vials were utilised. One millilitre of cells was loaded to each cryovial, and the cells were kept at -80°C for one night before being transferred to liquid nitrogen using a customised cool box (Mr. Frosty™).

2.2 Detection of protein expression in cell lines by Western blot

2.2.1 Collection of cell pellets

Pellets of cultivated cells were harvested when they reached 80% confluence or more. The old media was removed, and cells were rinsed with PBS, treated with trypsin, and centrifuged as

described previously. In a universal tube, the pellet was lysed with a combination of the CelLytic reagent and a protease inhibitor. The tube was then shaken for 15 minutes on a roller mixing shaker, followed by a 10-minute centrifugation at 11,200 x g to collect the supernatant for Western blot analysis.

2.2.2 Bradford assay

Protein concentrations in each sample loaded for Western blot analysis were determined with the Bradford assay. The principle for this assay is as following: when a protein attaches to the Coomassie Blue G250 dye, the dye's colour can be changed from brown to blue. The colour is proportional to the protein content and may be identified using a spectrometer (Biotech, UK) to measure absorbance. Protein concentrations can be quantified by comparing the absorbance of the protein to a standard curve composed of repeated dilutions of a common protein known as bovine serum albumin (BSA) [224].

Bradford dye was filtered through Whatman paper, and 1 ml was poured to each of a serial dilution tubes and protein tubes. Following that, transfer the serial dilutions and cell proteins in triplicate to a microplate reader and use a spectrometer to measure the absorbance at 595 nm. A standard linear curve was generated between protein concentration and associated absorbance values to identify unknown sample concentrations Figure 2.1.

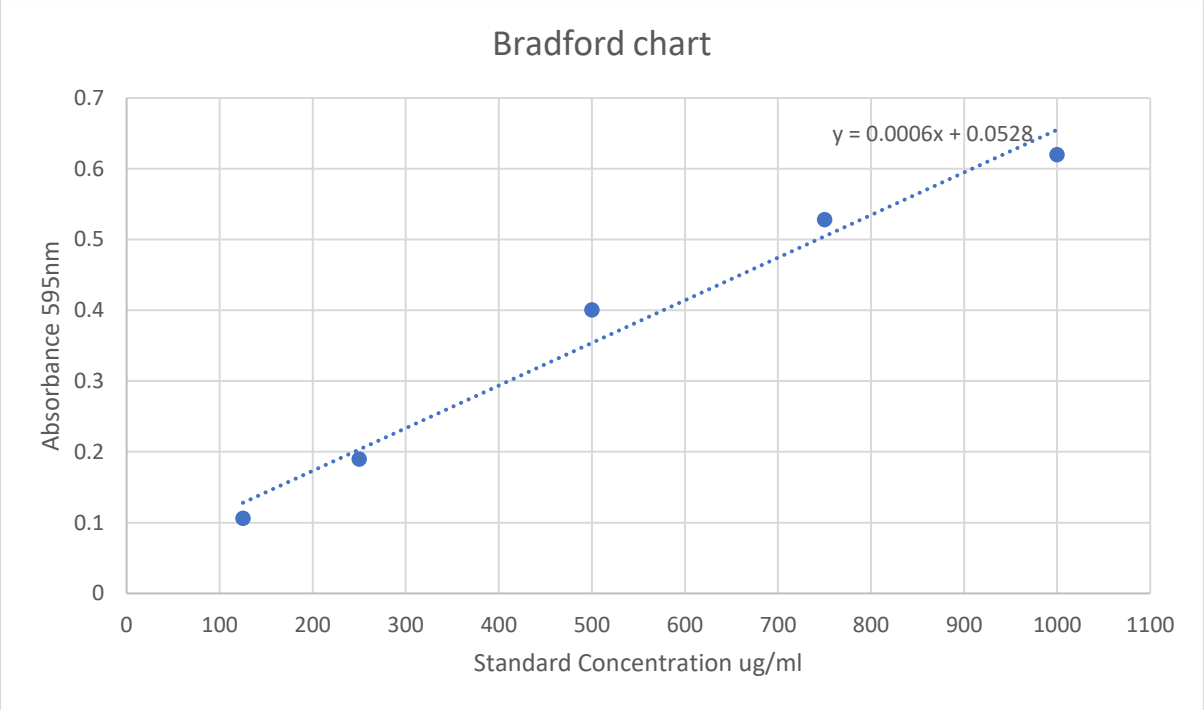

Figure 2.1 Standard linear curve between concentration and associated absorbance values.

2.2.3 Western blot

Electrophoresis with a Bio-Rad Mini-Protean gel technology was used to separate the total proteins obtained from each source (Bio-Rad, UK). All buffer reagents were made in advance according to the recipes included in the appendix A. The protein concentration of each sample was determined using the Bradford assay, and an equal quantity of total protein from each sample was loaded into each well of the polyacrylamide gel for polyacrylamide gel electrophoresis (PAGE). Sample buffer (Laemmli buffer), produced and stored in an Eppendorf tube, was added to each cell extract and mixed with β-mercaptoethanol to inhibit the formation

of disulfide bonds and thereby avoiding protein aggregation. The proteins at the reduced condition were then denatured by heating on a hot plate for 10 minutes at 95 °C. The mixture was then instantaneously kept on ice for three minutes. The gel was placed in a clamping frame and secured tightly. The tank was refilled with running buffer. As a reference, a molecular weight marker was loaded into a separate well, and cell protein (20 µl) was loaded into each well respectively. The electrophoresis was carried out for one hour at a voltage of 100 volts.

To transfer the separated proteins from the polyacrylamide gel to a PolyVinylidene DiFluoride (PVDF) membrane for subsequent immunodetection, the protein gel was laid on the membrane forming a sandwich and encapsulated in a cassette. As illustrated in figure 2.1, the cassette was produced utilizing sponges, filter papers, gel, membrane, and finally filter paper and sponge. A roller was used to eliminate bubbles and prevent the gel from being displaced. To avoid overheating and gel rupture, cold ice was applied. The PVDF membrane (Immobilon-P, Millipore, and USA) was activated by submerging for 2 minutes in methanol, then washed in cold transfer buffer and assembled in the cassette using Whatman filter papers and sponges. The transfer is carried out at 4 ^{o}C in a pre-prepared transfer buffer (appendix). Electroblotting was carried out for one hour at a voltage of 100 volts, with the ice pack replaced at half hour. After one hour, the membrane was removed from the gel and rinsed with distilled water.

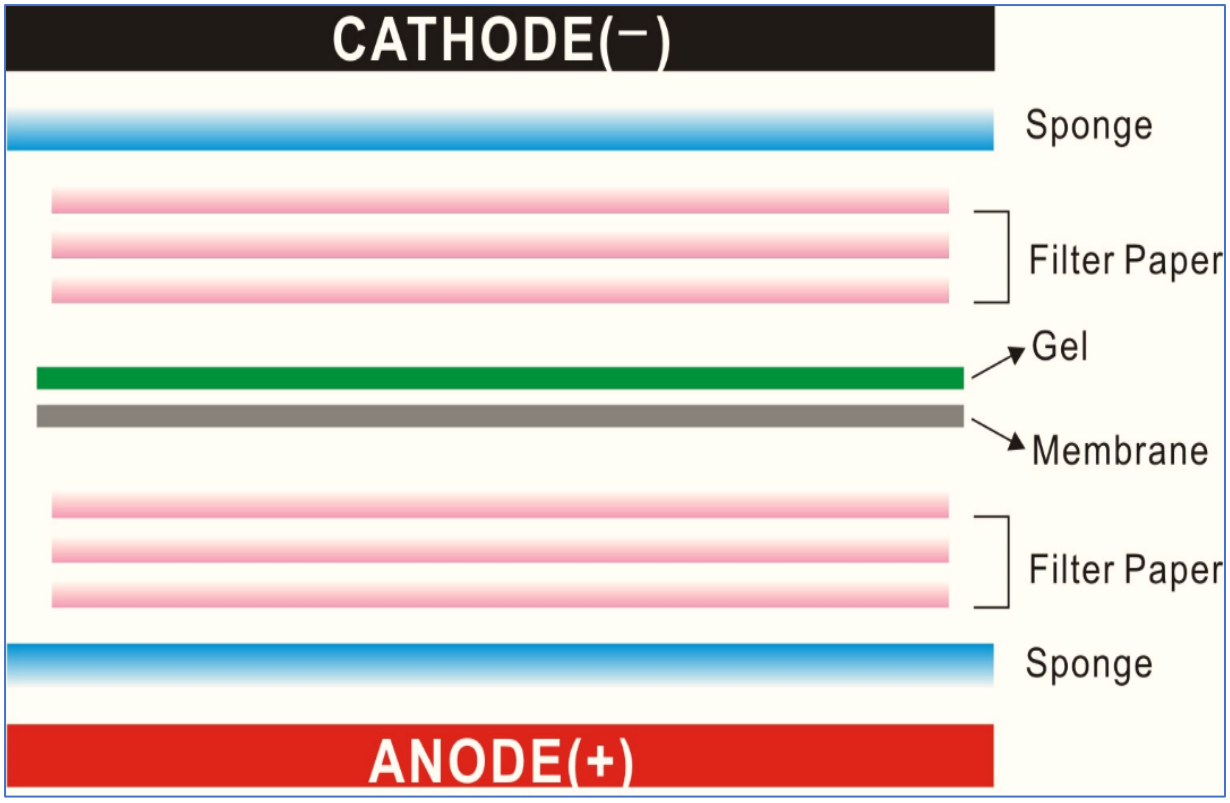

Figure 2.2. Western blot transfer cassette illustrated diagrammatically. Sponge, three filter sheets, gel, PVDF membrane, three filter papers, and sponge are arranged and layered from black to red. The electro-current flows between the negative black and positive red electrodes, so that the separated proteins can migrate from the gel to the membrane.

Upon the completion of the transfer of the proteins, an extra procedure was performed to check the transfer efficiency. The gel was stained with Coomassie blue, washed with distilled water overnight, and then stained with Ponceau S red for 3-5 minutes to check whether protein bands were transferred completely. After the assessment and confirmation of the transfer efficiency, the membrane was washed several times with TBS buffer on a shaker plate to remove the stain, kept at 4°C for antibody hybridization.

2.2.4 Immunodetection

The membrane was rinsed with TBS-T buffer to remove any potential gel residuals and then incubated for one hour on a shaker plate with the primary anti-PPARγ antibody (CST, 24435), Table 2.2, followed up by four washes (5 minutes each) with 1x TBS-T buffer to eliminate unbound antibody. The membrane was then incubated for one hour on a shaking plate with the secondary antibody conjugated with horseradish peroxidase, followed by four further washes (5 minutes each) to eliminate any unbound secondary antibody residuals. Following that, the membrane was incubated with Chemiluminescence ECL in dark. The ChemiDoc imaging equipment was used to view the protein bands, with exposure and timing optimised to obtain the best possible images.

To adjust for any loading discrepancies, the membrane was hybridised with an anti β-actin. To begin, the membrane was blocked for 30 minutes in TBS-T milk to avoid nonspecific binding. Then the membrane was incubated for 30 minutes with primary anti-β-actin mouse antibody (1:50000) in 20 ml milk, to be followed by four washes with TBS-T buffer (5 minutes each). After 30 minutes incubation with a secondary rabbit anti-mouse antibody (1:10000), the membrane was washed, and the actin band detected using the ECL using the same procedures as those used for other protein band detection.

Target Protein	Primary antibody	Secondary Antibody
PPARγ	Rabbit mAb (1:1000)	Anti-rabbit IgG, HRP-linked Antibody (1:2000)
β-actin	Monoclonal Mouse Anti- β-actin (1:5000)	Polyclonal Rabbit Anti-Mouse IgG-HRP (1:2000)

Table 2.2: Primary and secondary antibodies used in Western blot.

2.3 Gene editing

To assess the possible functional role of PPARγ in promoting malignant progression in prostate cancer cells, and to test whether it can be utilised as a pharmacological target, gene editing technique CRISPR/CAS9 was used to knock out the *PPARγ* gene from the genome of the prostate cancer cells to determine the effect of diminished PPARγ expression on tumorigenicity. Due to the fact that the CRISPR/Cas9 approach is a novel state-of-the-art methodology, the initial procedure required significant refinements. GeneArt® CRISPR Nuclease provided the plasmid (Invitrogen, U.K). It integrates both a guided RNA and the Cas9 nuclease to cleave the specifically targeted gene and to enable the development of prostate cancer cell clones lacking the target gene on both chromosomes. The procedures may be classified into two distinct steps: target gene knockout and generation of cell lines derived from a single isolated colony with diminished expression of the target gene. The following steps were used to accomplish gene knockout (figure 2.2):

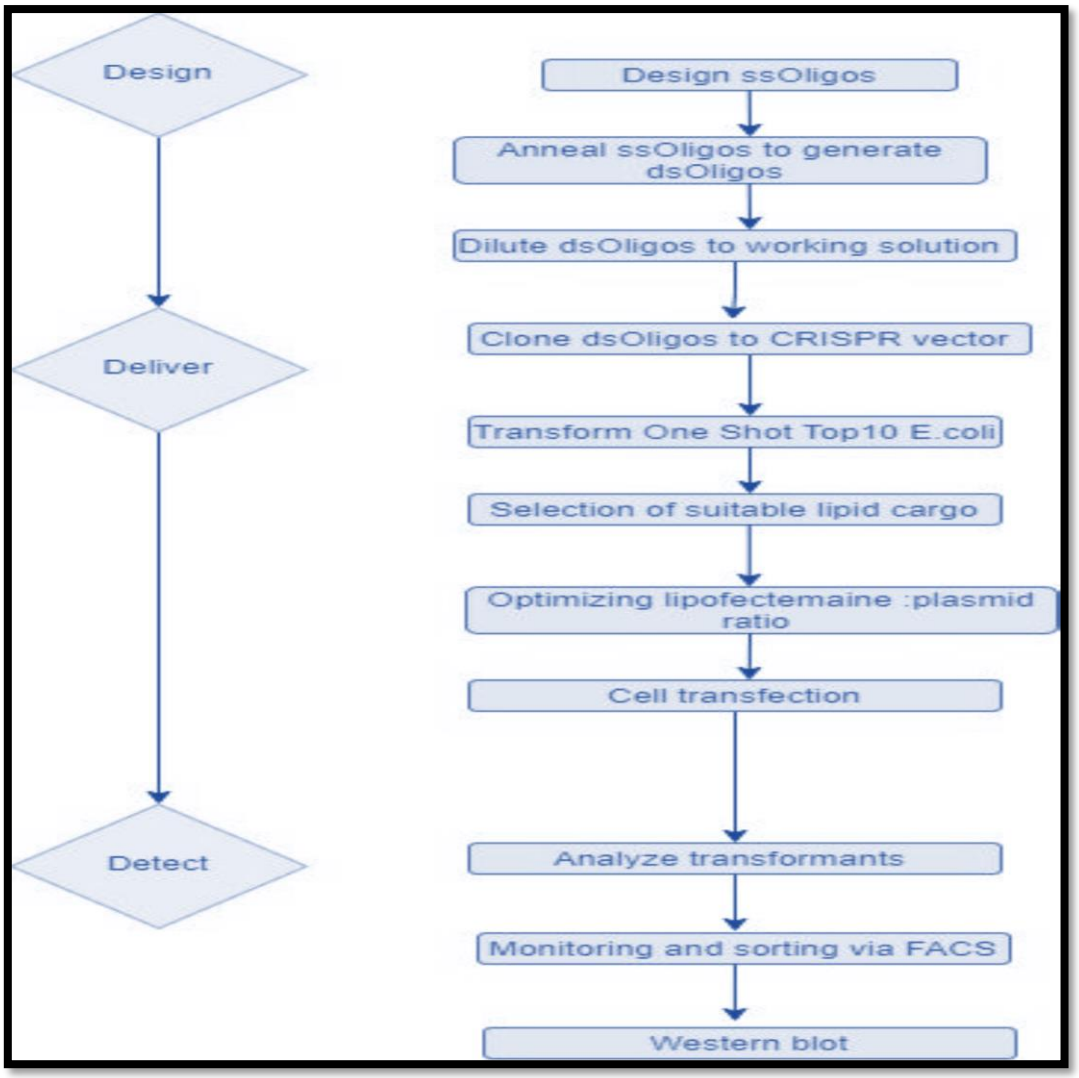

Figure 2.3. Diagram representing CRISPR/CAS9 knockout scheme. It begins with designing single stranded oligonucleotides, then annealing it to generate dsOligos. Afterwards, clone the dsOligos to the Crispr vector. Then to be transformed to E.Coli and then to be added to the lipid cargo. After optimizing the plasmid ratio, cell transfection is performed. Detection process is then applied, which contains a FACS sorting, western blot and/or sanger sequencing.

2.4.1 Guided RNA sequence design

The guided sequence was introduced into the plasmid and to direct Cas9 to the critical region of the target gene in order to trigger the knockout effect. After designing the guiding oligonucleotide, a complementary strand was made and annealed by complementary sequences to form a double-stranded DNA segment that was inserted into the plasmid's cloning site. The short DNA molecule had a length of 20 base pairs. Additional overhanging nucleotides complementary to the linearized plasmid overhangs were flanked to both ends to facilitate ligation with the vector. It is to be noted that the design of the Guided RNA sequence and expression vector were manufactured commercially. The target sequence was chosen using the following criteria:

1. The target sequence is 20 nucleotide long and immediately adjacent to the NGG proto-spacer adjacent motif (PAM), which is required for cleavage.
2. There is no evidence of considerable homology with other genes (verified using online sequence designing tool).
3. The target sequence is oriented correctly to suit PAM criteria, as illustrated in Figure 2.4.

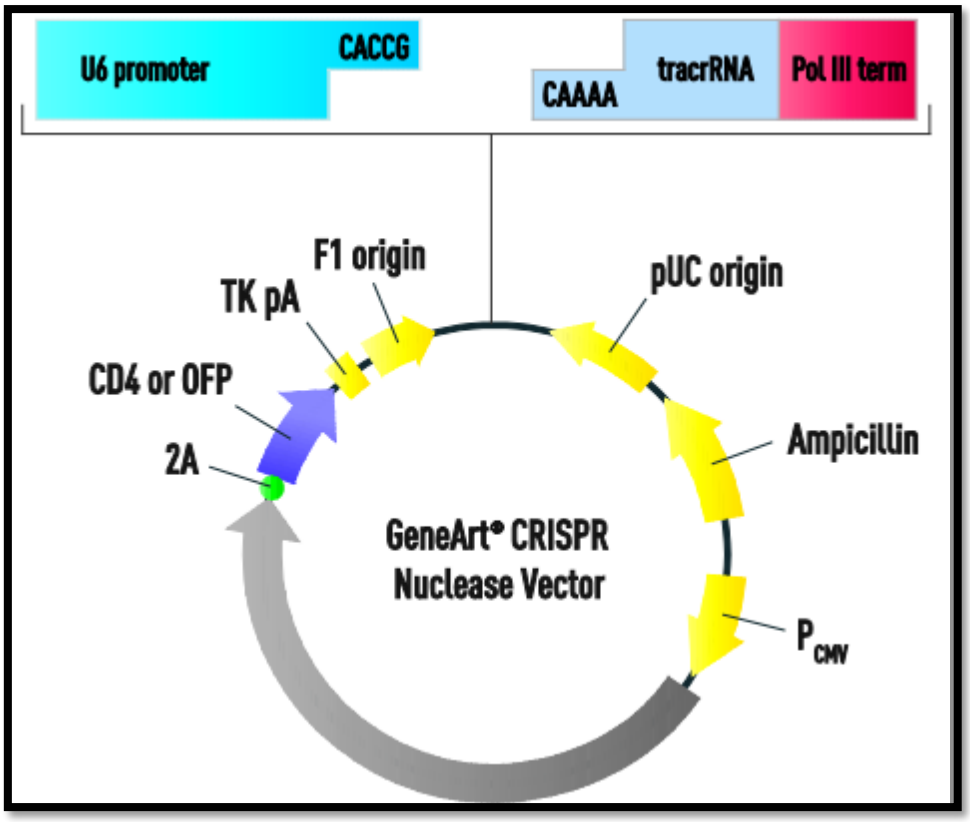

Figure 2.4. GeneArt CRISPR nuclease vector map (Invitrogen, UK). The diagram illustrates an example of the vector map of CRISPR/Cas9 vector, GeneArt CRISPR Nuclease vector, The guide RNA (gRNA) ligation which was enabled by using BbsI as a restriction enzyme. U6 promoter, CD4 Enrichment or orange fluorescent promoter, CMV enhancer, gRNA scaffold, Cas9, and ampicillin resistant gene (AmpR) are included in the sequence elements.

The crRNA and tracrRNA sequences of the GeneArt® CRISPR Nuclease Vector are combined to form a guide RNA that matches the natural crRNA-tracrRNA hybrid found in bacterial systems. The guide RNA is expressed under the control of a U6 polIII promoter. The vector contains a GFP gene to express a florescent protein that can be used as a marker to measure

transfection effectiveness, as well as 5 base pair 3′ overhangs on each strand as indicated. As described in 2.4.1, additional overhanging nucleotides complementary to the linearized plasmid overhangs were flanked on both ends to facilitate ligation with the vector.

SST 5′UTR Start codon- Mature Protein -Stop Codon- gRNA1-gRNA2PAM seq 3′UTR

5′UTR

GCCTTAACCTCTGCTGGTGACCAGAAGCCTGCATTTCTGCATTCTGCTTAATTCCCTTTCCTTAGATTTG

AAAGAAGCCAACACTAAACCACAAATATACAACAAGGCCATTTTCTCAAACGAGAGTCAGCCTTTAACGA

AATGACCATGGTTGACACAGAGATGCCATTCTGGCCCACCAACTTTGGGATCAGCTCCGTGGATCTCTCC

GTAATGGAAGACCACTCCCACTCCTTTGATATCAAGCCCTTCACTACTGTTGACTTCTCCAGCATTTCTA

CTCCACATTACGAAGACATTCCATTCACAAGAACAGATCCAGTGGTTGCAGATTACAAGTATGACCTGAA

ACTTCAAGAGTACCAAAGTGCAATCAAAGTGGAGCCTGCATCTCCACCTTATTATTCTGAGAAGACTCAG

CTCTACAATAAGCCTCATGAAGAGCCTTCCAACTCCCTCATGGCAATTGAATGTCGTGTCTGTGGAGATA

AAGCTTCTGGATTTCACTATGGAGTTCATGCTTGTGAAGGATGCAAGGGTTTCTTCCGGAGAACAATCAG

ATTGAAGCTTATCTATGACAGATGTGATCTTAACTGTCGGATCCACAAAAAAAGTAGAAATAAATGTCAG

TACTGTCGGTTTCAGAAATGCCTTGCAGTGGGGATGTCTCATAATGCCATCAGGTTTGGGCGGATGCCAC

AGGCCGAGAAGGAGAAGCTGTTGGCGGAGATCTCCAGTGATATCGACCAGCTGAATCCAGAGTCCGCTGA

CCTCCGGGCCCTGGCAAAACATTTGTATGACTCATACATAAAGTCCTTCCCGCTGACCAAAGCAAAGGCG

AGGGCGATCTTGACAGGAAAGACAACAGACAAATCACCATTCGTTATCTATGACATGAATTCCTTAATGA

TGGGAGAAGATAAAATCAAGTTCAAACACATCACCCCCCTGCAGGAGCAGAGCAAAGAGGTGGCCATCCG

CATCTTTCAGGGCTGCCAGTTTCGCTCCGTGGAGGCTGTGCAGGAGATCACAGAGTATGCCAAAAGCATT

CCTGGTTTTGTAAATCTTGACTTGAACGACCAAGTAACTCTCCTCAAATATGGAGTCCACGAGATCATTT

ACACAATGCTGGCCTCCTTGATGAATAAAGATGGGGTTCTCATATCCGAGGGCCAAGGCTTCATGACAAG

GGAGTTTCTAAAGAGCCTGCGAAAGCCTTTTGGTGACTTTATGGAGCCCAAGTTTGAGTTTGCTGTGAAG

TTCAATGCACTGGAATTAGATGACAGCGACTTGGCAATATTTATTGCTGTCATTATTCTCAGTGGAGACC

GCCCAGGTTTGCTGAATGTGAAGCCCATTGAAGACATTCAAGACAACCTGCTACAAGCCCTGGAGCTCCA

GCTGAAGCTGAACCACCCTGAGTCCTCACAGCTGTTTGCCAAGCTGCTCCAGAAAATGACAGACCTCAGA

CAGATTGTCACGGAACACGTGCAGCTACTGCAGGTGATCAAGAAGACGGAGACAGACATGAGTCTTCACC

CGCTCCTGCAGGAGATCTACAAGGACTTGTACTAGCAGAGAGTCCTGAGCCACTGCCAACATTTCCCTTC

TTCCAGTTGCACTATTCTGAGGGAAAATCTGACACCTAAGAAATTTACTGTGAAAAAGCATTTTAAAAAG

AAAAGGTTTTAGAATATGATCTATTTTATGCATATTGTTTATAAAGACACATTTACAATTTACTTTTAAT

ATTAAAAATTACCATATTATGAAA

3′UTR

Figure 2.5. Design of sgRNA's locations on PPARγ gene mRNA. This sequence illustrates the possible sgRNA's positions on the PPARγ gene mRNA. It includes the 5' untranslated region (5'UTR), start codon, mature protein, PAM sequence, gRNA1 sequence, gRNA2 sequence, stop codon and 3' untranslated region (3'UTR).

2.4.2 Annealing

After the sequences were designed, both oligonucleotides were purchased from a biosynthetic manufacturer (Thermofisher, UK). Separately, each dried oligonucleotide was suspended in T.E buffer. To anneal the two oligonucleotides together to form a double-stranded DNA, a combination of equal volumes of forward- and reverse-strand oligos were prepared with 10x annealing buffer containing DNase/RNase-free water. The mixture was first heated to 95°C for 4 minutes on a heating block and then steadily cooled to 25°C and maintained at that temperature for 10 minutes. The double-stranded oligos were then diluted in DNase/RNase-free water to obtain a 500 nM stock solution, which was aliquoted and stored at -20°C. To prepare a working solution, 500 nM oligos were diluted to 5nM ds oligos, and the newly prepared 5nM solution was stored and utilized in the experimental work.

2.4.3 Ligation reaction and transformation

To use DNA ligase to insert the short DNA molecule formed by the ds oligonucleotides into the plasmid which was linearized with restriction enzymes that can generate complementary

overhangs at each end with the corresponding end of the short DNA insert (Invitrogen, UK): The short DNA were ligated to the plasmid using a reaction mixture consisting of the ds oligos, the linearized plasmid, ligation buffer (final concentration 1x), and T4 DNA ligase. To complete the ligation reaction, the reaction mixture was incubated at 25°C for ten minutes. The ligation mixture was kept at 4°C and used for transformation into the One Shot® TOP10 competent E. coli cells provided with the plasmid kit (Thermofisher, UK).

Agar plates for bacterial growth were prepared at least one day before to the transformation experiment. After cooling the melted LB agar, ampicillin (100 µg/mL) was added and stirred. The mixture was then poured into Petri dishes and kept in a refrigerator and the gel was set to 4 °C. Before using the LB plates for transformation, they were pre-warmed for 30 minutes in a 37 °C incubator.

A vial of competent One Shot® TOP10 E. coli was thawed on ice, the ligation reaction mixture (5µl) was added, the tube gently tapped, and placed on ice for 30 minutes. The heat shock step was conducted by heating the tube for 30 seconds at 42 °C and immediately cooling it down on ice. The tube was then supplied with S.O.C medium and incubated in a shaking incubator for 60 minutes at 37°C with a shaking speed at 200 rpm. The S.O.C medium was then pipetted and distributed with a spreader onto a pre-warmed LB agar plate, which was then incubated overnight in a oven at 37°C. The effectiveness of transformation was determined by the number of colonies generated per µg of DNA.

2.4.4 Mini-preparation of DNA and sequence analysis

To verify that the guiding RNA sequence was correctly inserted into the plasmid with a correct orientation, the plasmid DNA was extracted from single E. Coli colonies using a mini-prep technique. Each mini-DNA preparation began with the selection of several colonies from the ampicillin-resistant LB agar plate using a flame-sterilized loop. Each colony was cultivated separately in a flask containing LB medium with 100ug/ml ampicillin and incubated overnight at 37 °C in a shaking oven. The plasmid DNA was recovered from each bacterial pellet using a DNA Mini-Prep kit (Invitrogen, UK, PureLink® HQ Mini Plasmid Purification Kit) following the manufacturer's instruction. The plasmid DNA was sent to Source BioScience (United Kingdom) for nucleotide sequence analysis to confirm that the guiding sequence was correctly inserted into the plasmid and that the inserted fragment was correctly orientated.

2.4.5 Transfection of the plasmid DNA into the recipient cancer cells

After confirming successful cloning and the precise orientation of the guide sequence, a sufficient quantity of plasmid DNA was prepared and purified from E. coli cells and transfected into the moderately malignant prostate cancer cell line 22Rv1 and highly malignant prostate cancer cell line DU145 to knock out the *PPARγ* gene. Prior to transfection, the purity of plasmid DNA was determined using the NanoDrop™ One spectrophotometer (Thermo Scientific, UK). The cationic lipid-based Lipofectamine® 2000 Reagent kit (Cat. no. 11668-027, Invitrogen, UK) was used to transfect the DNA construct into the recipient cells. When the cells reached

around 70% confluence in a 6 well plate, a mixture of plasmid and Lipofectamine was added to the cultures of the two cell lines, respectively.

2.4.6 Identifying of cells harbouring plasmid DNA

The effectiveness of transfection of 22Rv1 or DU145 cell lines was determined using a fluorescence microscope (Zeiss Axio Observer Z.1. Zeiss, Germany). The plasmid-containing cells were sorted using a fluorescence activated cell sorting (FACS) machine (BD FACSAria™ III, BD biosciences, USA). Due to the fact that the plasmid utilised in this study contains a *green fluorescent protein* (GFP) gene, cells that successfully took up the plasmid should express GFP and were detected using FACS. Thus, –ve GFP cells were discarded and +ve GFP cells were collected in FACS buffer, suspended in culture medium containing 100g/ml ampicillin (Ampicillin is a broad-spectrum antibiotic that inhibits bacterial growth, preventing potential bacterial contamination in cell culture), and incubated at 37°C in an CO_2 incubator. A series of repeated western blots were carried out to further insure the phenotype of the transfected cells were maintained.

2.4.7 Establishment of new sub-lines from single cell colonies

Two strategies were employed to establish a knockout colony from a single transfectant cell: machine-based FACS sorting and limited cell dilution. A number of sublines from both 22Rv1 and Du145 transfectants were established from different individual single cell clones. These

sublines, in which the PPARγ gene was completely knocked out, were established with the procedures summarised in the following flowchart (figure 2.5):

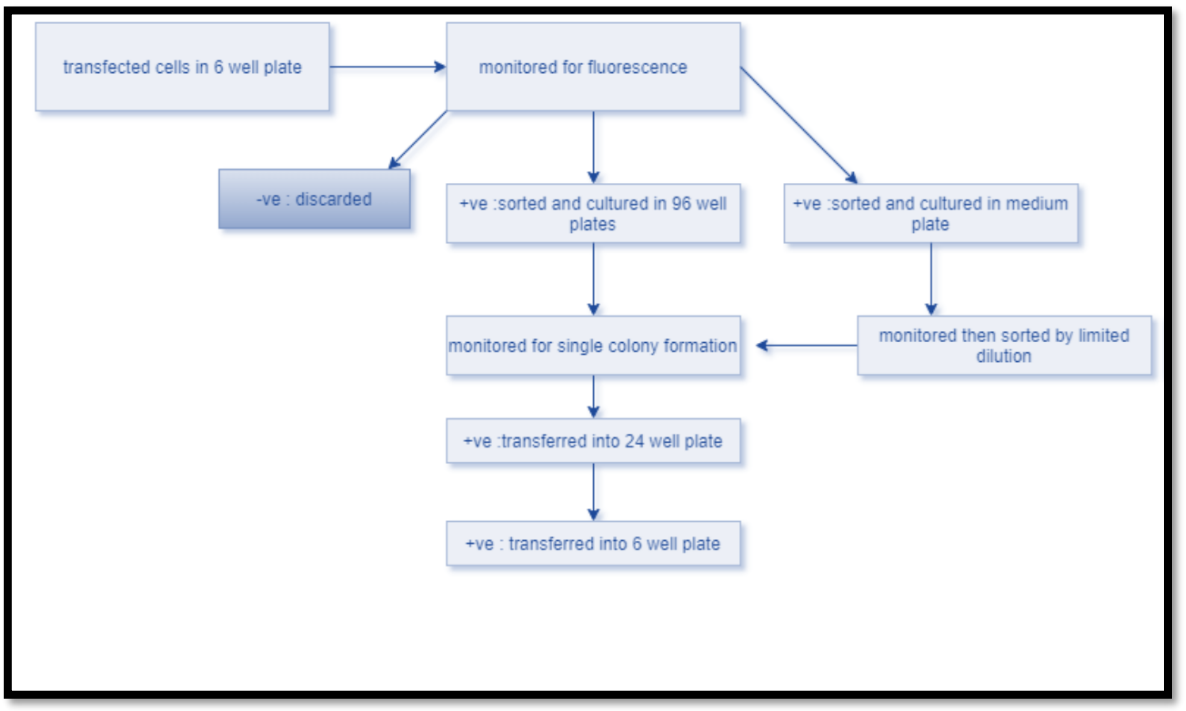

Figure 2.6. The flowchart illustrates the stages of cell transfection. After transfecting the cells, they will be monitored under a fluorescent microscope. Afterwards, they will be sorted using a FACS machine. Cells demonstrating no fluorescence will be discarded. Positive sorted cells will be cultured in adequate number of 96 well plates and one medium sized medium culture plate. Cells will be monitored under a regular microscope for colony formation. Afterwards, the colonies will be cultured in 24 well plates then 6 well plates for further analysis.

2.5 *In vitro* tests for malignant characteristics

2.5.1 Proliferation assay

A proliferation assay was utilised to test the effect of gene knock out on the rate of proliferation of the prostate cancer cell. The number of cells at various experimental time points was determined by analysing cell viability, which was determined by measuring cell metabolic activity using a Resazurin test kit (Thermofisher, UK) following the manufacturer's instruction. This test kit was specifically designed for detecting cell viability and death. Once the resazurin compound (a blue, non-fluorescent compound) reaches living cells, it is chemically reduced to red resorufin in the cytosol. The chemical reducing process is maintained in living cells. The colour change caused by this reduction activity is proportional to the number of cells that are metabolically active. This leads to a change in colour that can be measured quantitatively by measuring the absorbance of the cells with fluorescence plate readers to accurately quantitate the cell viability. Due to the fact that dead cells cannot diminish the resazurin, the colour change occurred only in active cells. Thus, the number of living cells can be quantitated by measuring their absorbents at specific wavelength of 570nm. We used the PrestoBlue® Cell Viability Reagent (Invitrogen, USA) kit to quantitate the live cells. Using this time-saving viability reagent kit, accurate results can be obtained in as little as ten minutes after reagent administration.

The assay was carried out on a 96-well plate (corning™), with cells (22Rv1, DU145 parents cells and their 100% gene knockout-derivatives) growing in separate wells for 6 days.

Every day, the PrestoBlue® reagent was applied to wells and incubated for two hours in a cell culture incubator. The absorbance at 570 nm was measured using a spectrophotometer (Labtech, UK), and the absorbance at 600 nm was measured and utilized as a baseline wavelength.

The assay was performed in triplicate, with two controls: parental cells growing in the wells, and wells containing only growth media with no cells.

2.5.2 Motility assay

Also known as wound healing or scratch assay, this assay is utilised to evaluate the effect of a gene knockout on the ability of cells to migrate. Cell migratory behaviour was evaluated in this experiment using Ibidi culture-Insert (Ibidi™, Germany). These insertions comprise two cell culture reservoirs separated by a wall; once a cell suspension is introduced to the reservoirs, cell growth is observed. The insert will then be withdrawn following cell attachment, resulting in a gap of 500 μm. The capacity of cells to migrate is determined by the rate of wound healing.

After reaching a confluency of 70%-80%, Cell suspension was made as stated in the cell culture section, and 70 μl of suspension was carefully added to each well of cell cultures, followed by at least 24 hours of incubation in a humidified cell culture incubator at 37 °C and 5% CO_2. After allowing cells to reach full confluence and forming a complete monolayer, the insert was carefully removed without disrupting the cell layer using sterile tweezers. The dish was examined under a microscope and photographs were taken at various time intervals to

determine cell migration based on the diameters of the closing gaps. The photos were captured using a microscope and analysed quantitatively using ImageJ software.

2.5.3 Invasion assay

The invasion assay was used to determine cells' capacity to invade the extracellular matrix. This was accomplished with the aid of a Boyden chamber apparatus. It comes in the form of chambers with plates and inserts, the latter of which has a membrane with an 8µm pore size and a Matrigel basement membrane matrix. Cells were introduced in the top chamber and their capacity to migrate to the bottom compartment was determined. Through Matrigel holes, invasive cells were able to detach and invade; however, non-invading cells were blocked by the pores. The assay's duration takes about 24 hours including staining.

Chambers were pre-warmed on the day of the test by adding warm medium and placing them in a cell culture incubator set to 37°C for two hours. The medium was then cautiously aspirated. In the lower chamber, medium containing FBS was introduced; the FBS acts as a chemoattractant. A cell suspension containing $1.25x10^5$ cells/ml was transferred to the upper chamber along with serum-free media and cultured for 22 hours in a cell culture incubator. The following day, cells that did not penetrate the membrane were gently scraped out of the top chamber with a cotton swab; invaded cells on the other side of the membrane were stained with crystal violet. Under a microscope, the invading cells were counted (EVOS, Thermo Scientific, UK). For cell quantification analysis, nine random fields were counted.

2.5.4 Soft agar assay

To analyse the cells' anchorage-independent growth, the soft agar assay was employed to determine the effect of the gene knockout on the cells' colony forming capacity (as an indicator of tumorigenicity) in soft agar.

The Cell Transformation Assay Kit-Colorimetric (Abcam Cat No. ab235698) was used to perform cell transformation assays in prostate cancer cells (22RV1, DU145), following the instructions of the manufacturer. Two layers of agarose (base and top layer) were prepared as instructed. Prior to the experiment, we generated a cell dose curve by serially diluting the cells (2-fold) and incubating them for 4 hours at 37°C in WST working solution. Following that, using linear regression on SPSS™ (SPSS Inc., Chicago, IL., USA), the absorbance at 450nm was obtained and the cell-dose curve was constructed ($y = \alpha x + \beta$). To conduct the experiment, $2.5x10^4$ cells per sample were blended with the top agarose layer in 10x DMEM solution and seeded in triplicates alongside blank wells in a 96-well plate. After plating the cells for 7 days at 37°C, colony formation was evaluated. The cells were photographed in the microscope after 7 days. The cells were then treated for 4 hours at 37°C in WST working solution. A plate reader was used to determine the absorbance at 450nm. To assess the result, the average value of the blank wells was subtracted from all experimental condition values. The final number of transformed cells was then calculated by relating the corrected data into the pre-experiment cell-dose curve. In this assay two types of controls were used: wild type cells grown in the same condition and wells containing media but no cells.

2.6 In vivo work

2.6.1 Nude mouse tumorigenicity assay

To test the effect of the *PPARγ* gene knockout on tumorigenicity in vivo, Du145 parental cells and Du145-PPARγ-KO cells were transfected with the pGL4.50 [*luc2*/CMV/Hygro] vector to establish stable transfectants expressing strong bioluminescence signals. Individual colonies were isolated by ring cloning and 3 colonies that stably-expressed the highest bioluminescence signals were identified using D-luciferin (Promega) with a Varioskan Flash Reader (Thermo Scientific). A number of colonies expressing strongest signals from both the parental Du145 and the Du145-PPARγ-KO cells were selected by the relative light units. The colony expressing the strongest signal from each original cell line was identified and used for further test in the nude mouse model.

Two groups of nude mice were used, each group contained five mice, the first group is the wild type group, and the other is the knocked-out group. Prior to the procedure, 8-10-week old male Balb/c nude mice were analgised with Novalgin and then maintained anaesthetically with isofluorane. The mouse was immobilised in the supine position using surgical adhesive tape. The lower abdomen was disinfected with 10% povidone-iodine, and scissors were used to make a peritoneal incision approximately 1.5cm superior to the external genitalia. The urinary bladder was externalised using tissue forceps after being elevated as a yellow-light spherical organ. Two separate lobes of the prostate gland were positioned just beneath the bladder (left and right). Suspension of Du145-luc and Du145-ko-luc cells (5×10^5) in 30μL PBS were

injected orthotopically into the prostate glands of two groups of nude mice, and a tiny bubble was noticed in the prostate. Sutures were used in two layers to close the peritoneum and skin using 6.0 absorbable vicryl monofilament. The mouse was analgised subcutaneously with Novalgin following surgery. All animal work (irrespective of the experimental sites) was conducted in accordance with Cancer Research UK Guidelines under Home Office Project (PPL No. P3CDF5A55 to Professor YK).

2.6.2 Bioluminescence imaging of mice

The IVIS imaging technology (Perkin Elmer) was used to image mice. We dissolved 15mg/ml potassium Dluciferin (Promega) in PBS and filtered the solution using a 0.2m filter. All mice were anaesthetized with isoflurane and subcutaneously injected with 150mg/kg Dluciferin. After 15 minutes, they were imaged after a two second exposure. Following D-luciferin injection, tumour loci were monitored weekly using the IVIS system. Mice were maintained sedated in the IVIS imaging chamber using isoflurane administered by nasal cones. Following the acquisition of photographic photographs of mice, autoexposure time was used to acquire bioluminescent images. The IVIS Living Image Software (Xenogen) was used to superimpose the bioluminescent images, and the measurements were made in terms of total photons per second (p/s) inside distinct defined region of interest (ROI). A manually formed ROI around the signal was used to determine the signal's strength.

2.7 Data analysis

The following software was used to analyse the data in this work: Microsoft Excel, ImageJ, and Statistical Package for Social Sciences (SPSS). In all statistical tests, the p value < 0.05 was regarded as significance. In this work Student t-test was used to assess the experiment results. This test is a commonly used statistical method for data analysis. When the variables have a normal distribution, it compares the means of two groups [225]. In this work, Student's t-test was employed to compare the results obtained from the experimental group and the control group in western blot, proliferation, invasion, motility assays, soft agar and *in-vivo* assay.

CHAPTER THREE

Result-1: Editing *PPARγ* gene in prostate cancer cells

In order to assess the possible functional role of PPARγ in promoting malignant progression in prostate cancer cells, and to test whether it can be utilised as a pharmacological target, gene editing technique CRISPR/CAS9 was used to knock out the *PPARγ* gene from the genome of the prostate cancer cells to determine the effect of diminished PPARγ expression on tumorigenicity. To further validate the knockout, western-blot immunodetection and sanger sequencing is performed.

3. Gene editing

Crispr/cas9 has recently emerged as an effective state-of-the-art gene editing technology, that can produce reliable, robust and reproduceable outcome. As discussed previously, PPARγ1 is highly expressed in prostate cancer cell lines, unlike PPARγ2 which has been proven not to be expressed in PCa, I have targeted the PPARγ1 gene in this work. Crispr/cas9 technique was used to successfully knock-out PPARγ gene from 22Rv1 and Du145 prostate cancer cells. The gRNA was obtained from (Life Technologies, UK), and the knock-out procedures were carried out according to the manufacturer's instructions in the official protocol, as detailed in the methodology.

Analyses of the sequences were performed to determine which included the altered genomic material. The selected sequence was verified to choose the one with the edited genomic material. The chosen sequence is shown in figure 3.1. Afterwards, it was utilised to transfect the moderately malignant prostate cancer cell 22Rv1 and highly malignant Du145 to knockout the PPARγ gene. To achieve the knock-out, three sgRNA's were selected as mentioned in the

methodology, Figure 3.2 represents localization of guide sequence Three guides were screened to identify the one that is efficiently active, which include:

1- sgRNA1: GAGCTGATCCCAAAGTTGGT

2- sgRNA2: TTCCATTACGGAGAGATCCA

3- sgRNA3: CTCCGTGGATCTCTCCGTAA

AAAGATTTTGGGTAGTTTGCAGTTGTAAATTATGTTTTAAAATGGACTATCATAT
GCTTACCGTAACTTGAAAGTATTTCGATTTCTTGGCTTTATATATCTTGTGGAAAG
GACGAAACACCG**GAGCTGATCCCAAAGTTGGT**GTTTTAGAGCTAGAAATAGCA
AGTTAAAATAAGGCTAGTCCGTTATCAACTTGAAAAAGTGGCACCGAGTCGGTG
CTTTTTTGTTTTAGAGCTAGAAATAGCAAGTTAAAATAAGGCTAGTCCGTTTTTA
GCGCGTGCGCCAATTCTGCAGACAAATGGCTCTAGAGGTACCCGTTACATAACTT
ACGGTAAATGGCCCGCCTGGCTGACCGCCCAACGACCCCCGCCCATTGACGTCA
ATAGTAACGCCAATAGGGACTTTCCATTGACGTCAATGGGTGGAGTATTTACGGT
AAACTGCCCACTTGGCAGTACATCAAGTGTATCATATGCCAAGTACGCCCCCTAT
TGACGTCAATGACGGTAAATGGCCCGCCTGGCATTGTGCCCAGTACATGACCTTA
TGGGACTTTCCTACTTGGCAGTACATCTACGTATTAGTCATCGCTATTACCATGGT
CGAGGTGAGCCCCACGTTCTGCTTCACTCTCCCCATCTCCCCCCCCTCCCCACCCC
CAATTTTGTATTTATTTATTTTTTAATTATTTTGTGCAGCGATGGGGGCGGGGGGG
GGGGGGGGGCGCGCGCCAGGCGGGGCGGGGCGGGGCGAGGGGCGGGGCGGGCC
GAGGCGAAAAGGTGCGGCGGCAGCCAATCAGAGCGGCGCGCTCCGAAAGTTTCC
TTTTATGGCGAGGCGGCGGCGGCGGCGGCCCTATAAAAAGCGAAGCGCGCGGCG
GGCGGAAGTCGCTGCGCGCTGCCTTCGCCCCGTGCCCCGCTCCGCCGCCGCCTCG
CGCCGCCCGCCCCGGCTCTGACTGACCGCGTTACTCCCACAGTGGAGCGGGCGG
GACGGCCCTTCTCCTCCGGGCTGTAATTAGCTGAACAAGAAGGTAAGGGTTTTAA
GGGAATGTTTGTTTGGTGGGGGTATTAATGTTTAATTACCTGGGAGCCCCCTGCC
GGAAAATCCCTTTTTTTCGGGTGGCCGGGGCCCCCCCGGGGCCATTAAGGGCC

Figure 3.1 Nucleotide sequence of the CRISPR nuclease plasmid starting from 5'to 3'. The red letters represent the guiding sequence. This sequence was acquired from the plasmid DNA

of a positive transformant colony and this sequencing analysis result indicated that the guide sequence is successfully inserted into the plasmid in a proper orientation.

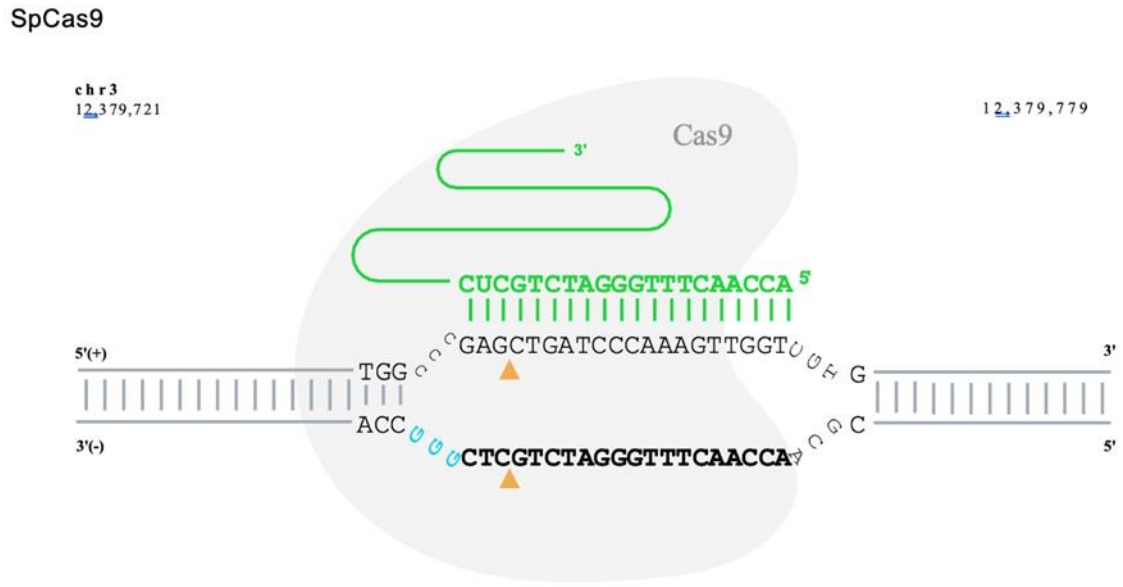

Figure 3.2 Scheme represents localization of guide sequence.

3.1 Gene editing 22Rv1 cells

3.1.1 Fluorescens monitoring of transfected 22Rv1 cells

After the transfection of 22Rv1, the transfection process was monitored through a fluorescence microscope (Zeiss Axio Observer Z.1. Zeiss, Germany). As shown in Figure 3.3, cells

harbouring the plasmid exhibited a green fluorescence due to the expressed green fluorescent protein (GFP). It is to be noted that parental 22Rv1 cells were used as controls.

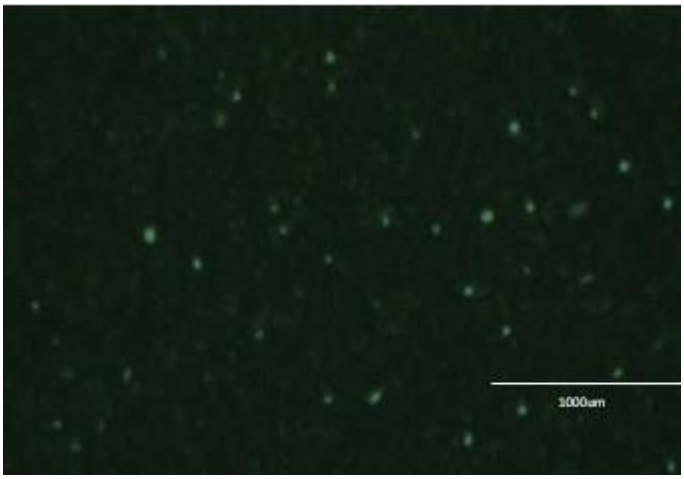

Figure 3.3 Transfection with plasmid containing GFP in 22Rv1 cells. Positively transfected cells expressing GFP appear in a green colour.

3.1.2 FACS sorting of knocked out 22Rv1 cells

After the transfection, cells were collected in 500 µl prewarmed PBS, transported to sterile FACS tubes (STEMCELL Technologies), GFP positive cells were sorted using a sterile FACS Aria II sorter (BD Biosciences) and ejected into 100 µl of complete media in each well of a 96-well plate. Figure 3.4 represents the transfection efficiency obtained from the FACS machine in 22Rv1 which is 58.6%.

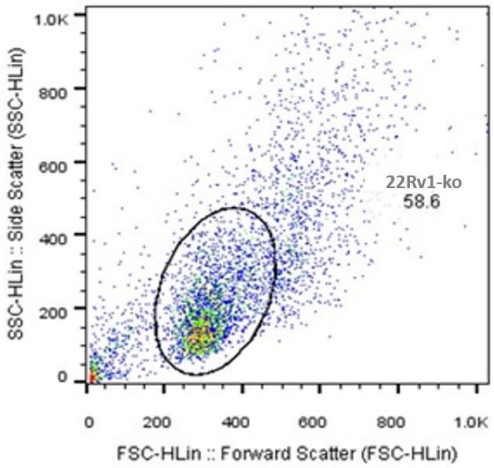

Figure 3.4 Transfection efficiency in 22Rv1. GFP-expressing vector was subject to flow cytometry analysis to green (GFP) positive cells depicting a 58.6% transfection efficiency.

3.1.3 Western blot conformation of 22Rv1 knockout cells

In order to assess the gene knockout on the protein level, western blots were performed to assess the PPARγ expression in the parental 22Rv1 cells and sub-lines of the cells sorted using the FACS machine. Only the fully knocked-out cells have been chosen for the experiments due to the large number of samples. 22Rv1 parental cells were used as control.

Two sub-cells from 22Rv1 cells that showed no PPARγ expression was chosen and named PPARγ-KO-1 and PPARγ-KO-2 respectively. As illustrated in figure 3.5.A, parental 22Rv1 cells expressed an extremely high level of PPARγ. For the sublines 22Rv1-PPARγ-KO-1 and 2 both did not express PPARγ. Figure 3.5.B illustrates a quantitative examination of the intensities of the peak regions of the bands on the blot. When the amount of PPARγ expression

in 22Rv1-PPARγ-KO-1 cells was adjusted to 1, the relative PPARγ levels of 22Rv1was 3354±66.05, which is considered to be extremely significant.

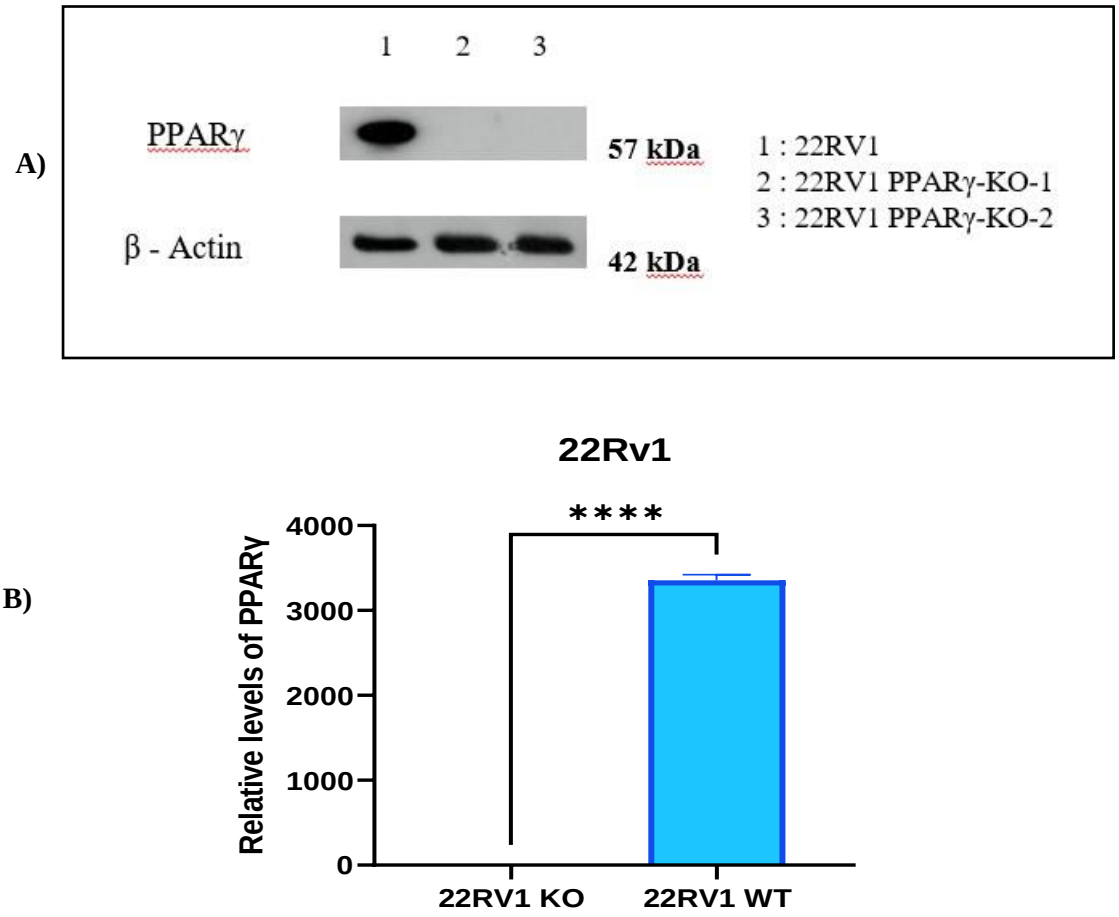

Figure 3.5 Detection of PPARγ in parental 22Rv1 cells. A) Western blot of PPARγ, B) Quantitative analysis of the relative levels of PPARγ in control and KO cells. Results were generated from three different measurements (Mean±SD).

3.1.4 Sanger sequence conformation of knockout 22Rv1 cells

To further confirm the knock-out verification of PPARγ from 22Rv1 cells, samples from 22Rv1-PPARγ-KO-1 and 2 colonies was sent to GENEWIZ for PCR and sanger sequencing; the genomic analysis findings are provided below figure 3.6. The PCR was performed on a lysate of the prostate cell line colonies, which had the greatest decrease in PPARγ expression, as shown in figure 3.5.A . The firm supplied primers (not shared with consumer for commercial reasons). The amplicons are then subjected to Sanger sequencing using the same primers that were used to create them.

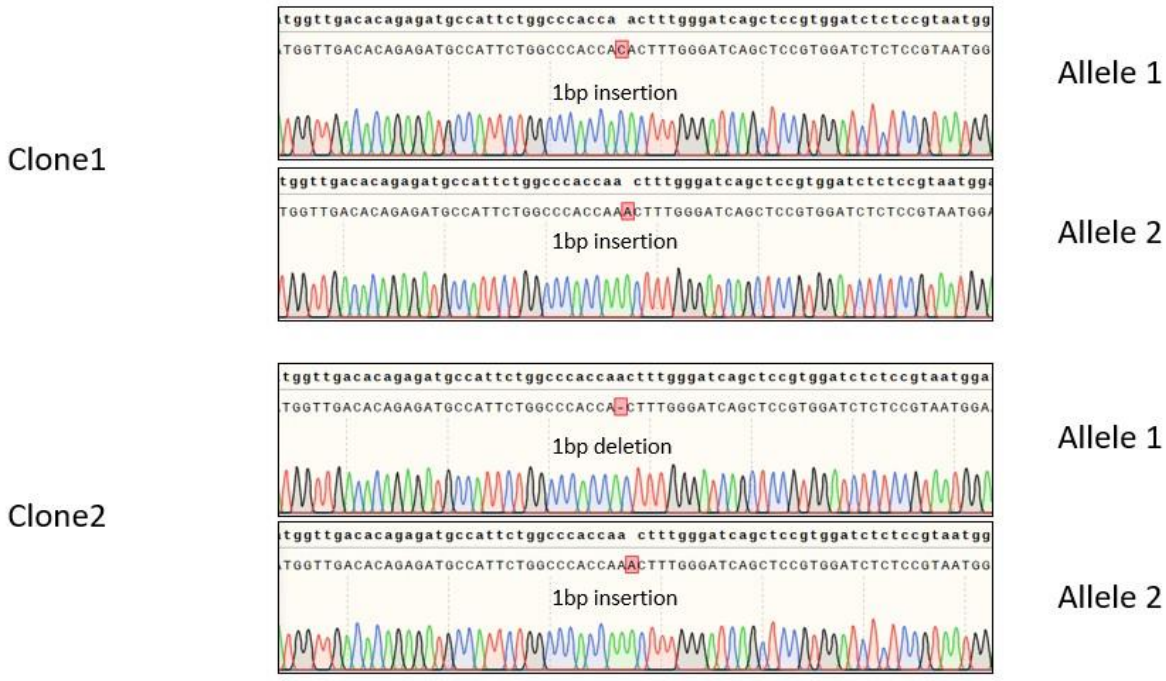

Figure 3.6 Sanger sequencing results of ko cells: Sanger sequence data for 22Rv1-PPARγ-KO-1 and 2 colonies shows a 1bp insertion in each allele of clone 1 and clone 2.

3.2 Gene editing Du145 cells

3.2.1 Fluorescens monitoring of transfected Du145 cells

After the transfection of Du145, The transfection process was monitored through a fluorescence microscope (Zeiss Axio Observer Z.1. Zeiss, Germany). As shown in Figure 3.7, cells harbouring the plasmid exhibited a green fluorescence due to the expressed green fluorescent protein (GFP). It is to be noted that parental Du145 cells were used as controls.

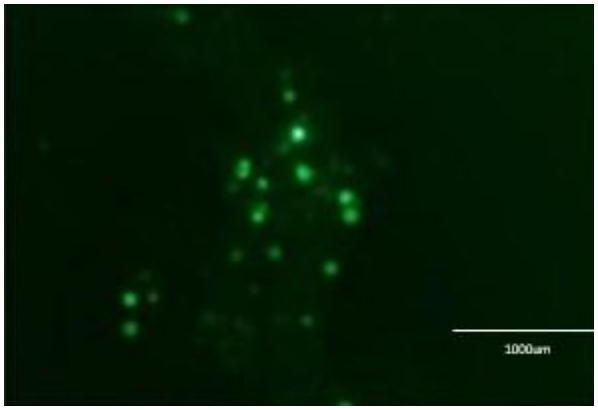

Figure 3.7 Transfection with plasmid containing GFP in DU145 cells. Positively transfected cells expressing GFP appear in a green colour.

3.2.2 FACS sorting of knocked out Du145 cells

After the transfection, cells were collected in 500 µl prewarmed PBS, transported to sterile FACS tubes (STEMCELL Technologies), GFP positive cells were sorted using a sterile FACS Aria II sorter (BD Biosciences) and ejected into 100 µl of complete media in each well of a 96-

well plate. Figure 3.8 represents the transfection efficiency obtained from the FACS machine in Du145 which is 86.1%.

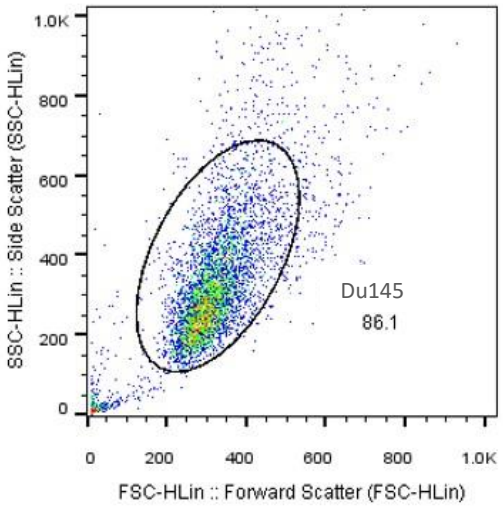

Figure 3.8 Transfection efficiency in Du145. GFP-expressing vector was subject to flow cytometry analysis to green (GFP) positive cells showing a 86.1% transfection efficiency.

3.2.3 Western blot conformation of Du145 knockout cells

In order to assess the gene knockout on the protein level, western blots were performed to assess the PPARγ expression in the parental 22Rv1 cells and sub-lines of the cells sorted using the FACS machine. Only the fully knocked-out cells have been chosen for the experiments due to the large number of samples. It is to be noted that parental Du145 cells were used as controls.

As illustrated in Figure 3.9.A, parental DU145 cells expressed an extremely high level of PPARγ. For the sublines DU145-PPARγ-KO-1 and 2 both did not express PPARγ. Figure 3.9 B illustrates a quantitative examination of the intensities of the peak regions of the bands on the blot. When the amount of PPARγ expression in DU145-PPARγ-KO-1 cells was adjusted to 1, the relative PPARγ levels of DU145 was 1177±83.44, which is considered to be extremely significant.

A)

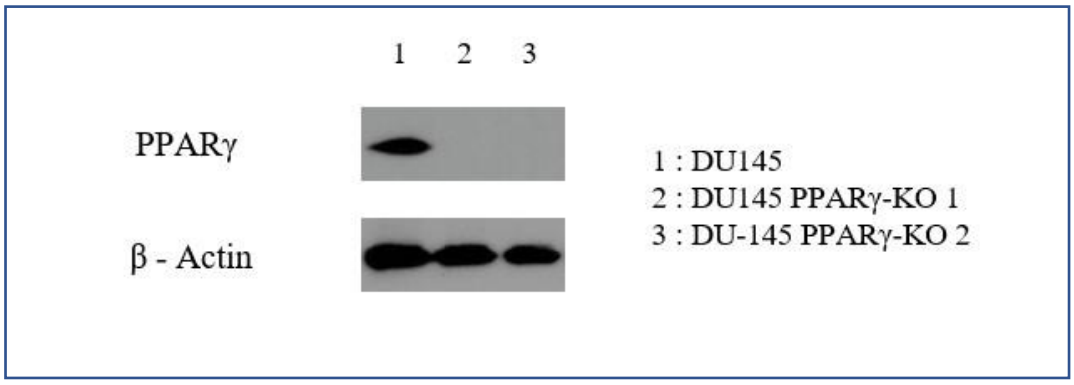

B)

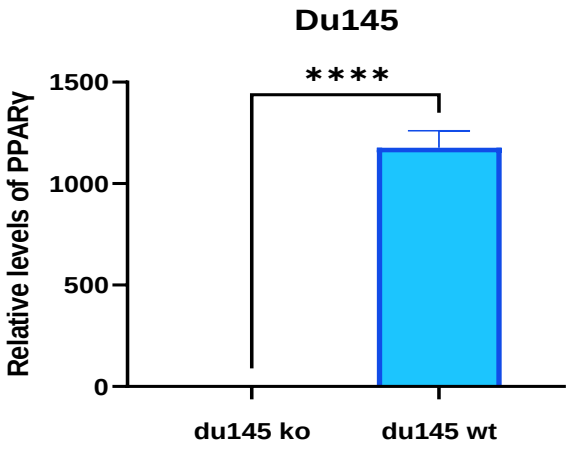

Figure 3.9 Detection of PPARγ in parental Du145 cells. A) Western blot of PPARγ, B) Quantitative analysis of the relative levels of PPARγ in control and KO cells. Results were generated from three different measurements (Mean±SD).

3.2.4 Sanger sequence conformation of knockout Du145 cells

To further confirm the knock-out verification of PPARγ from Du145 cells, samples from Du145-PPARγ-KO-1 and 2 colonies was sent to GENEWIZ for PCR and sanger sequencing; the genomic analysis findings are provided below figure 3.10. The PCR was performed on a lysate of the prostate cell line colonies, which had the greatest decrease in PPARγ expression, as shown in figure 3.9.A. The firm supplied primers (not shared with consumer for commercial reasons). The amplicons are then subjected to Sanger sequencing using the same primers that were used to create them.

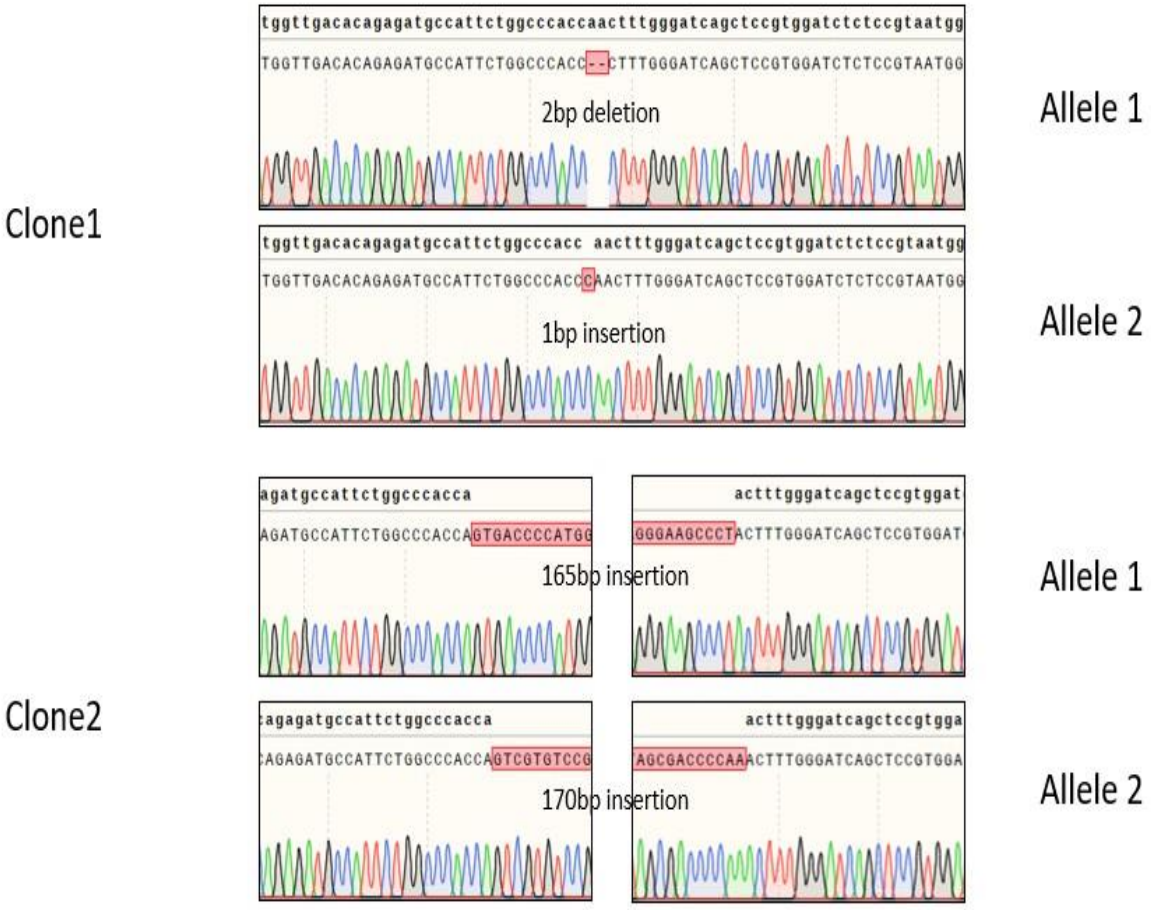

Figure 3.10 Sanger sequencing results of ko cells: Sanger sequence data for DU145-PPARγ-KO-1 and 2 colonies shows a 2bp deletion in allele 1 and 1bp insertion in allele 2 of clone 1, a 165bp and 170bp insertion in allele 1 and allele 2 of clone 2 respectively.

3.3 Discussion

In order to assess the possible suppressive effect of PPARγ in both androgen-dependant and androgen-independent cancer cell lines, we edited the PPARγ gene and successfully produced a full bi-allelic deletion both 22Rv1 and Du145 prostate cancer cells with the

CRISPR/Cas9 method. When the sub-lines eatablsihed from individual knockout clonies were subjected to further verifications with Western blot analyis, the PPARγ bands were not detectable in the knockout cell lines, but it was highly expressed in the parental cells (Figures 3.5 , 3.9). Further analysis with Sanger sequencing technique on both PPARγ-KO-sublines established from 22Rv-1, one subline gained an one base-pair insertion in each of both alleles. This inserted one pair of nucleotide produced a shift in all coding codens of this protein and thus completely eliminated the PPARγ expression. When Sanger sequencing analysis was performed to assess the nucleotide sequence of 22Rv1-PPARγ-KO-2, it was revealed that one bp was deleted in one allele, and one bp was inserted into the other allele of the PPARγ gene (Figure 3.6). Sanger sequencing analysis was also performed to check the nucleotide sequences of the PPARγ gene Du145-KO lines and the result obtained was different from the analysis of 22Rv-1 sublines. While a 1-bp insertion and a 2-bp insertion was found in allele 1 and allele 2 in Du145-PPARγ-KO-1 respectively; a 165-bp insertion and a 170-bp insertion was detected in allele 1 and allele 2 in Du145-PPARγ-Ko-2 respectively (Figure 3.10). These sequencing analysis results, combined with the Western blot analysis suggested that these bp-insertion or deletions generated by CRISR/Cas9 gene editing technique have completely altered the PPARγ translation process and led to a full 100% PPARγ suppression in both 22Rv1 and Du145 cell lines.

CHAPTER 4:

RESULT-2: THE EFFECT OF *PPARγ* GENE KNOCKOUT ON THE PROLIFERATION RATE OF THE PROSTATE CANCER CELLS

A proliferation assay was utilised to test the effect of gene knock out on the rate of proliferation of the prostate cancer cell. The number of cells at various experimental time points was determined by analysing cell viability, which was determined by measuring cell metabolic activity using a Resazurin test kit. Both 22Rv1 and Du145 parental cells were used as controls.

4.1 The effect of PPARγ knockout on the proliferation rate of 22Rv1 cells

To accurately quantitate the number of the cells in each experimental time points, the standard growth curve for both the 22Rv-KO cells was established, the relationship between the value of the light absorbent (at the wave length 570nm) and the number of the cells was plotted with linear regression and shown **Figure 4.1.**

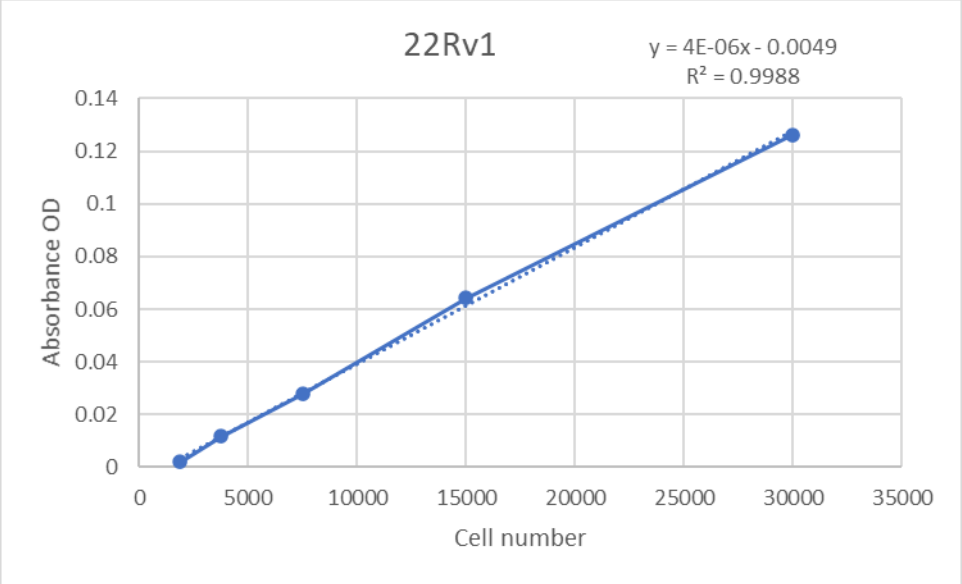

Figure 4.1. The relative curve for 22RvKO cell lines. Media absorbance is to be accredited to the line not passing through the origin. It was deducted from absorbance readings.

Proliferation assay was performed to compare the proliferation rates between 22Rv1-PPARγ-KO-1 (22Rv-KO) cells and their parental cell line 22Rv-1. During the proliferation assay, the numbers of cells were collected from different experimental time points, and were shown in **Figure 4.2.** Whereas the starting numbers of both cell lines (5000 cells) were the same, the numbers started to exhibit differences from day 2 and difference was keeping increase until the end of the experiment at day 5. Overall, the average cell number from 22Rv-KO cells was significantly lower than that from the parental 22Rv-1 cells (Student t-test, P=<0.0001).

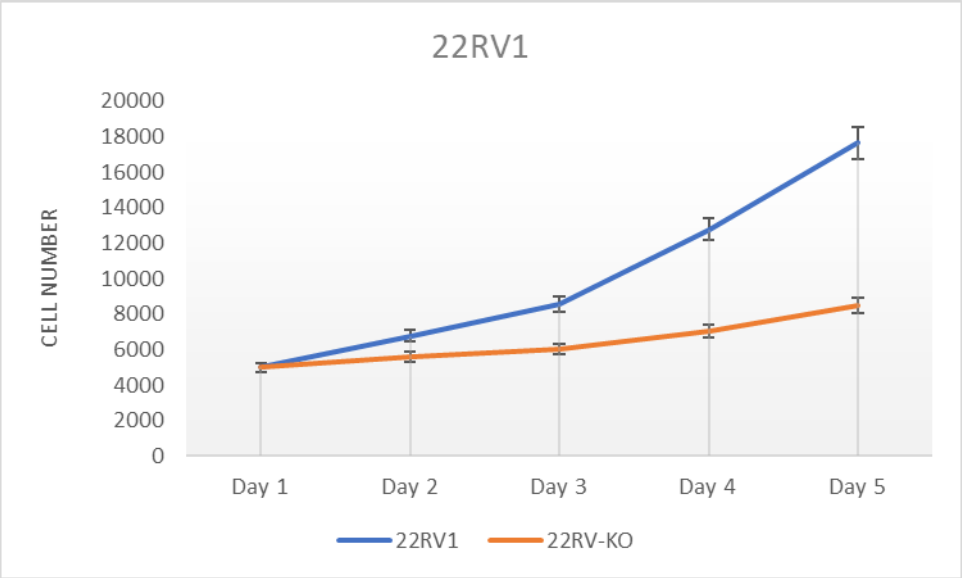

Figure 4.2 Cell proliferation rates for 22Rv-KO cells and the parental 22Rv1cells. 5000 from each cell line was cultured in triplicate in six 96 well plates and in each day one plate were removed to make cell number count. Assay was carried in triplicates for 6 days and the 2 tested cell lines were the parental 22Rv1 and22Rv-KO. The difference was assessed by Student t-test. X axis shows the time (in days), while Y axis shows cell number.

Further detailed analysis on the proliferation results (**Figure 4.3A-D**) was performed on cell numbers collected from day 2. On day 2 (Figure 4.3A), the number of 22Rv1 cells was 6782±186, the number of 22Rv-KO cells was 5610±278. Comparing with the cell number of 22Rv-1 cells, the number of 22Rv-KO cells was significantly reduced by 1.21-fold (Student t-test, $p<0.004$). On day 3 (Figure 4.3B), the number of 22Rv1 cells was 8568±220, and the number of 22Rv-KO cells was 6029±281. When comparing with the cell number of 22Rv1, the number of 22Rv-KO cells was significantly reduced by 1.42-fold (Student t-test, $P< 0.0002$). On day 4 (Figure 4.3C), the number of 22Rv1 cells was 12784 ± 445, and the number of 22Rv-KO was 7049±177. Comparing with the cell number of 22Rv1, the number of 22Rv-KO cells were significantly reduced by 1.81-fold (Student t-test, $P <0.0001$). On day 5 (Figure 4D), the number of 22Rv1 cells was 17636±507, and the number of 22Rv-KO was 8510±278. When compared with the cell number of 22Rv1, the number of 22Rv-KO cells was significantly reduced by 2.07-fold (Student t-test, $P <0.0001$).

A)

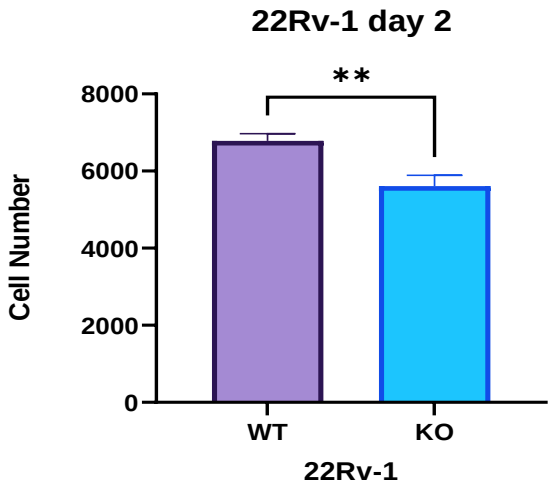
22Rv-1 day 2
**
8000
6000
4000
2000
0
Cell Number
WT
KO
22Rv-1

B)

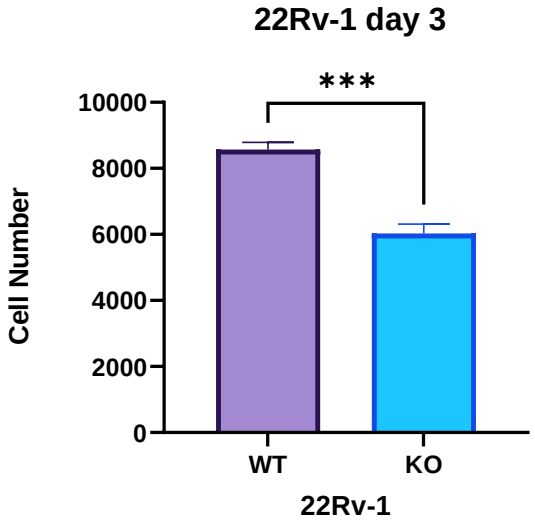
22Rv-1 day 3
***
10000
8000
6000
4000
2000
0
Cell Number
WT
KO
22Rv-1

C)

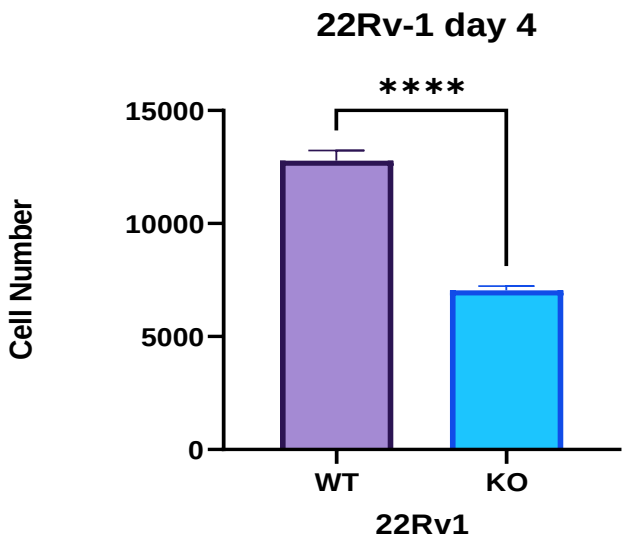

D)

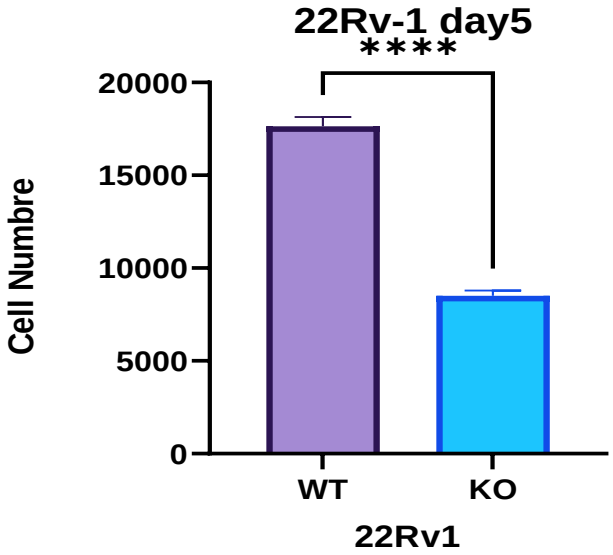

Figure 4.3 Proliferation assay of parental 22Rv1 cell line vs. 22Rv-KO on days 2 to 5.

4.2 The effect of PPARγ knockout on the proliferation rate of Du145 cells

To accurately quantitate the number of the cells in each experimental time points, the standard growth curve for both the Du145-ko cells was established, the relationship between the value of the light absorbent (at the wave length 570nm) and the number of the cells was plotted with linear regression and shown **Figure 4.4.**

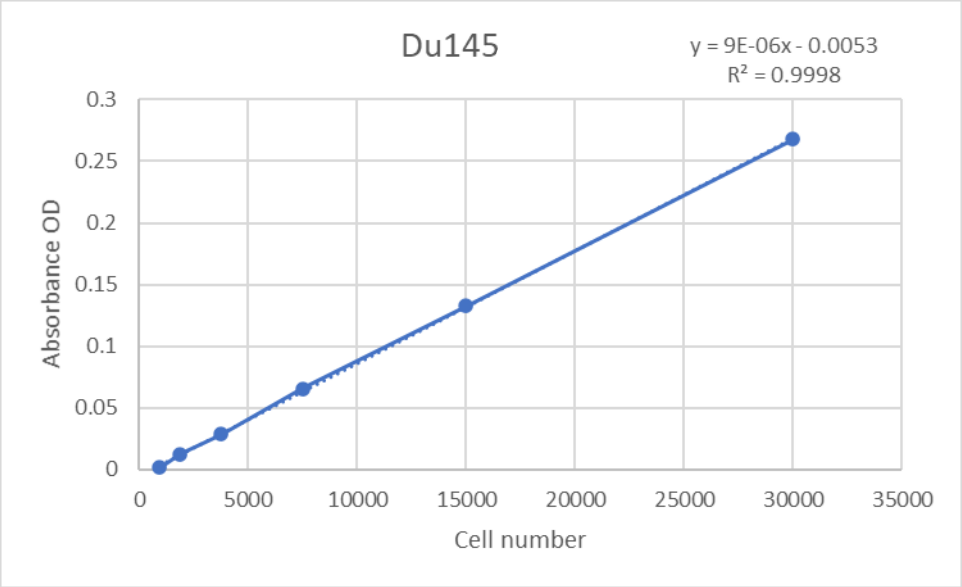

Figure 4.4 The relative curve of Du145-ko cells. Media absorbance is to be accredited to the line not passing through the origin. It was deducted from absorbance readings.

Proliferation assay was performed to compare the proliferation rates between Du145-PPARγ-KO-1 (Du145-ko) cells and their parental cell line Du145. During the proliferation assay, the numbers of cells were collected from different experimental time points, and were shown in

Figure 4.5. Whereas the starting numbers of both cell lines (5000 cells) were the same, the numbers started to exhibit differences from day 2 and difference was keeping increase until the end of the experiment at day 5. Overall, the average cell number from Du145-ko cells was significantly lower than that from the parental Du145 cells (Student t-test, P<0.0001).

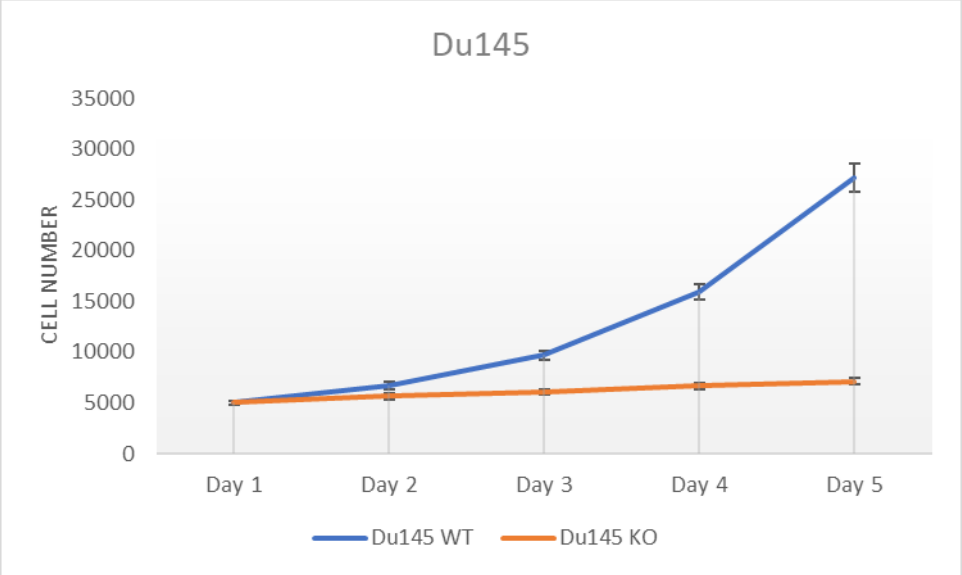

Figure 4.5 Cell proliferation assay for Du145-ko, and the parental cell Du145. Cell proliferation rates for Du145-KO cells and the parental Du145 cells. 5000 from each cell line was cultured in triplicate in six 96 well plates and in each day one plate were removed to make cell number count. Assay was carried in triplicates for 6 days and the 2 tested cell lines were the parental Du145 and Du145-KO. The difference was assessed by Student t-test. X axis shows the time (in days), while Y axis shows cell number.

Further detailed analysis on the proliferation results (**Figure 4.6A-D**) was performed on cell numbers collected from day 2. On day 2 (Figure 4.6A), the number of Du145 cells was 6717±462.6, the number of Du145-KO cells was 5638±72. Comparing with the cell number of Du145 cells, the number of Du145-KO cells was significantly reduced by 1.19-fold (Student t-test, p<0.0.02). On day 3 (Figure 4.6B), the number of Du145 cells was 9682±483, and the number of Du145-KO cells was 6065±170. When comparing with the cell number of Du145, the number of Du145-KO cells was significantly reduced by 1.60-fold (Student t-test, P< 0.0003). On day 4 (Figure 4.6C), the number of Du145 cells was 15950±66, and the number of Du145-KO was 6680±202. Comparing with the cell number of Du145, the number of Du145-KO cells were significantly reduced by 2.39-fold (Student t-test, P< <0.0001). On day 5 (Figure 4.6D), the number of Du145 cells was 27223±1078, and the number of Du145-KO was 7125±169. When compared with the cell number of Du145, the number of Du145-KO cells was significantly reduced by 3.82-fold (Student t-test, P <0.0001).

A)

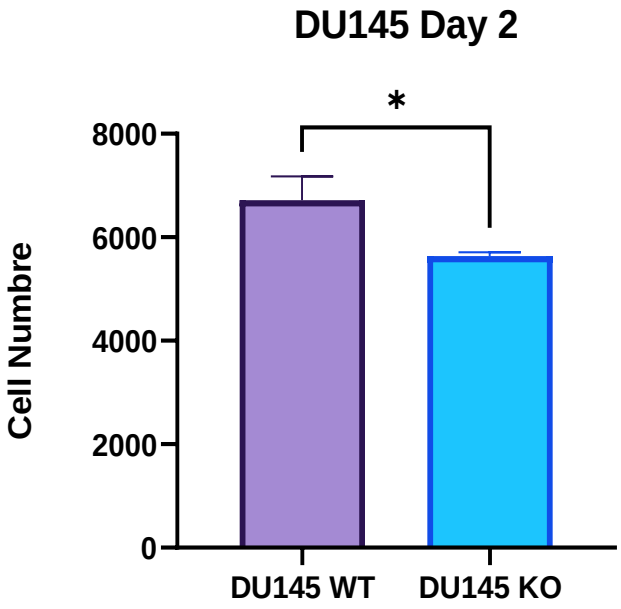
DU145 Day 2
*
8000
6000
4000
2000
0
Cell Numbre
DU145 WT
DU145 KO

B)

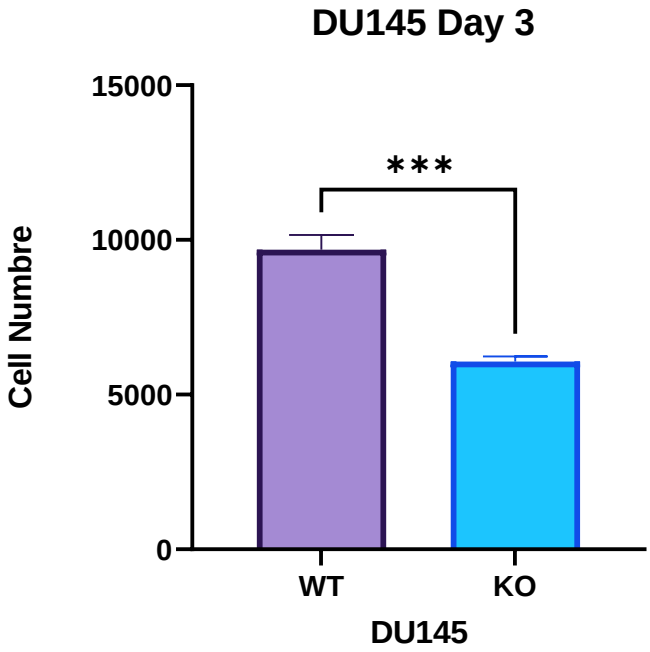
DU145 Day 3
***
15000
10000
5000
0
Cell Numbre
WT
KO
DU145

C)

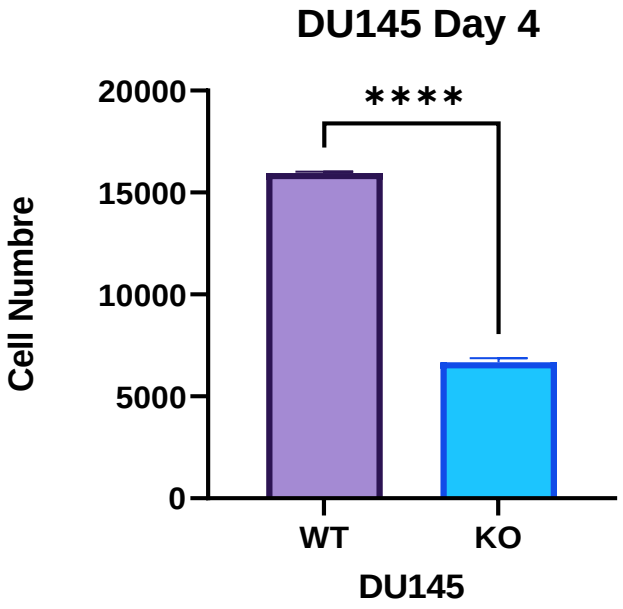

D)

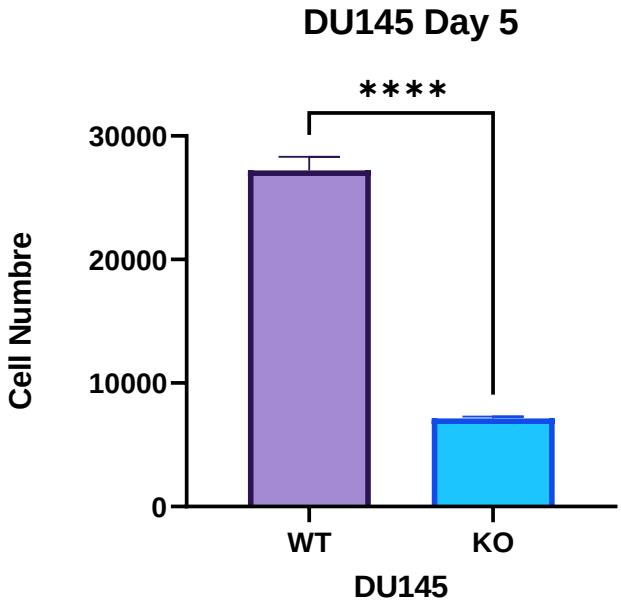

Figure 4.6 Proliferation assay of parental Du145 cell line vs. Du145-KO on days 2 to 5 of assay.

4.3 Discussion

On the fifth day of the assay of 22Rv1-ko, the cell numbers of 22Rv1-ko were significantly reduced by 2.07-fold ($P<0.0001$) when compared with the 22Rv1 control cells. Meanwhile, on the fifth day of the assay of Du145, the cell numbers of Du145-ko were significantly reduced by 3.82-fold ($P<0.0001$) when compared to the Du145 control cells. This result proves that PPARγ plays a role in the promotion of the growth of prostate cancer cells via the FABP5-PPARγ-VEGF signalling pathway as shown in our lab's previous study [191].

CHAPTER 5:

Result-3: THE EFFECT OF *PPARγ* GENE KNOCKOUT ON THE INVASIVNESS OF THE PROSTATE CANCER CELLS.

(INVASION ASSAY RESULTS)

The invasion assay was used to determine cells' capacity to invade the extracellular matrix. This was accomplished with the aid of a Boyden chamber apparatus. Both 22Rv1 and Du145 parental cells were used as controls.

5.1 Invasion assay results for 22rv1 knockout cells

For this invasion assay I chose 22Rv1-PPARγ-KO-1 referred to as (22Rv-KO) knockout clone and 22Rv1 parental cell as a control.

The invasiveness of 22rv-KO cancer cells was determined utilising invasion chambers covered with BD Matrigel with parental 22Rv1 cells as a control. both cells were cultured in serum-free RPMI 1640 media for 24 hours prior to setting up the invasion test in order to deplete the growth factors to keep them from interfering with the migration process. Cells were extracted and counted after 24 hours of deprivation to create a combination containing 5×10^4 cells in serum-free media. Chambers were rehydrated for two hours prior to loading 2.5×10^4 cells in 0.5ml media supplemented with inhibitors into each top compartment of chambers. Lower compartments were filled with routine medium (including 10% (v/v) FBS). Triplicate cell lines of each were established and the experiment was conducted for 24 hours in a humidified tissue culture incubator. Finally, residual cells in the top section were gently removed and rinsed with PBS using cotton swabs. For ten minutes, migrating cells were fixed and stained with 2% crystal violet and counted in random areas using a light microscope.

As illustrated in table 5.1, the number of invaded cells from 22Rv1 parental cell and 22Rv-KO was 73±2 and 20 ±1 respectively. When comparing the invaded cells from the KO to the parental 22Rv1, the 22Rv-KO was significantly reduced (student t-test, p <0.0001). (Figure 5.1, A and B).

Cell Line	No. of invaded Cells/ nine random locations	*P* Value
Parental 22Rv1	73	……
22Rv-KO	20	*P*<0.0001

Table 5.1 Number of invaded cells from 22Rv1 parental cell and 22Rv-KO. Cell numbers were taken from nine random locations. The results were taken from three separate experiments (Mean ± SD).

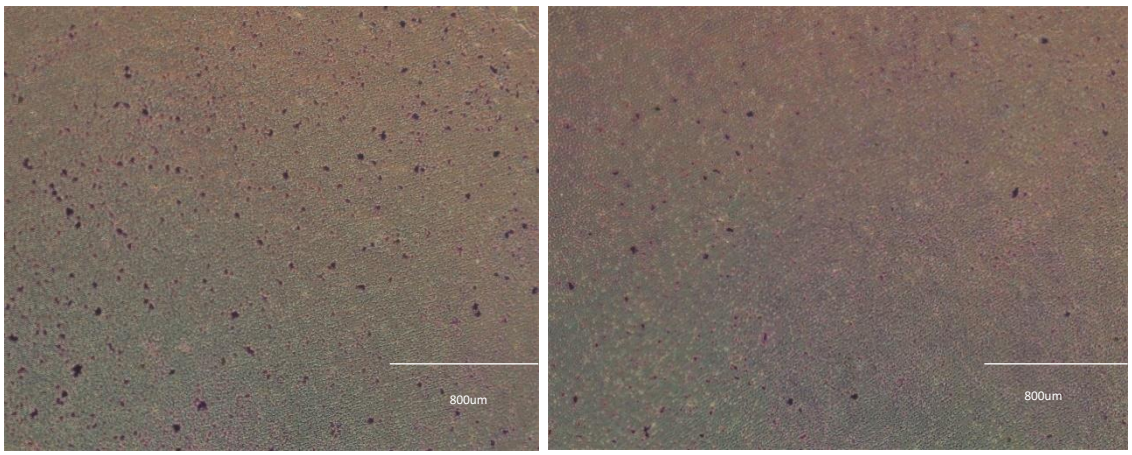

1 **2**

Figure 5.1 Number of invading cells from the control 22Rv1 (1), 22Rv-KO (2) taken from nine random locations. Results were obtained from three separate measurements (mean ± SD).

5.2 Invasion assay results for Du145 knockout cells

For this invasion assay I chose Du145-PPARγ-KO-1 referred to as (Du145-KO) knockout clone and Du145 parental cell as a control. The invasiveness of Du145-KO cancer cells was determined utilising invasion chambers covered with BD Matrigel with parental Du145 cells as a control, just as described in 5.1.

As illustrated in table 5.2, the number of invaded cells from DU145 parental cell and Du145-KO was 102±3 and 29 ±2 respectively. When comparing the invaded cells of the KO cells to the parental Du145, the Du145-KO was significantly reduced (student t-test, p <0.0001). (Figure 5.2, A and B).

Cell Line	No. of invaded Cells/nine random locations	*P* Value
Parental Du145	102	……
Du145-KO	29	*P*<0.0001

Table 5.2 Number of invaded cells from Du145 parental cell and Du145-KO. Cell numbers were taken from nine random locations. The results were taken from three separate experiments (Mean ± SD).

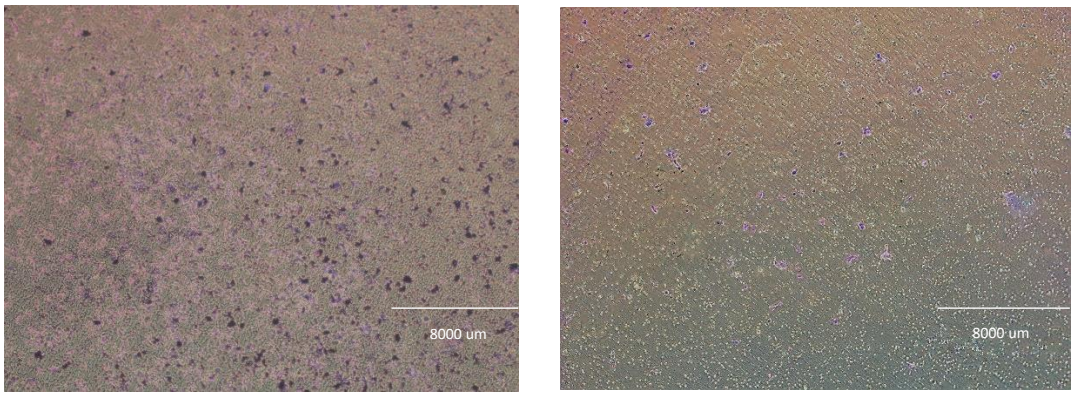

1 2

Figure 5.2 Number of invading cells from the control Du145 (1), Du145-KO (2) taken from nine random locations. Results were obtained from three separate measurements (mean ± SD).

5.3 Discussion

Analysing the invasion assay of 22Rv1-ko compared to its parental cell 22Rv1, demonstrated that cellular invasion was drastically affected by PPARγ knockout, it has produced a 72.6% decrease in invaded cells when compared to 22Rv1 control cells. Meanwhile, analysing the

invasiveness of Du145-ko compared to its parental Du145 cell demonstrated an extremely huge decrease by 71.6% in the number of the invaded cells of Du145-ko compared to parental Du145 cells. These results show that PPARγ knocked out has a great suppressive effect on tumorigenicity of prostate cancer.

CHAPTER 6

Result-4: THE EFFECT OF *PPARγ* GENE KNOCKOUT ON THE MOTILITY OF THE PROSTATE CANCER CELLS

Also known as wound healing or scratch assay, this assay is utilised to evaluate the effect of a gene knockout on the ability of cells to migrate. Cell migratory behaviour was evaluated in this experiment using Ibidi culture-Insert (Ibidi™, Germany). Both 22Rv1 and Du145 parental cells were used as controls.

6. Motility assay

To assess the functional effect of PPARγ knockout on the migratory ability of cells, motility assay was conducted, as migration is a core aspect of living cells. The capacity of cancer cells to migrate is a reliable indicator of their metastatic potential [226]. Ibidi inserts (Ibidi™, Germany) were utilized in this research to replicate the natural wound healing process. The wound area was then measured at three separate time intervals to determine the potential of parental and knocked-out cell lines to migrate. Images were taken at the beginning of the assay and then at regular intervals.

6.1 Motility assay results of 22Rv1

In this assay I studied the cell motility ability of 22Rv1-PPARγ-KO-1 (22Rv-KO), using 22Rv1 parental cell as a control. When analysing the 24 hours data, 22Rv1 demonstrated a significantly higher migration rate than 22Rv-KO cells (Student's t-test, $P < 0.0001$). These values are also the same for 22Rv1 cells at 48 and 72 hours respectively (Student's t-test,

P<0.0001). I must point that the 22Rv1 wound almost closed after 72 hours. Representative data and photos are shown in Figure 6.1 A and B.

A)

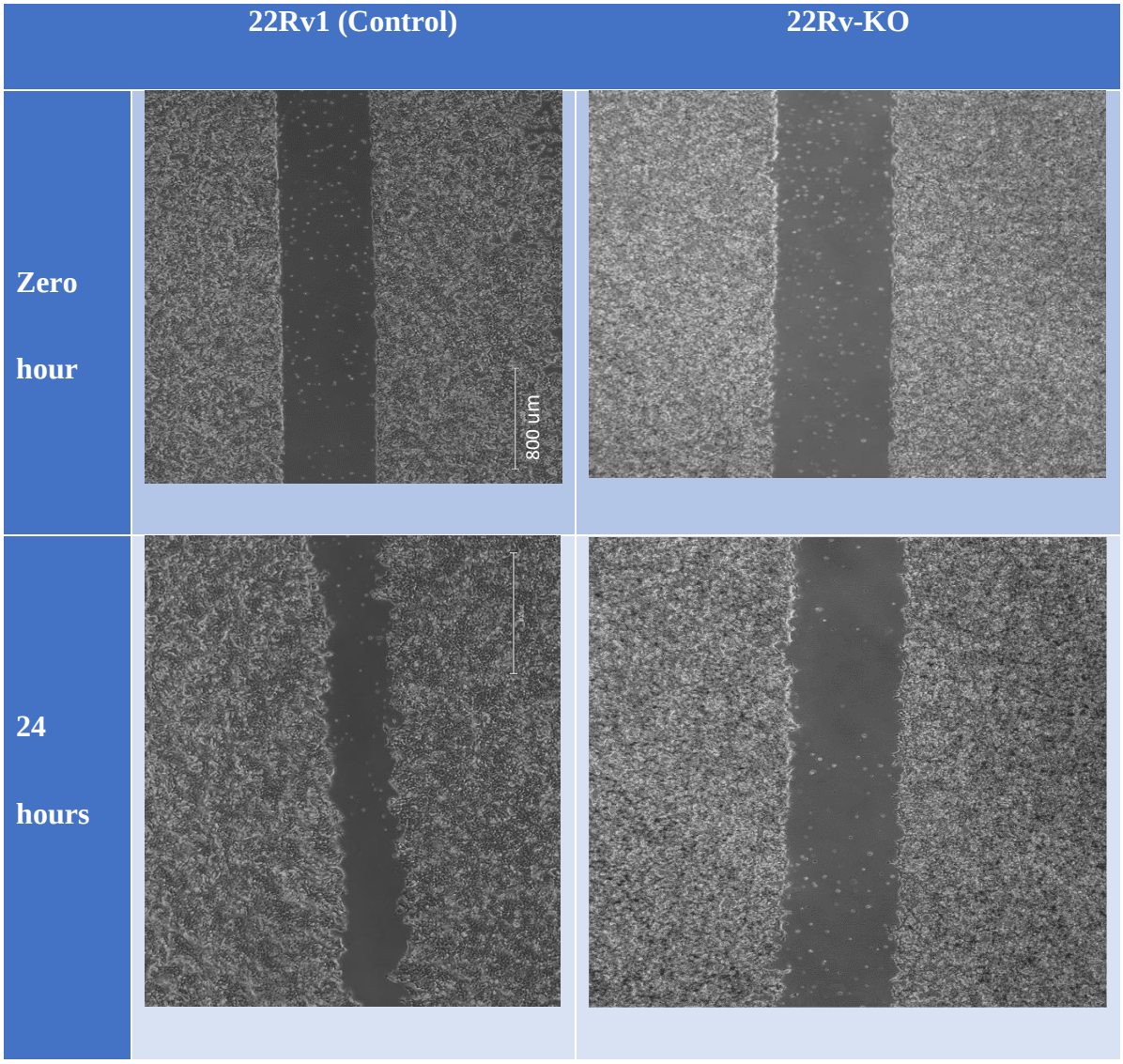

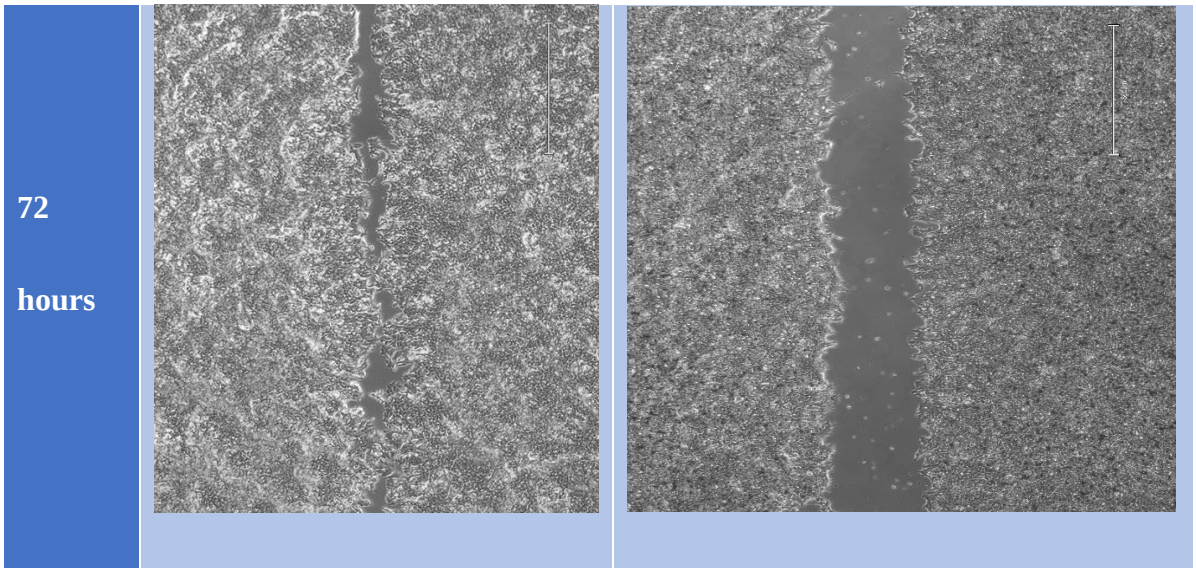
72
hours

B)

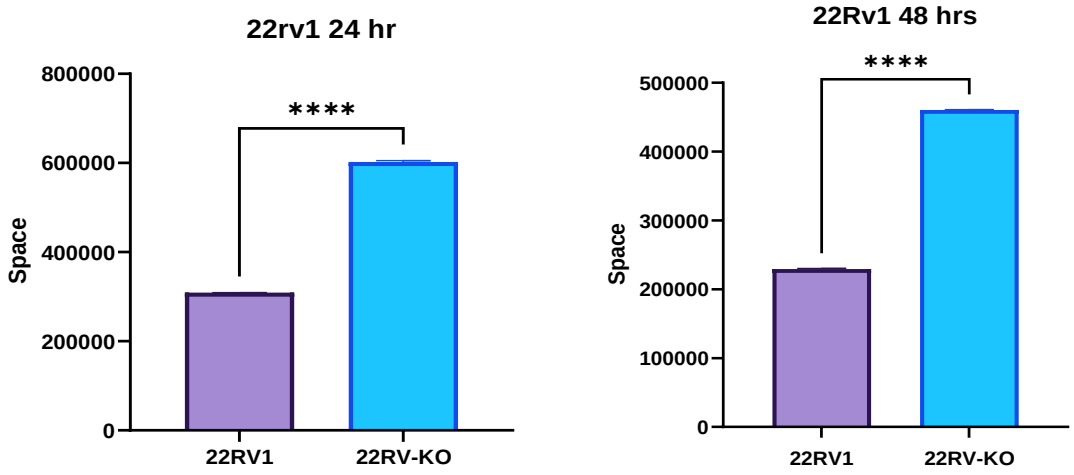
22rv1 24 hr
Space
800000
600000
400000
200000
0
****
22RV1
22RV-KO
22Rv1 48 hrs
Space
500000
400000
300000
200000
100000
0
****
22RV1
22RV-KO

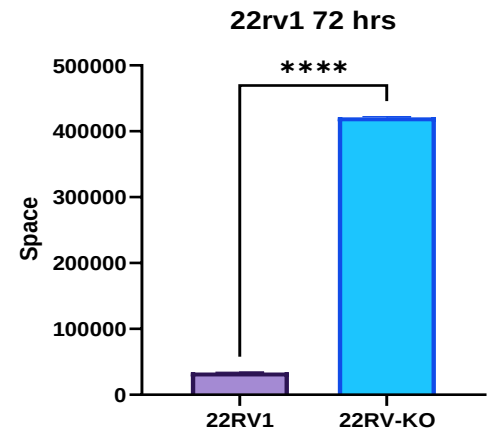

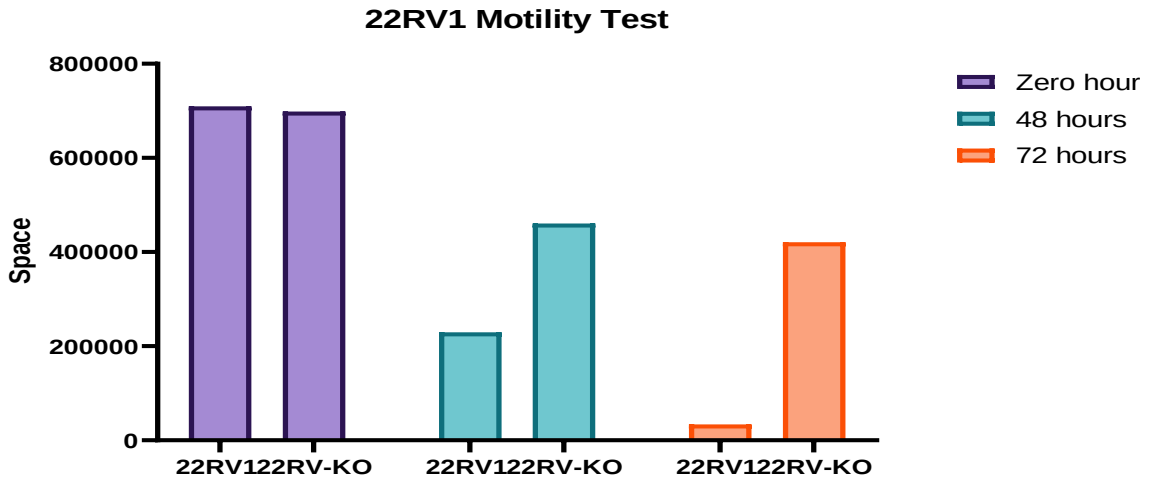

Figure 6.1. The impact of PPARγ knockout on the migration rate of 22Rv1 cells.

A) Images representing migration rate of parental and knockout cells at different time intervals (Zero, 24 and 72 hours) taken from three different experiments.

B) Quantitative assessment of cell migration at different time intervals (Zero, 24 and 72 hours).

6.2 Motility assay results of Du145:

In this assay I studied the cell motility ability of Du145-PPARγ-KO-1 (Du145-KO), using Du145 parental cell as a control. When analysing the 12 hours data, Du145 demonstrated a significantly higher migration rate than Du145-KO cells (Student's t-test, P=<0.0001). These values are also the same for Du145 cells at 24 hours (Student's t-test, P=<0.0001). I must point here that the Du145 parental cell line wound has closed in about 24 hours. Representative data and photos are shown in Figure 6.2 A and B.

A)

	Du145 (Control)	Du145-KO
Zero hour	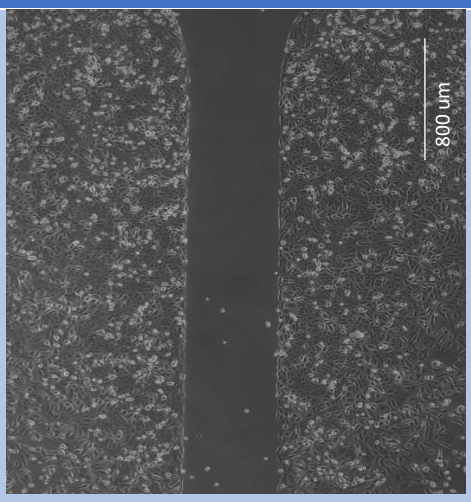	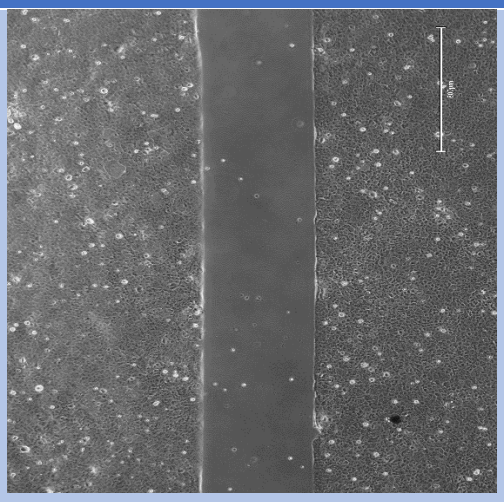
12 hours		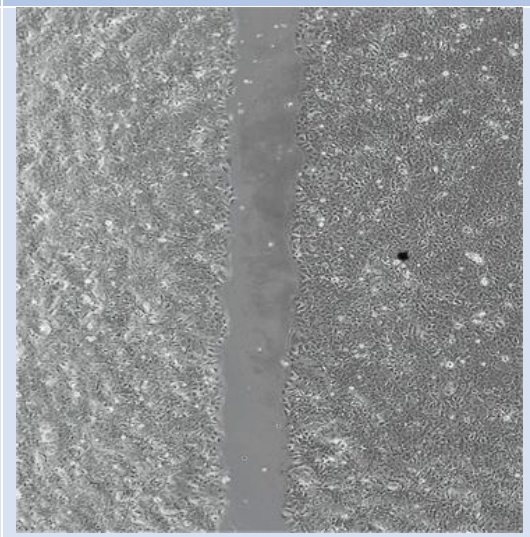
24 hours	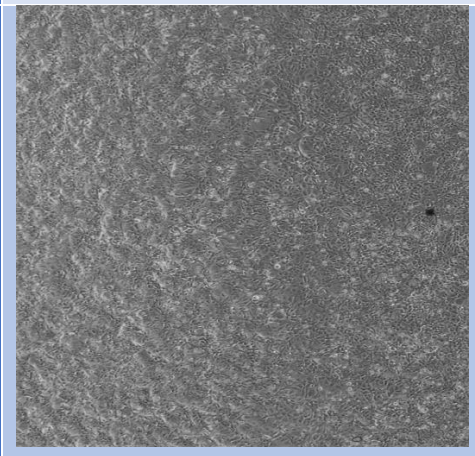	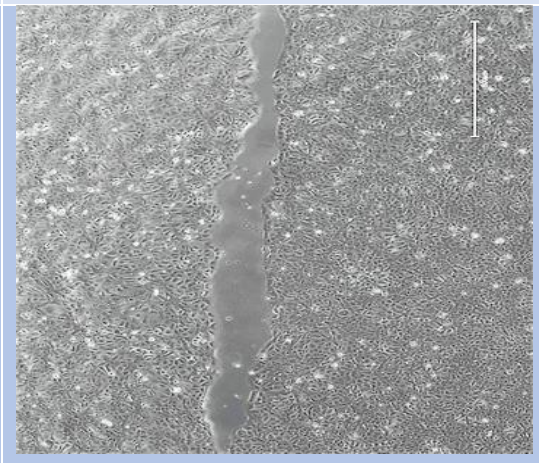

B)

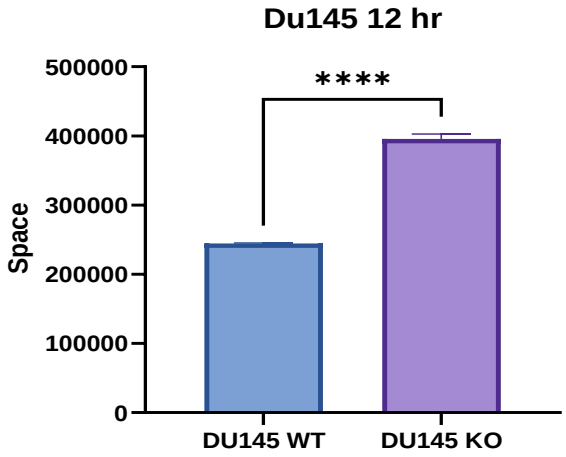
Du145 12 hr
****
500000
400000
300000
200000
100000
0
Space
DU145 WT
DU145 KO

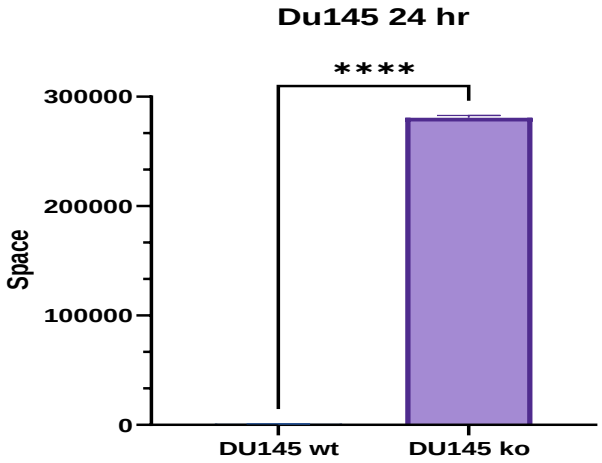
Du145 24 hr
****
300000
200000
100000
0
Space
DU145 wt
DU145 ko

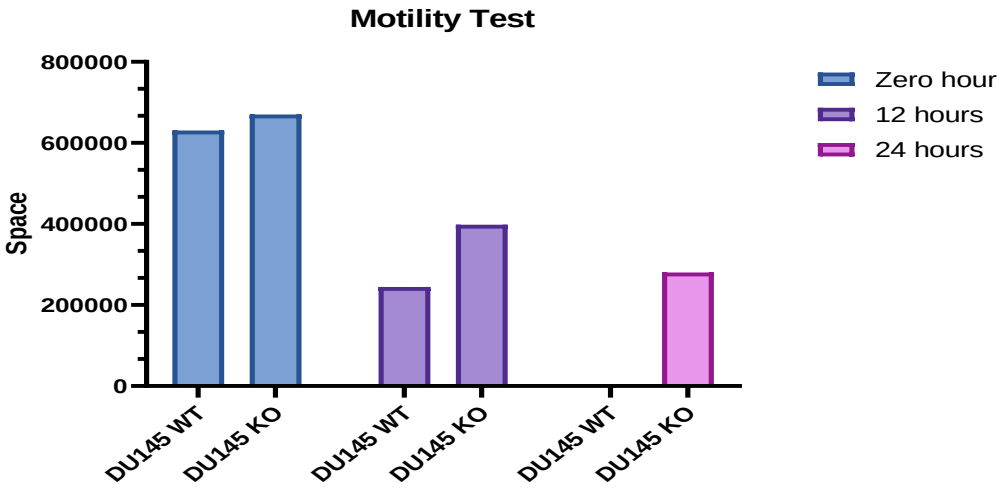
Motility Test
800000
600000
400000
200000
0
Space
DU145 WT
DU145 KO
DU145 WT
DU145 KO
DU145 WT
DU145 KO
Zero hour
12 hours
24 hours

Figure 6.1. The impact of PPARγ knockout on the migration rate of 22Rv1 cells.

A) Images representing migration rate of parental and knockout cells at different time intervals (Zero, 12 and 24 hours) taken from three different experiments.

B) Quantitative assessment of cell migration at different time intervals (Zero, 12 and 24 hours).

6.3 Discussion

Comparison of cell migration capabilities of 22Rv1-ko cells when compared to parental 22Rv1 cells, showed a highly significant migration rate of parental 22rv1 cells ($P<0.0001$) when compared to 22Rv1-ko knocked-out cells. Similarly, Du145 parental cells showed a highly significant migration rate ($P<0.0001$) when compared to Du145-ko knocked out cells. These results confirm the previous results suggesting that PPARγ knocked-out has a remarkable suppressive effect on tumorigenicity of prostate cancer.

CHAPTER 7

Result-5: THE EFFECT OF *PPARγ* GENE KNOCKOUT ON THE ANCHORAGE-INDEPENDENT GROWTH OF THE PROSTATE CANCER CELLS

To analyse the cells' anchorage-independent growth, the soft agar assay was employed to determine the effect of the gene knockout on the cells' colony forming capacity (as an indicator of tumorigenicity) in soft agar. The Cell Transformation Assay Kit-Colorimetric (Abcam Cat No. ab235698) was used to perform cell transformation assays in prostate cancer cells (22RV1, DU145). Both 22Rv1 and Du145 parental cells were used as controls.

7.1 Soft agar assay of 22Rv1 cells

To accurately quantitate the number of the cells in each experimental time points, the standard growth curve for the 22Rv1 cells was established, the relationship between the value of the light absorbent (at the wavelength 460nm) and the number of the cells was plotted with linear regression and shown **Figure 7.1.**

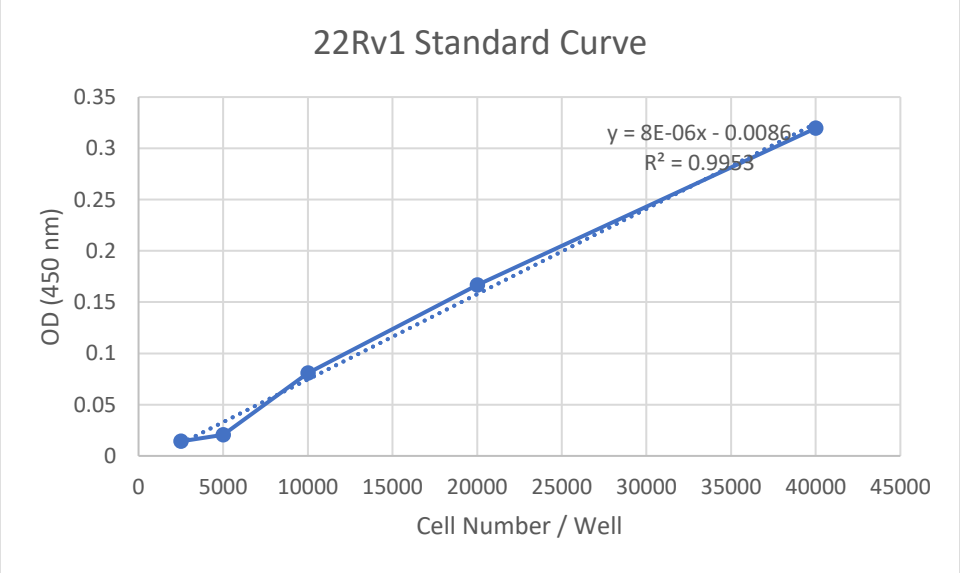

Figure 7.1. The standard curve for 22Rv1 cell lines.

To analyse the cells' anchorage-independent growth, the soft agar assay was employed to determine the effect of the gene knockout on the cells' colony forming capacity (as an indicator of tumorigenicity) in soft agar. 22Rv1 parental cell was used as a control and 22Rv-KO as a test.

After plating the cells for 7 days at 37°C, colony formation was evaluated, (Figure 7.2 A to C). On day 7, the number of 22Rv1 cells was 146706±196, the number of 22Rv-KO cells was 8907±175.8. Comparing with the cell number of 22Rv-1 cells, the number of 22Rv-KO cells was significantly reduced by 16.5-fold (Student t-test, $p<0.0001$) figure 7.3.

A) 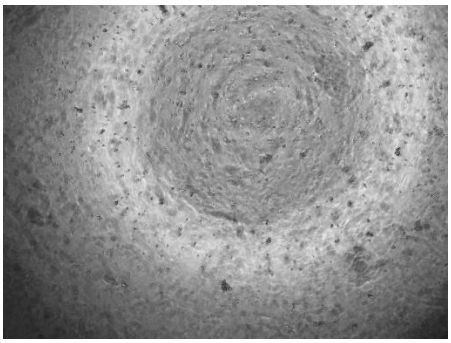 **B)** 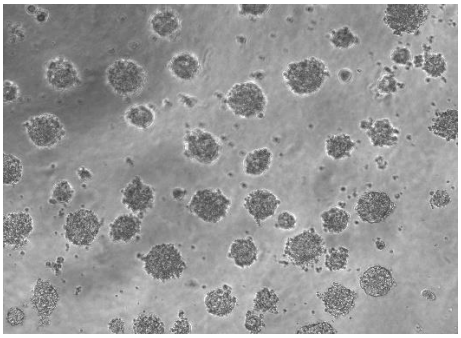

C) 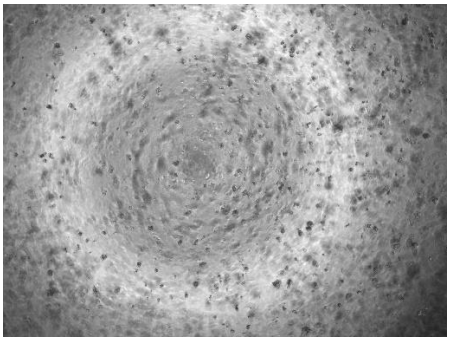 **D)** 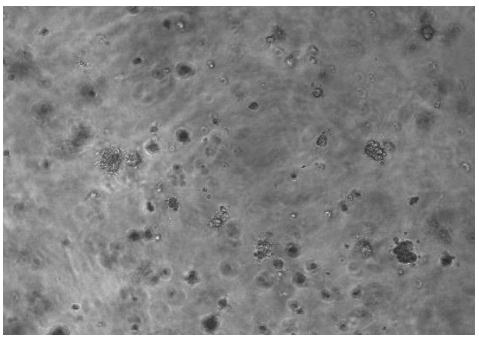

Figure 7.2: 22Rv1 and 22Rv-KO cells cultured in soft agar, cells were plated in triplicates and then visioned 7 days later: A) 22Rv1 cells at day zero. **B)** 22Rv1 at day 7. **C)** 22Rv-KO at day zero. **D)** 22Rv-KO at day 7. Photos were taken at 10x.

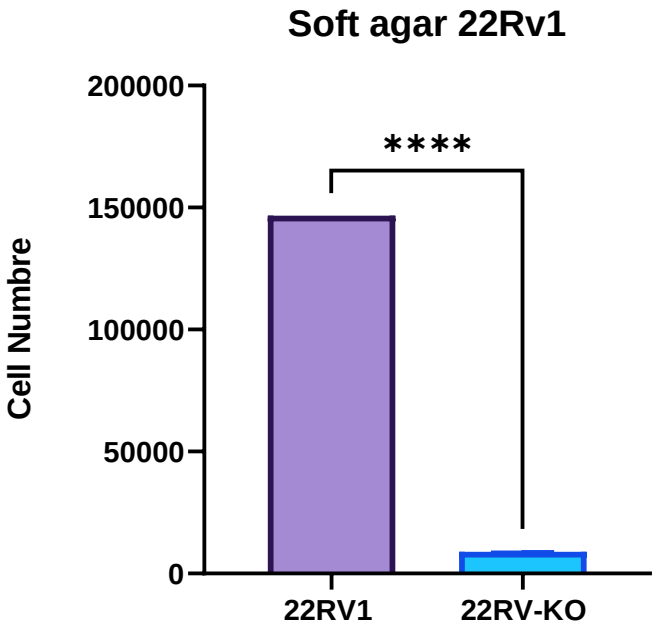

Figure 7.3: Quantification of soft agar data of 22Rv1 cells. Cell number was calculated through the relationship between the value of the light absorbent (at the wavelength 460nm)

and the number of the cells was plotted with linear regression. Readings were taken after seven days of cell culture.

7.2 Soft agar assay of Du145 cells

To accurately quantitate the number of the cells in each experimental time points, the standard growth curve for the Du145 cells was established, the relationship between the value of the light absorbent (at the wave length 460nm) and the number of the cells was plotted with linear regression and shown Figure 7.4.

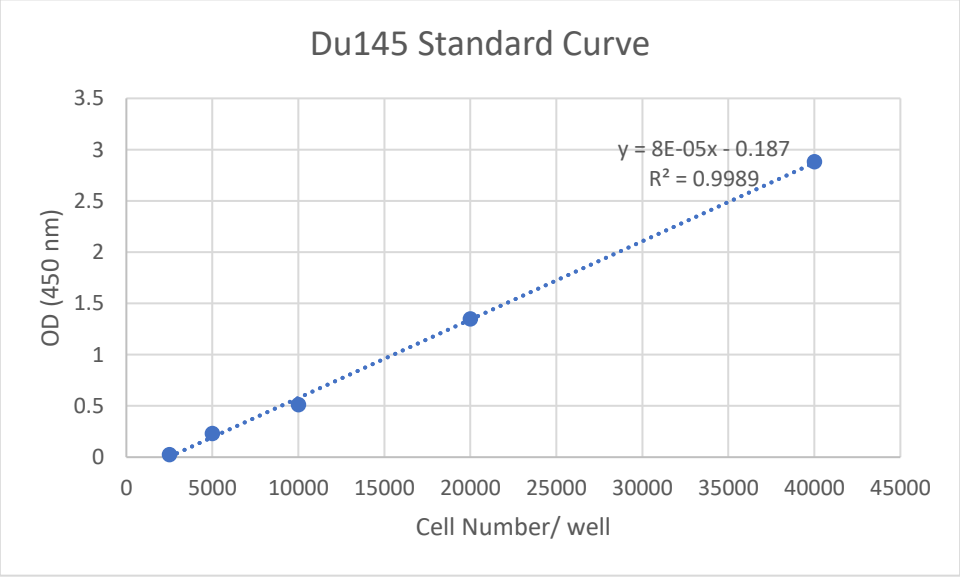

Figure 7.4. The standard curve for Du145 cell lines.

To analyse the cells' anchorage-independent growth, the soft agar assay was employed to determine the effect of the gene knockout on the cells' colony forming capacity (as an indicator of tumorigenicity) in soft agar. Du145 parental cell was used as a control and Du145-KO as a test.

After plating the cells for 7 days at 37°C, colony formation was evaluated, (Figure 7.5 A to C). On day 7, the number of Du145 cells was 29271±163, the number of Du145-KO cells was 6293±247. Comparing with the cell number of Du145 cells, the number of Du145-KO cells was significantly reduced by 4.7-fold (Student t-test, $p<0.0001$) figure 7.6.

A) 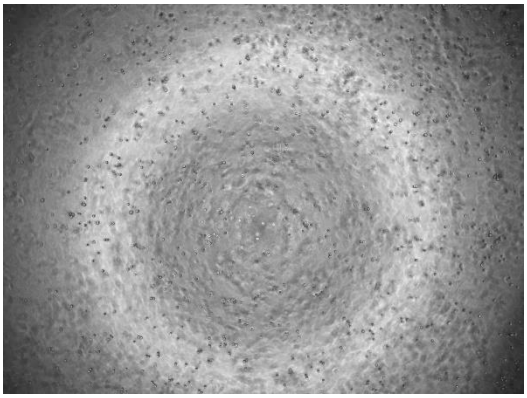 **B)** 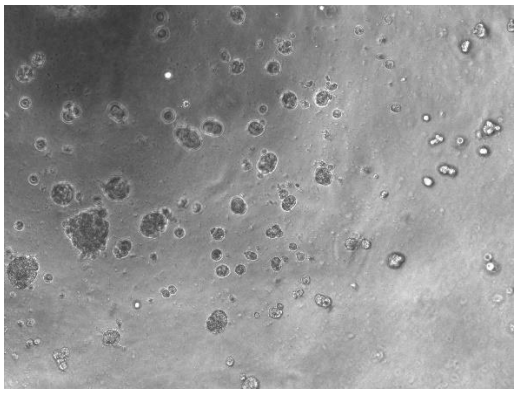

C) 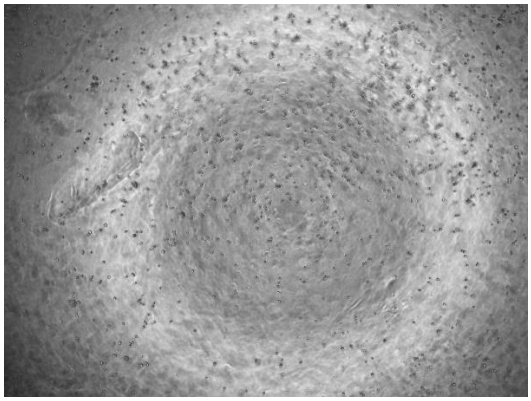 D) 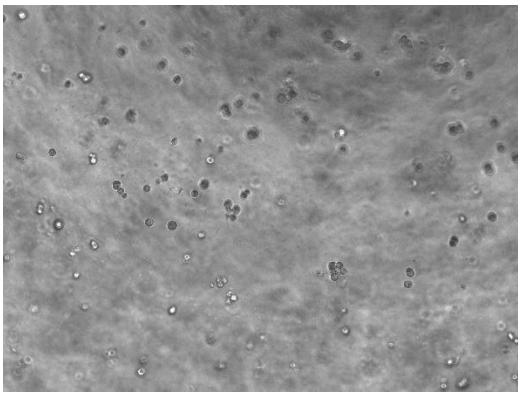

Figure 7.5: Du145 and Du145-KO cells cultured in soft agar, cells were plated in triplicates and then visioned 7 days later: A) Du145 at day zero. **B)** Du145 at day 7. **C)** Du145-KO at day zero. **D)** D145-KO at day 7. Photos were taken at 10x.

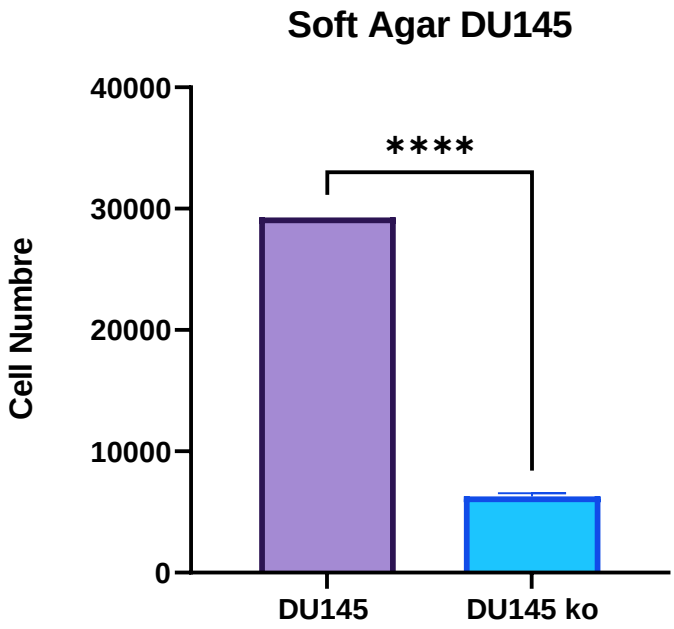

Figure 7.3: Quantification of soft agar data of Du145 cells. Cell number was calculated through the relationship between the value of the light absorbent (at the wavelength 460nm)

and the number of the cells was plotted with linear regression. Readings were taken after seven days of cell culture.

7.3 Discussion

Assessing the anchorage independent growth in soft agar of 22Rv1-ko compared to 22Rv1 control cell showed a highly significant 16.5-fold reduction ($P<0.0001$). Likewise, when comparing the anchorage independent growth of Du145-ko compared to Du145 control cells demonstrated a significant 4.7-fold reduction ($P<0.0001$).

CHAPTER 8

RESULT-6: THE EFFECT OF *PPARγ* GENE KNOCKOUT ON TUMORIGENICITY *IN VIVO*

This is to test the effect of the *PPARγ* gene knockout on tumorigenicity in vivo. It is to be noted that Du145 parental cells were used as controls.

8.1 Effect on tumorigenicity of Du145-ko cells implanted orthotopically into the nude mouse prostate gland

First of all, two groups of male Balb/c nude mice were utilised in this experiment. Each group consisted of five mise. Then, luciferase labelled Du145 parental cells and Du145-ko cells (5×10^5) were suspended in 30uL of PBS and orthotopically implanted into the dorsal prostate gland of each mouse, five with Du145-luc and five with Du145-ko-luc. The tumorigenic loci were monitored every eight days for 24 days using the IVIS system after the mice were injected subcutaneously with D-luciferin. Unfortunately, one mouse of the control died 7 days before the end point of the experiment due to an extremely large tumour size and thus was excluded from the result assessment.

On day 8, when comparing the bioluminescence signal (p/sec/cm^2) of Du145-ko (4.56×10^7) against Du145 (4.25×10^8), there is a substantial 9.32-fold decrease (Student's t test, $P < 0.0012$). On day 16, the bioluminescence signal of Du145-ko (4.45×10^8) compared to Du145 (3.64×10^9) with an 8.18-fold decrease (Student's t test, $P <0.0001$). Finally, on day 24, the bioluminescence signal of Du145-ko (1.02×10^9) compared to Du145 (2.33×10^9) with a decrease of 2.27-fold (Student's t test, $P < 0.008$) Figure 8.1.

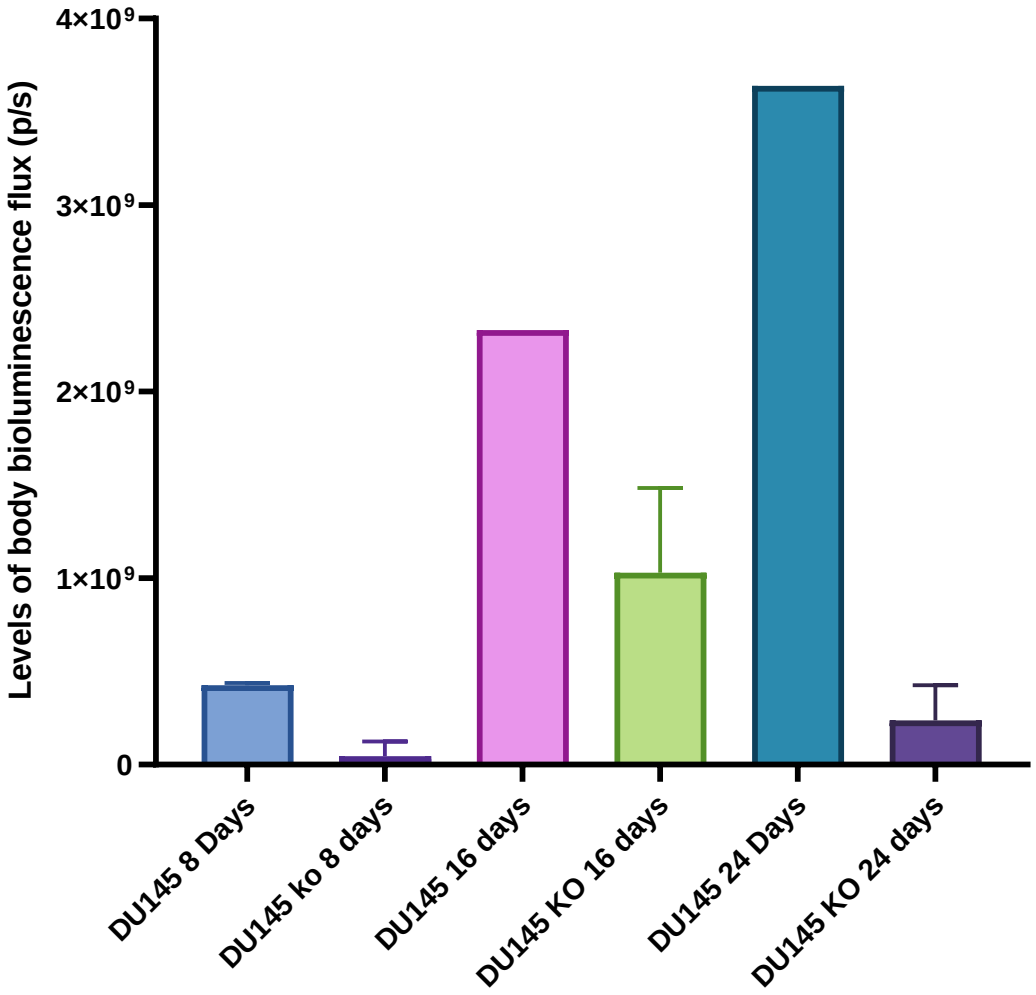

Figure 8.1 Whole body tumour bioluminescence flux produced by two groups of nude mice after orthotopic implantation of luciferase-labelled Du145 and Du145-ko cells for 24 days. Values were plotted as mean ± SD, (n = 5); the difference between the control and each of the testing groups was assessed by two-tailed unpaired t test ***, $P < 0.0001$.

A)

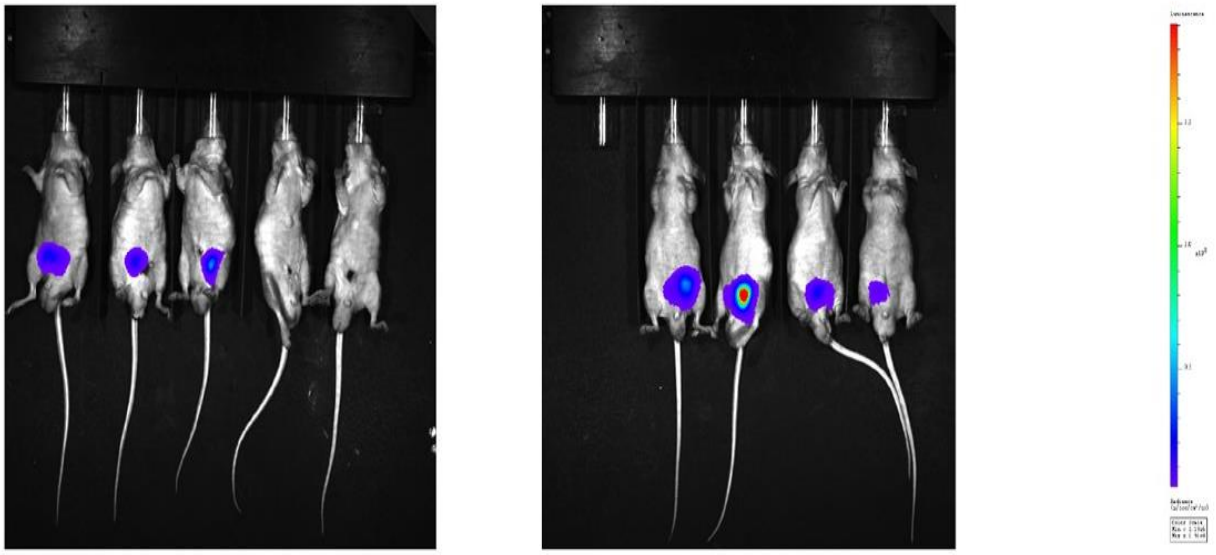

B)

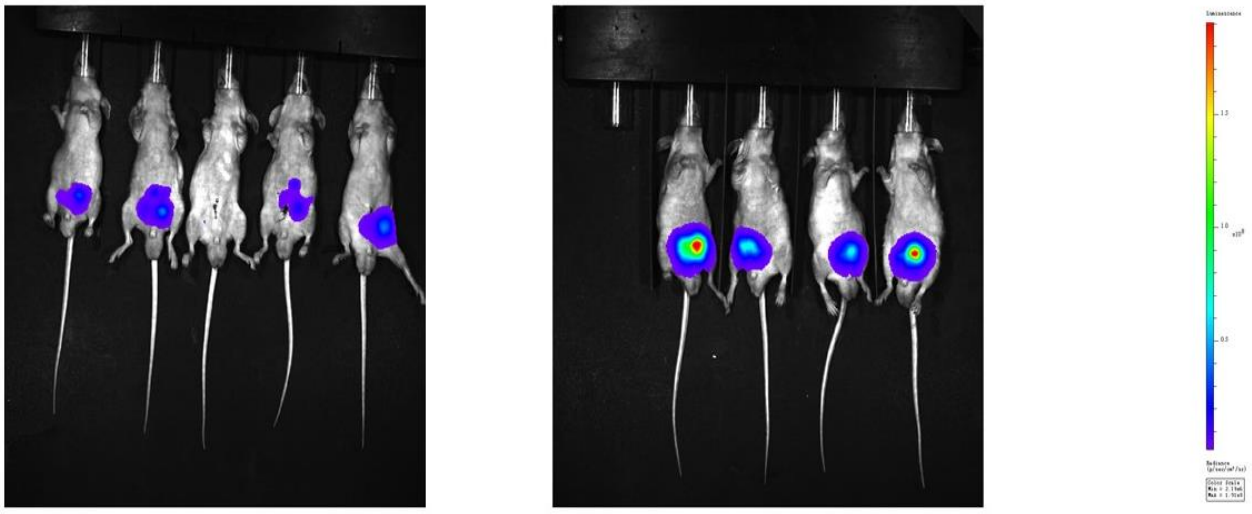

C)

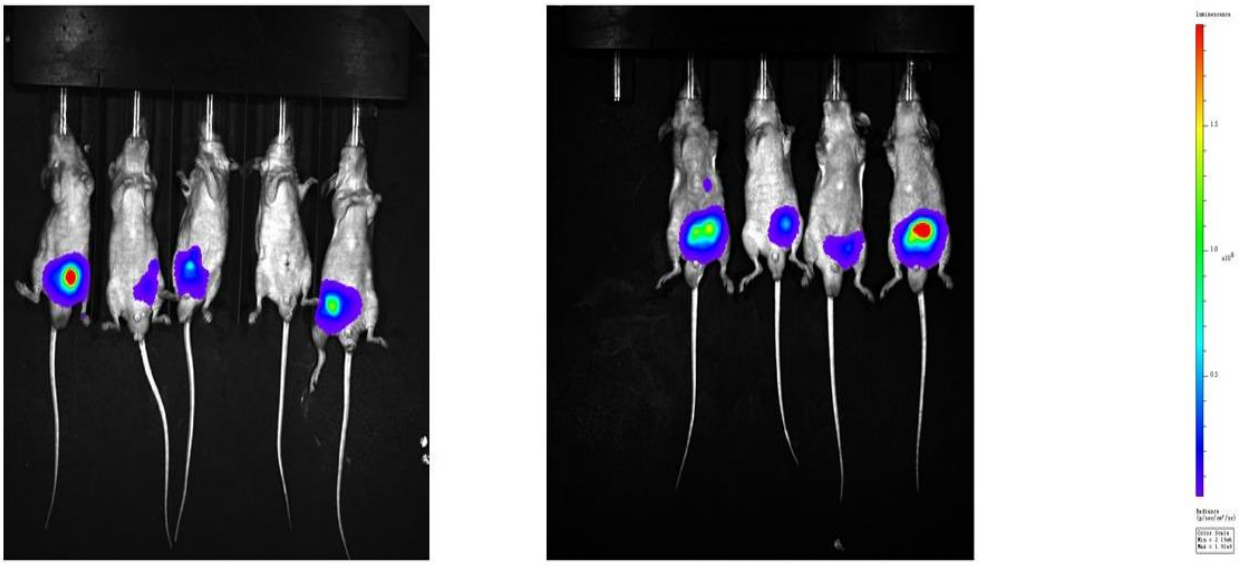

Figure 8.2 Tumorigenicity and metastatic ability of Du145 and Du145-ko cells implanted orthotopically in mice. Bioluminescence images of primary tumours in all 2 groups of experimental mice at day 8, 16 and 24 after treatment. The colour bar on the right indicates the signal intensity range (photons/second/cm2). **A)** Bioluminescence images of primary tumours in all 2 groups of experimental mice at day 8 after treatment (control on the right). **B)** Bioluminescence images of primary tumours in all 2 groups of experimental mice at day 16 after treatment (control on the right). **C)** Bioluminescence images of primary tumours in all 2 groups of experimental mice at day 24 after treatment (control on the right). All images were taken after two second exposure.

8.2 Discussion

Testing the effect of the *PPARγ* gene knockout on tumorigenicity *in vivo* using Du145-ko cells showed at least a 2.27-fold reduction in tumour mass when compared to that produced by the parental Du145 cells. These results suggest that *PPARγ* gene knockout may be an ideal strategy for suppressing the malignant progression of prostate cancer cells.

CHAPTER 9

GENERAL DISCUSSION

Prostate cancer diagnosis and treatment remain to be a persistent burden to health care systems worldwide, lack of novel treatment target is an important issue in prostate cancer research field. Identification and determination of new therapeutic targets is of great importance. The involvement of PPARγ in malignant progression of prostate cancer cells has been noticed since a long time ago [189]. Initially, PPARγ was believed to be a tumour suppressor for prostate cancer, a number of reports showed that it played a suppressive role in malignant progression of prostate cancer cells [189]. Contrary to these results, many other studies showed that supressing PPARγ activity played an inhibitive role to tumorigenicity and metastasis of prostate cancer [203].

Previous work of our laboratory showed that the increased FABP5 levels contributed considerably to development and spread of the cancer cells in CRPC cell lines by binding to and transporting the increased quantities of fatty acids into cells and delivers the fatty acids to their nuclear receptor PPARγ and activate it [219]. It was established in the early work of our group that it was the FABP5-PPARγ-VEGF signalling axis, rather than the androgen receptor-initiated route, that is the primary channel for malignant signal transduction in CRPC cells [195].

Despite all previous investigations, including the work performed by our group, there is still a need for further classify and to acertain the role of PPARγ on the process of CRPC progression. Whether therapeutic manipulation of the PPARγ gene expression can be used as a strategy for CRPC treatment is not completely sure. In this study I have adapted a resolute measure to

systmatically assess the possability of using PPARγ as a therapeutic target for the treatment of prostate cancer. As shown in results, this work demonstrated that PPARγ can be utilised as a therapeutic target, as knocking-out PPARγ led to a significant decrease in malignancy of the cancer cells.

The direct method that can be used to determine whether PPARγ can be used as a therapeutic target is to test whether the eliminated PPARγ expression will result in a reduced tumorigencicity of the cancer cells. In chosing the key technique used to interfere the expression of *PPARγ*, we faced 2 options: the RNA interference technique (RNAi) [227] and the reecntly developed gene editing technique Clustered Regularly Interspaced Short Palindromic Repeats or CRISPR/Cas9. Although the RNAi technique was well established in our laboratory and repeatedly used by our colleagues previously, a shortcome for this technique is the difficulty to generate a complete suppression. In normal circumastance when RNAi is used to perform functional role assessment studies, it is easy to detect a readuced functional activity when the expression level of a gene is significantly reduced. For these type of studies, a complete elimination of the activity of the gene is not essential, and thus RNAi technique is an ideal choice, except the occationally observed off-target effect when using RNAi technique. For some genes, the short interference RNA molecules could produce an exactly the oppositte effect: increase, rather than deacrease, the expression levels of the target genes. This phenomenon is called RNA activation or RNAa [228]. Considering the possible versatile nature of the functional activity of the *PPARγ* gene, particularly the controversial results observed

from the previous investigations [229], the RNAi is not an ideal choice for the current study. To test the functional role of PPARγ in prostate cancer cells, it is necessary to use a technique that can completely exclude the interference of PPARγ left over from the incompleted suppression, so as to assess its fuctional role under a complete abrogation of PPARγ expression. In this work, I used the CRISPR/Cas9 technique to knock out completely the *PPARγ* gene from the cancer cells. This is a reliable and robust technique, which can produce sustainable total knock-out of a gene when using a suitable sgRNA. It is also reprodusable, irreversable, and can be easily verified using numerous methods. In addition, CRISPR/cas9 is a well established technique and repeatedly used in our the research work of our laboratory [230].

9.1 Gene editing using Crispr/Cas9

In order to assess the possible suppressive effect of PPARγ in both androgen-dependant and androgen-independent cancer cell lines, we edited the PPARγ gene and successfully produced a full bi-allelic deletion both 22Rv1 and Du145 prostate cancer cells with the CRISPR/Cas9 method. When the sub-lines eatablsihed from individual knockout clonies were subjected to further verifications with Western blot analyis, the PPARγ bands were not detectable in the knockout cell lines, but it was highly expressed in the parental cells (Figures 3.5 , 3.9). Further analysis with Sanger sequencing technique on both *PPARγ*-KO-sublines established from 22Rv-1, one subline gained an one base-pair insertion in each of both alleles. This inserted one

pair of nucleotide produced a shift in all coding codens of this protein and thus completely elminated the PPARγ expression. When Sanger sequencing analysis was performed to assess the nucleotide sequence of 22Rv1-PPARγ-KO-2, it was revealed that one bp was deleted in one allele, and one bp was inserted into the other allele of the PPARγ gene (Figure 3.6). Sanger sequencing analysis was also performed to check the nucleotide sequences of the *PPARγ* gene Du145-KO lines and the result obtained was different from the analysis of 22Rv-1 sublines. While a 1-bp insertion and a 2-bp insertion was found in allele 1 and allele 2 in Du145-PPARγ-KO-1 respectively; a 165-bp insertion and a 170-bp insertion was detected in allele 1 and allele 2 in Du145-PPARγ-Ko-2 reectively (Figure 3.10). These sequencing analysis results, combined with the Western blot analysis suggested that these bp-insertion or deletions genearted by CRISR/Cas9 gene editing technique have completely altered the PPARγ translation process and led to a full 100% PPARγ supression in both 22Rv1 and Du145 cell lines.

9.2 Proliferation assay

I also utilised the proliferation assay to determine the effect of gene deletion on PCa cell growth. On the fifth day of the assay of 22Rv1-ko, the cell numbers of 22Rv1-ko were significantly reduced by 2.07-fold ($P<0.0001$) when compared with the 22Rv1 control cells. Meanwhile, on the fifth day of the assay of Du145, the cell numbers of Du145-ko were significantly reduced by 3.82-fold ($P<0.0001$) when compared to the Du145 control cells. This

result proves that PPARγ plays a role in the promotion of the growth of prostate cancer cells via the FABP5-PPARγ-VEGF signalling pathway as shown in our lab's previous study [191].

9.3 Invasion assay

Analysing the invasion assay of 22Rv1-ko compared to its parental cell 22Rv1, demonstrated that cellular invasion was drastically affected by PPARγ knockout, it has produced a 72.6% decrease in invaded cells when compared to 22Rv1 control cells. Meanwhile, analysing the invasiveness of Du145-ko compared to its parental Du145 cell demonstrated an extremely huge decrease by 71.6% in the number of the invaded cells of Du145-ko compared to parental Du145 cells. These results show that PPARγ knocked out has a great suppressive effect on tumorigenicity of prostate cancer.

9.4 Motility assay

Comparison of cell migration capabilities of 22Rv1-ko cells when compared to parental 22Rv1 cells, showed a highly significant migration rate of parental 22rv1 cells ($P<0.0001$) when compared to 22Rv1-ko knocked-out cells. Similarly, Du145 parental cells showed a highly significant migration rate ($P<0.0001$) when compared to Du145-ko knocked out cells. These results confirm the previous results suggesting that PPARγ knocked-out has a remarkable suppressive effect on tumorigenicity of prostate cancer.

9.5 Transformation assay (Soft agar assay)

Assessing the anchorage independent growth in soft agar of 22Rv1-ko compared to 22Rv1 control cell showed a highly significant 16.5-fold reduction (P=<0.0001). Likewise, when comparing the anchorage independent growth of Du145-ko compared to Du145 control cells demonstrated a significant 4.7-fold reduction (P=<0.0001). As the results of the transformation assay indicate a low anchorage independent growth value, indicating that PPARγ knocked-out 22-Rv-1 cells may not be able to produce tumours in nude mice. Thus, the result obtained *in vitro* has sufficiently proved that knocking out *PPARγ* gene can significantly suppress the malignant progression of the 22Rv-1 cells and there is no need to test the 22Rv1-Ko cells in the animal model. Thus, the nude mouse assay was conducted to test the Du145 and its derivative cells.

9.6 *In vivo* work utilising Du145-ko cells

Testing the effect of the *PPARγ* gene knockout on tumorigenicity *in vivo* using Du145-ko cells showed at least a 2.27-fold reduction in tumour mass when compared to that produced by the parental Du145 cells. These results suggest that *PPARγ* gene knockout may be an ideal strategy for suppressing the malignant progression of prostate cancer cells. Comparing the suppression effect by knocking out the *PPARγ* gene obtained from this current study with those obtained by the bio-inhibitors of FABP5 gene in our previous study [186], the effect of suppressing FABP5 with dmrFABP5 was much stronger than that obtained by *PPARγ* gene knockout.

These results suggested that FABP5 may play a much stronger promotive role than PPARγ in prostate cancer cells. Therefore, it is possible that FABP5 promoted malignant progression of the cancer cells through other unknown mechanisms, apart from transporting fatty acids to active PPARγ. More study is needed to identify these unknown mechanisms for FABP5 to promote tumorigenicity of the prostate cancer cells.

A risk assessment technique is used to aid in the proper treatment of prostate cancer patients. The National Institute for Health and Clinical Excellence (https://www.nice.org.uk/guidance/ng131) and the European Association of Urology [62] have developed clinical guidelines for prostate cancer assessment and treatment that classify localized prostate cancer into three risk groups based on the likelihood of biochemical relapse following surgery or external beam radiotherapy. Patients with locally advanced prostate cancer may benefit from a variety of treatment options, including active surveillance (AS), watchful waiting (WW), and many radical therapies. Prostate cancer is removed surgically during a radical prostatectomy. It is still considered the most effective treatment method, outperforming WW and AS [63-65]. External beam radiotherapy in combination with ADT (and maybe high-dose-rate brachytherapy) is an option for patients with locally advanced prostate cancer, as is radical prostatectomy (usually followed by ADT and radiotherapy), ADT alone, and WW [62]. ADT comes in a variety of formulations that aim to mitigate the effects of androgen. The most frequently used forms of ADT are surgical castration, which involves the removal of the testicles, luteinizing hormone releasing hormone agonists (e.g. Goserelin)

and GnRH antagonists (e.g. degarelix), which reduce the amount of androgen, anti-androgens (e.g. Flutamide, Enzalutamide, and Bicalutamide), which compete with androgen to reduce androgen binding to AR, and CYP17 inhibitor (e.g. Aberaterone) that blocks the formation of androgen [66].

While ADT is initially useful for the majority of patients, resistance always develops, rendering the treatment ineffective. Castration-resistant prostate cancer (CRPC) is a term that refers to a situation that has progressed, either radiographically or biochemically, in the presence of a castration level of circulating testosterone (<50ng/dl) [71]. Notably, CRPC is not fully resistant to hormones, as different forms of ADT may be beneficial as second line hormone therapy [72]. The CRPC stage of prostate cancer appears to be incurable, with a poor prognosis for the majority of patients who develop metastases [73]. At the moment, patients with metastatic CRPC (mCRPC) have a limited number of treatment options, including ADT with abiraterone and enzalutamide [76, 77], immunotherapy with sipuleucel-T, which uses activated patient-derived antigen-presenting cells to act as an immune modulator or vaccine [78], and the alpha emitter Ra 223 [79]. Docetaxel is only effective in around 50% of patients as a first-line therapy [74, 76]. According to one study, PPARγ agonists decreased cell proliferation by boosting transcription factor specificity protein 1 (SP1) proteasomal degradation [199]. Other studies have suggested a variety of mechanisms by which PPARγ agonists inhibit prostate cancer cell growth in a PPARγ-independent manner, including inhibition of BclxL/Bcl2 functions [200], inhibition of the CXC chemokine receptor type 4/CXC motif chemokine 12

(CXCR4/CXCL12) axis [201], and inhibition of the AKT signalling pathway [212]. Additionally, PPARγ agonists enhanced AR signalling in C42 prostate cancer cells in a PPARγ-dependent manner [213]. As a result, whereas PPARγ agonists are expected to increase AR signalling, their activities on SP1 or other signalling pathways result in indirect AR repression and lower prostate cancer cell proliferation in some cell types. Our laboratory previously demonstrated that treatment of PC3-M cells with the PPARγ antagonist GW9662 reduces tumour formation in a manner comparable to that observed with the FABP5 inhibitor dmrFABP5 [191]. This has resulted in a debate over the involvement of PPARγ agonists and antagonists in the advancement of prostate cancer.

The role of PPARγ in prostate cancer needs more scrutiny to be clearly understood. Initially, it was assumed that PPARγ worked as a tumour suppressor in prostate cells since agonist ligands suppressed the production of prostate cancer cells; however, subsequent study demonstrated that PPARγ agonists inhibit cell proliferation in a manner unrelated to PPARγ [198-202]. Additionally, PPARγ expression is correlated with an increase in the grade/stage of cancer [203-205]. This indicates that PPARγ activity is not a tumour suppressor, but may instead promote to the development and/or advancement of prostate cancer, as tumour suppressor protein expression frequently declines during malignant progression. The presence of PPARγ appears to be strongly related with advanced stages and grades of prostate cancer, implying that it is an oncogene. For example, researchers discovered that PPARγ expression was much greater and more intense in prostate cancer and prostatic intraepithelial neoplasia (PIN) tissues

than in benign prostatic hyperplasia (BPH) and normal prostate tissues in around 200 samples [205]. Similarly, further studies demonstrated that advanced prostate cancer tissues expressed considerably more PPARγ than low-risk prostate cancer and BPH samples ($P<0.001$) [204]. Additionally, two studies found that malignant tissues expressed more PPARγ than benign tissues [206, 207]. The heterozygous deletion of the PPARγ gene in the TRAMP mouse prostate cancer model was found to have no effect on the development or progression of the disease, which was surprising [231].

These controversial results that cannot clearly define the role PPARγ in prostate cancer progression can mainly be attributed to lack of a proper gene editing technique. Therefore, in this work I have proved that CRISPR/CAS9 has been a very useful technique, it lead to generating a full knock-out of PPARγ gene from both 22Rv1 and Du145 prostate cancer cell lines. These knocked-out cell lines have been utilised many times giving reproducible reults in both *in vitro* and *in vivo* work.

Cancer patients have been treated with a variety of therapies, including traditional techniques such as chemo, radiotherapy, and targeted therapy, as well as immunotherapy such as checkpoint inhibitors, vaccines, and cell therapy, among others. Therefore, finding a new approach, like crispr/cas9, can be a promising method to treat various cancers. Recently, in a study that targeted prostate cancer using crispr/cas9, an aptamer-liposome-CRISPR/Cas9 delivery chimera-based strategy that combines effective delivery and modified flexibility was developed. The aptamer-liposome-CRISPR/Cas9 chimeras not only demonstrated significant

cell-type specificity in binding and a remarkable gene silencing impact in vitro, but also demonstrated significant tumor regression in vivo while exhibiting a reduced immune response. The adaptability of the targeting moiety or liposome allows for universal cell type-specific CRISPR/Cas9 distribution, which is essential for the widespread therapeutic application of CRISPR/Cas9 or other nucleic acid medicines [232].

CHAPTER 10

CONCLUSION

In this study, I have proved that knoking-out the PPARγ gene from androgen-dependent 22Rv1 and androgen-independent Du145 cell line lead to a significant decrease in prostate cancer malignancy.

In this work, I characterised the PPARγ gene's functional role in prostate cancer cells and my results confirmed that increased PPARγ promoted the cancer cells' malignant progression. I also discovered that prostate cancer's malignant progression can be suppressed by completely knocking-out the PPARγ gene. Thus, PPARγ represents a novel target for PCa therapy.

References

1. Sung, H., et al., *Global cancer statistics 2020: GLOBOCAN estimates of incidence and mortality worldwide for 36 cancers in 185 countries.* CA: a cancer journal for clinicians, 2021. **71**(3): p. 209-249.
2. ONS. *Cancer Registration Statistics, England: 2015*. 2017; Available from: https://www.ons.gov.uk/peoplepopulationandcommunity/healthandsocialcare/conditionsanddiseases/bulletins/cancerregistrationstatisticsengland/2015
3. Torre, L.A., et al., *Global cancer statistics, 2012.* CA: a cancer journal for clinicians, 2015. **65**(2): p. 87-108.
4. CRUK. *Prostate cancer statistics*. 2018; Available from: https://www.cancerresearchuk.org/health-professional/cancer-statistics/statistics-by-cancer-type/prostate-cancer#heading-Zero.
5. Hsing, A.W., L. Tsao, and S.S. Devesa, *International trends and patterns of prostate cancer incidence and mortality.* International journal of cancer, 2000. **85**(1): p. 60-67.
6. Ferlay, J., et al., *GLOBOCAN 2012 v1. 0.* Cancer incidence and mortality worldwide: IARC CancerBase, 2013. **11**.
7. Bray, F., et al., *Prostate cancer incidence and mortality trends in 37 European countries: an overview*. European journal of cancer, 2010. **46**(17): p. 3040-3052.
8. CRUK. *Prostate cancer incidence statistics*. 2018; Available from: http://www.cancerresearchuk.org.
9. CRUK. *Prostate cancer mortality statistics*. 2018; Available from: http://www.cancerresearchuk.org.
10. CRUK. 2016 [cited 2021; Available from: https://www.cancerresearchuk.org/.
11. Hsing, A.W. and A.P. Chokkalingam, *Prostate cancer epidemiology*. Front Biosci, 2006. **11**(5): p. 1388-413.

12. Merrill, R.M. and J.S. Bird, *Effect of young age on prostate cancer survival: a population-based assessment (United States).* Cancer Causes & Control, 2002. **13**(5): p. 435-443.

13. Krieger, N., et al., *Social class, race/ethnicity, and incidence of breast, cervix, colon, lung, and prostate cancer among Asian, Black, Hispanic, and White residents of the San Francisco Bay Area, 1988–92 (United States).* Cancer Causes & Control, 1999. **10**(6): p. 525-537.

14. Woods, V.D., et al., *Culture, black men, and prostate cancer: what is reality?* Cancer control, 2004. **11**(6): p. 388-396.

15. Baade, P.D., et al., *Epidemiology of prostate cancer in the Asia-Pacific region.* Prostate international, 2013. **1**(2): p. 47-58.

16. Goldgar, D.E., et al., *Systematic population-based assessment of cancer risk in first-degree relatives of cancer probands.* JNCI: Journal of the National Cancer Institute, 1994. **86**(21): p. 1600-1608.

17. Bratt, O., *Hereditary prostate cancer: clinical aspects.* The Journal of urology, 2002. **168**(3): p. 906-913.

18. Kalish, L.A., W.S. McDougal, and J.B. McKinlay, *Family history and the risk of prostate cancer.* Urology, 2000. **56**(5): p. 803-806.

19. Cerhan, J.R., et al., *Family history and prostate cancer risk in a population-based cohort of Iowa men.* Cancer Epidemiology and Prevention Biomarkers, 1999. **8**(1): p. 53-60.

20. Powell, I.J., *The precise role of ethnicity and family history on aggressive prostate cancer: a review analysis.* Archivos espanoles de urologia, 2011. **64**(8): p. 711.

21. Kiciński, M., J. Vangronsveld, and T.S. Nawrot, *An epidemiological reappraisal of the familial aggregation of prostate cancer: a meta-analysis.* PloS one, 2011. **6**(10): p. e27130.

22. Beebe-Dimmer, J.L., et al., *Familial clustering of breast and prostate cancer and risk of postmenopausal breast cancer in the W omen's H ealth I nitiative S tudy.* Cancer, 2015. **121**(8): p. 1265-1272.

23. Foster, C.S., et al., *Cellular and molecular pathology of prostate cancer precursors.* Scandinavian Journal Of Urology And Nephrology. Supplementum, 2000(205): p. 19-43.

24. Rose, D.P., *Effects of dietary fatty acids on breast and prostate cancers: evidence from in vitro experiments and animal studies.* The American journal of clinical nutrition, 1997. **66**(6): p. 1513S-1522S.

25. Russell, P.J., P. Jackson, and E.A. Kingsley, *Prostate cancer methods and protocols*. Vol. 81. 2003: Springer.

26. Cook, L.S., et al., *Incidence of adenocarcinoma of the prostate in Asian immigrants to the United States and their descendants.* The Journal of urology, 1999. **161**(1): p. 152-155.

27. Harman, S.M., et al., *Serum levels of insulin-like growth factor I (IGF-I), IGF-II, IGF-binding protein-3, and prostate-specific antigen as predictors of clinical prostate cancer.* The Journal of Clinical Endocrinology & Metabolism, 2000. **85**(11): p. 4258-4265.

28. Stattin, P.r., et al., *Plasma insulin-like growth factor-I, insulin-like growth factor-binding proteins, and prostate cancer risk: a prospective study.* Journal of the National Cancer Institute, 2000. **92**(23): p. 1910-1917.

29. Shimizu, H., et al., *Cancers of the prostate and breast among Japanese and white immigrants in Los Angeles County.* British journal of cancer, 1991. **63**(6): p. 963-966.

30. Whittemore, A.S., et al., *Prostate cancer in relation to diet, physical activity, and body size in blacks, whites, and Asians in the United States and Canada.* JNCI: Journal of the National Cancer Institute, 1995. **87**(9): p. 652-661.

31. Chan, J.M., et al., *Plasma insulin-like growth factor-I and prostate cancer risk: a prospective study.* Science, 1998. **279**(5350): p. 563-566.

32. Crawford, E.D., *Epidemiology of prostate cancer.* Urology, 2003. **62**(6): p. 3-12.

33. Hiatt, R.A., et al., *Alcohol consumption, smoking, and other risk factors and prostate cancer in a large health plan cohort in California (United States).* Cancer Causes & Control, 1994. **5**(1): p. 66-72.

34. Kasivisvanathan, V. and B. Challacombe, *The big prostate*. 2018: Springer.

35. Lilja, H., D. Ulmert, and A.J. Vickers, *Prostate-specific antigen and prostate cancer: prediction, detection and monitoring.* Nature Reviews Cancer, 2008. **8**(4): p. 268-278.

36. Miller, M.C., G.V. Doyle, and L.W. Terstappen, *Significance of circulating tumor cells detected by the CellSearch system in patients with metastatic breast colorectal and prostate cancer.* Journal of oncology, 2010. **2010**.

37. Mcneal, J., et al., *Patterns of progression in prostate cancer.* The Lancet, 1986. **327**(8472): p. 60-63.

38. Fine, S.W. and V.E. Reuter, *Anatomy of the prostate revisited: implications for prostate biopsy and zonal origins of prostate cancer.* Histopathology, 2012. **60**(1): p. 142-152.

39. Hayward, S.W. and G.R. Cunha, *The prostate: development and physiology.* Radiologic Clinics of North America, 2000. **38**(1): p. 1-14.

40. Mawhinney, M. and A. Mariotti, *Physiology, pathology and pharmacology of the male reproductive system.* Periodontology 2000, 2013. **61**(1): p. 232-251.

41. Humphrey, P.A., *Histological variants of prostatic carcinoma and their significance.* Histopathology, 2012. **60**(1): p. 59-74.

42. Foster, C., et al., *Cellular and molecular pathology of prostate cancer precursors.* Scandinavian Journal of Urology and Nephrology, 2000. **34**(205): p. 19-43.

43. Long, R.M., et al., *Prostate epithelial cell differentiation and its relevance to the understanding of prostate cancer therapies.* Clinical science, 2005. **108**(1): p. 1-11.

44. Bonkhoff, H., U. Stein, and K. Remberger, *The proliferative function of basal cells in the normal and hyperplastic human prostate.* The Prostate, 1994. **24**(3): p. 114-118.

45. Rizzo, S., G. Attard, and D. Hudson, *Prostate epithelial stem cells.* Cell proliferation, 2005. **38**(6): p. 363-374.

46. Ruscica, M., et al., *Role of neuropeptide Y and its receptors in the progression of endocrine-related cancer.* Peptides, 2007. **28**(2): p. 426-434.

47. Ruscica, M., et al., *Relevance of the neuropeptide Y system in the biology of cancer progression.* Current topics in medicinal chemistry, 2007. **7**(17): p. 1682-1691.

48. Costello, L.C. and R.B. Franklin, *Concepts of citrate production and secretion by prostate 1. Metabolic relationships.* The Prostate, 1991. **18**(1): p. 25-46.

49. McLatchie, G., N. Borley, and J. Chikwe, *Oxford handbook of clinical surgery*. 2013: OUP Oxford.

50. Emberton, M., J.M. Fitzpatrick, and J. Rees, *Risk stratification for benign prostatic hyperplasia (BPH) treatment.* BJU international, 2011. **107**(6): p. 876-880.

51. Bostwick, D.G. and J. Qian, *High-grade prostatic intraepithelial neoplasia.* Modern pathology, 2004. **17**(3): p. 360-379.

52. Bostwick, D.G. and M.K. Brawer, *Prostatic intra-epithelial neoplasia and early invasion in prostate cancer.* Cancer, 1987. **59**(4): p. 788-794.

53. Zlotta, A. and C. Schulman, *Clinical evolution of prostatic intraepithelial neoplasia.* European urology, 1999. **35**(5-6): p. 498-503.

54. Sakr, W., et al., *High grade prostatic intraepithelial neoplasia (HGPIN) and prostatic adenocarcinoma between the ages of 20-69: an autopsy study of 249 cases.* In Vivo (Athens, Greece), 1994. **8**(3): p. 439-443.

55. Cheville, J.C., M.J. Reznicek, and D.G. Bostwick, *The focus of "atypical glands, suspicious for malignancy" in prostatic needle biopsy specimens: incidence, histologic features, and clinical follow-up of cases diagnosed in a community practice.* American journal of clinical pathology, 1997. **108**(6): p. 633-640.

56. Ayala, A.G. and J.Y. Ro, *Prostatic intraepithelial neoplasia: recent advances.* Archives of pathology & laboratory medicine, 2007. **131**(8): p. 1257-1266.

57. Molinié, V. *Le score de Gleason en 2008*. in *Annales de pathologie*. 2008. Elsevier.

58. Roehrborn, C.G., *Clinical management of lower urinary tract symptoms with combined medical therapy.* BJU international, 2008. **102**: p. 13-17.

59. Humphrey, P.A., *Gleason grading and prognostic factors in carcinoma of the prostate.* Modern pathology, 2004. **17**(3): p. 292-306.

60. Shah, R.B., *Current perspectives on the Gleason grading of prostate cancer.* Archives of pathology & laboratory medicine, 2009. **133**(11): p. 1810-1816.

61. Epstein, J.I., et al., *A contemporary prostate cancer grading system: a validated alternative to the Gleason score.* European urology, 2016. **69**(3): p. 428-435.

62. Ahmed, H.U., et al., *Diagnostic accuracy of multi-parametric MRI and TRUS biopsy in prostate cancer (PROMIS): a paired validating confirmatory study.* The Lancet, 2017. **389**(10071): p. 815-822.

63. Cimitan, M., et al., *[18F] fluorocholine PET/CT imaging for the detection of recurrent prostate cancer at PSA relapse: experience in 100 consecutive patients.* European journal of nuclear medicine and molecular imaging, 2006. **33**(12): p. 1387-1398.

64. Mottet, N., et al., *EAU-ESTRO-SIOG guidelines on prostate cancer. Part 1: screening, diagnosis, and local treatment with curative intent.* European urology, 2017. **71**(4): p. 618-629.

65. Hamdy, F.C., et al., *10-year outcomes after monitoring, surgery, or radiotherapy for localized prostate cancer.* N Engl J Med, 2016. **375**: p. 1415-1424.

66. Bill-Axelson, A., et al., *Radical prostatectomy or watchful waiting in early prostate cancer.* New England Journal of Medicine, 2014. **370**(10): p. 932-942.

67. Wilt, T.J., et al., *Radical prostatectomy versus observation for localized prostate cancer.* N Engl J Med, 2012. **367**: p. 203-213.

68. Society, A.C. *Hormone therapy for prostate cancer.* . 2019 [cited 2021; Available from: www.cancer.org/cancer/prostate-cancer/treating/hormone-therapy.html.

69. Cornford, P., et al., *EAU-ESTRO-SIOG guidelines on prostate cancer. Part II: treatment of relapsing, metastatic, and castration-resistant prostate cancer*. European urology, 2017. **71**(4): p. 630-642.

70. James, N.D., et al., *Addition of docetaxel, zoledronic acid, or both to first-line long-term hormone therapy in prostate cancer (STAMPEDE): survival results from an adaptive, multiarm, multistage, platform randomised controlled trial.* The Lancet, 2016. **387**(10024): p. 1163-1177.

71. Gravis, G., et al., *Androgen-deprivation therapy alone or with docetaxel in non-castrate metastatic prostate cancer (GETUG-AFU 15): a randomised, open-label, phase 3 trial.* The lancet oncology, 2013. **14**(2): p. 149-158.

72. Sweeney, C.J., et al., *Chemohormonal therapy in metastatic hormone-sensitive prostate cancer.* New England Journal of Medicine, 2015. **373**(8): p. 737-746.

73. Scher, H.I., et al., *Design and end points of clinical trials for patients with progressive prostate cancer and castrate levels of testosterone: recommendations of the Prostate Cancer Clinical Trials Working Group.* Journal of clinical oncology: official journal of the American Society of Clinical Oncology, 2008. **26**(7): p. 1148.

74. Chandrasekar, T., et al., *Mechanisms of resistance in castration-resistant prostate cancer (CRPC).* Translational andrology and urology, 2015. **4**(3): p. 365.

75. Kirby, M., C. Hirst, and E. Crawford, *Characterising the castration-resistant prostate cancer population: a systematic review.* International journal of clinical practice, 2011. **65**(11): p. 1180-1192.

76. Petrylak, D.P., et al., *Docetaxel and estramustine compared with mitoxantrone and prednisone for advanced refractory prostate cancer.* New England Journal of Medicine, 2004. **351**(15): p. 1513-1520.

77. Tannock, I.F., et al., *Docetaxel plus prednisone or mitoxantrone plus prednisone for advanced prostate cancer.* New England Journal of Medicine, 2004. **351**(15): p. 1502-1512.

78. Ryan, C.J., et al., *Abiraterone acetate plus prednisone versus placebo plus prednisone in chemotherapy-naive men with metastatic castration-resistant prostate cancer (COU-AA-302): final overall survival analysis of a randomised, double-blind, placebo-controlled phase 3 study.* The Lancet Oncology, 2015. **16**(2): p. 152-160.

79. Beer, T.M., et al., *Enzalutamide in metastatic prostate cancer before chemotherapy.* New England Journal of Medicine, 2014. **371**(5): p. 424-433.

80. Kantoff, P.W., et al., *Overall survival analysis of a phase II randomized controlled trial of a Poxviral-based PSA-targeted immunotherapy in metastatic castration-resistant prostate cancer.* Journal of Clinical Oncology, 2010. **28**(7): p. 1099.

81. Parker, C., et al., *Alpha emitter radium-223 and survival in metastatic prostate cancer.* New England Journal of Medicine, 2013. **369**(3): p. 213-223.

82. Cussenot, O., et al., *Immortalization of human adult normal prostatic epithelial cells by liposomes containing large T-SV40 gene.* The Journal of urology, 1991. **146**(3): p. 881-886.

83. BERTHON, P., et al., *Functional expression of sv40 in normal human prostatic epithelial and fibroblastic cells-differentiation pattern of nontumorigenic cell-lines.* International journal of oncology, 1995. **6**(2): p. 333-343.

84. Sobel, R. and M. Sadar, *Cell lines used in prostate cancer research: a compendium of old and new lines—part 1.* The Journal of urology, 2005. **173**(2): p. 342-359.

85. Horoszewicz, J.S., et al., *LNCaP model of human prostatic carcinoma.* Cancer research, 1983. **43**(4): p. 1809-1818.

86. Yu, P., et al., *Androgen-independent LNCaP cells are a subline of LNCaP cells with a more aggressive phenotype and androgen suppresses their growth by inducing cell cycle arrest at the G1 phase.* International journal of molecular medicine, 2017. **40**(5): p. 1426-1434.

87. Hartel, A., et al., *Characterisation of gene expression patterns in 22RV1 cells for determination of environmental androgenic/antiandrogenic compounds.* The Journal of steroid biochemistry and molecular biology, 2003. **84**(2-3): p. 231-238.

88. Sramkoski, R.M., et al., *A new human prostate carcinoma cell line, 22Rv1.* In Vitro Cellular & Developmental Biology-Animal, 1999. **35**(7): p. 403-409.

89. van Bokhoven, A., et al., *Molecular characterization of human prostate carcinoma cell lines.* The Prostate, 2003. **57**(3): p. 205-225.

90. Stone, K.R., et al., *Isolation of a human prostate carcinoma cell line (DU 145).* International journal of cancer, 1978. **21**(3): p. 274-281.

91. Kaighn, M., et al., *Establishment and characterization of a human prostatic carcinoma cell line (PC-3).* Investigative urology, 1979. **17**(1): p. 16-23.

92. Kozlowski, J.M., et al., *Metastatic behavior of human tumor cell lines grown in the nude mouse.* Cancer research, 1984. **44**(8): p. 3522-3529.

93. Alford, A.V., et al., *The use of biomarkers in prostate cancer screening and treatment.* Reviews in urology, 2017. **19**(4): p. 221.

94. Avgeris, M., K. Mavridis, and A. Scorilas, *Kallikrein-related peptidases in prostate, breast, and ovarian cancers: from pathobiology to clinical relevance.* Biological chemistry, 2012. **393**(5): p. 301-317.

95. Gaudreau, P.-O., et al., *The present and future of biomarkers in prostate cancer: proteomics, genomics, and immunology advancements: supplementary issue: biomarkers and their essential role in the development of personalised therapies (A).* Biomarkers in cancer, 2016. **8**: p. BIC. S31802.

96. Filella, X., et al., *Emerging biomarkers in the diagnosis of prostate cancer.* Pharmacogenomics and personalized medicine, 2018. **11**: p. 83.

97. *4Kscore*. Available from: https://www.4kscore.com/.

98. Vickers, A.J., et al., *A panel of kallikrein marker predicts prostate cancer in a large, population-based cohort followed for 15 years without screening.* Cancer Epidemiology and Prevention Biomarkers, 2011. **20**(2): p. 255-261.

99. Carlsson, S., et al., *Predictive value of four kallikrein markers for pathologically insignificant compared with aggressive prostate cancer in radical prostatectomy*

specimens: results from the European Randomized Study of Screening for Prostate Cancer section Rotterdam. European urology, 2013. **64**(5): p. 693-699.

100. Voigt, J.D., et al., *The Kallikrein Panel for prostate cancer screening: its economic impact.* The Prostate, 2014. **74**(3): p. 250-259.

101. Leyten, G.H., et al., *Prospective multicentre evaluation of PCA3 and TMPRSS2-ERG gene fusions as diagnostic and prognostic urinary biomarkers for prostate cancer.* European urology, 2014. **65**(3): p. 534-542.

102. Heinlein, C.A. and C. Chang, *Androgen receptor (AR) coregulators: an overview.* Endocrine reviews, 2002. **23**(2): p. 175-200.

103. Foj, L., et al., *Real-time PCR PCA3 assay is a useful test measured in urine to improve prostate cancer detection.* Clinica Chimica Acta, 2014. **435**: p. 53-58.

104. Hessels, D., et al., *Predictive value of PCA3 in urinary sediments in determining clinico-pathological characteristics of prostate cancer.* The Prostate, 2010. **70**(1): p. 10-16.

105. Tomlins, S.A., et al., *Recurrent fusion of TMPRSS2 and ETS transcription factor genes in prostate cancer.* science, 2005. **310**(5748): p. 644-648.

106. Abeshouse, A., et al., *The molecular taxonomy of primary prostate cancer.* Cell, 2015. **163**(4): p. 1011-1025.

107. Storch, J. and B. Corsico, *The emerging functions and mechanisms of mammalian fatty acid–binding proteins.* Annual review of nutrition, 2008. **28**.

108. Pettersson, A., et al., *The TMPRSS2: ERG rearrangement, ERG expression, and prostate cancer outcomes: a cohort study and meta-analysis.* Cancer Epidemiology and Prevention Biomarkers, 2012. **21**(9): p. 1497-1509.

109. Hisatake, J.-i., et al., *Down-regulation of prostate-specific antigen expression by ligands for peroxisome proliferator-activated receptor γ in human prostate cancer.* Cancer research, 2000. **60**(19): p. 5494-5498.

110. Gopalan, A., et al., *TMPRSS2-ERG gene fusion is not associated with outcome in patients treated by prostatectomy.* Cancer research, 2009. **69**(4): p. 1400-1406.

111. Sahin, E., et al., *Resveratrol reduces IL-6 and VEGF secretion from co-cultured A549 lung cancer cells and adipose-derived mesenchymal stem cells.* Tumor Biology, 2016. **37**(6): p. 7573-7582.

112. Sen, M., et al., *Mechanism of action of selective inhibitors of IL-6 induced STAT3 pathway in head and neck cancer cell lines.* Journal of chemical biology, 2017. **10**(3): p. 129-141.

113. Nguyen, D.P., J. Li, and A.K. Tewari, *Inflammation and prostate cancer: the role of interleukin 6 (IL-6).* BJU international, 2014. **113**(6): p. 986-992.

114. Bharti, R., et al., *Diacerein-mediated inhibition of IL-6/IL-6R signaling induces apoptotic effects on breast cancer.* Oncogene, 2016. **35**(30): p. 3965-3975.

115. Shao, G., et al., *GCN5 inhibition prevents IL-6-induced prostate cancer metastases through PI3K/PTEN/Akt signaling by inactivating Egr-1.* Bioscience Reports, 2018. **38**(6).

116. Mauer, J., J.L. Denson, and J.C. Brüning, *Versatile functions for IL-6 in metabolism and cancer.* Trends in immunology, 2015. **36**(2): p. 92-101.

117. Velazquez-Salinas, L., et al., *The role of interleukin 6 during viral infections.* Frontiers in microbiology, 2019. **10**: p. 1057.

118. Giannoni, E., et al., *Reciprocal activation of prostate cancer cells and cancer-associated fibroblasts stimulates epithelial-mesenchymal transition and cancer stemness.* Cancer research, 2010. **70**(17): p. 6945-6956.

119. Mäkinen, T., et al., *Family history and prostate cancer screening with prostate-specific antigen.* Journal of clinical oncology, 2002. **20**(11): p. 2658-2663.

120. Zieglschmid, V., C. Hollmann, and O. Böcher, *Detection of disseminated tumor cells in peripheral blood.* Critical reviews in clinical laboratory sciences, 2005. **42**(2): p. 155-196.

121. Turajlic, S. and C. Swanton, *Metastasis as an evolutionary process.* Science, 2016. **352**(6282): p. 169-175.

122. Scher, H.I., et al., *Phenotypic heterogeneity of circulating tumor cells informs clinical decisions between AR signaling inhibitors and taxanes in metastatic prostate cancer.* Cancer research, 2017. **77**(20): p. 5687-5698.

123. Liberko, M., K. Kolostova, and V. Bobek, *Essentials of circulating tumor cells for clinical research and practice.* Critical reviews in oncology/hematology, 2013. **88**(2): p. 338-356.

124. Neri, E., et al., *Radiomics and liquid biopsy in oncology: the holons of systems medicine.* Insights into Imaging, 2018. **9**(6): p. 915-924.

125. Taube, J.M., et al., *Colocalization of inflammatory response with B7-h1 expression in human melanocytic lesions supports an adaptive resistance mechanism of immune escape.* Science translational medicine, 2012. **4**(127): p. 127ra37-127ra37.

126. Dermani, F.K., et al., *PD-1/PD-L1 immune checkpoint: potential target for cancer therapy.* Journal of cellular physiology, 2019. **234**(2): p. 1313-1325.

127. Zheng, Y., Y.C. Fang, and J. Li, *PD-L1 expression levels on tumor cells affect their immunosuppressive activity.* Oncology letters, 2019. **18**(5): p. 5399-5407.

128. Topalian, S.L., *Targeting immune checkpoints in cancer therapy.* Jama, 2017. **318**(17): p. 1647-1648.

129. Fay, A.P. and E.S. Antonarakis, *Blocking the PD-1/PD-L1 axis in advanced prostate cancer: are we moving in the right direction?* Annals of translational medicine, 2019. **7**(Suppl 1).

130. Graff, J.N., et al., *Early evidence of anti-PD-1 activity in enzalutamide-resistant prostate cancer.* Oncotarget, 2016. **7**(33): p. 52810.

131. Haffner, M.C., et al., *Comprehensive evaluation of programmed death-ligand 1 expression in primary and metastatic prostate cancer.* The American journal of pathology, 2018. **188**(6): p. 1478-1485.

132. Carter, R.E., A.R. Feldman, and J.T. Coyle, *Prostate-specific membrane antigen is a hydrolase with substrate and pharmacologic characteristics of a neuropeptidase.* Proceedings of the National Academy of Sciences, 1996. **93**(2): p. 749-753.

133. Chang, S.S., *Overview of prostate-specific membrane antigen.* Reviews in urology, 2004. **6**(Suppl 10): p. S13.

134. Israeli, R.S., et al., *Expression of the prostate-specific membrane antigen.* Cancer research, 1994. **54**(7): p. 1807-1811.

135. Murphy, G., et al., *Evaluation of prostate cancer patients receiving multiple staging tests, including ProstaScint® scintiscans.* The Prostate, 2000. **42**(2): p. 145-149.

136. Lastraioli, E., J. Iorio, and A. Arcangeli, *Ion channel expression as promising cancer biomarker.* Biochimica et Biophysica Acta (BBA)-Biomembranes, 2015. **1848**(10): p. 2685-2702.

137. Stanbrough, M., et al., *Prostatic intraepithelial neoplasia in mice expressing an androgen receptor transgene in prostate epithelium.* Proceedings of the National Academy of Sciences, 2001. **98**(19): p. 10823-10828.

138. Taplin, M.E. and S.-M. Ho, *The endocrinology of prostate cancer.* The Journal of Clinical Endocrinology & Metabolism, 2001. **86**(8): p. 3467-3477.

139. Attar, R.M., C.H. Takimoto, and M.M. Gottardis, *Castration-resistant prostate cancer: locking up the molecular escape routes.* Clinical Cancer Research, 2009. **15**(10): p. 3251-3255.

140. Heinlein, C.A. and C. Chang, *Androgen receptor in prostate cancer.* Endocrine reviews, 2004. **25**(2): p. 276-308.

141. Buchanan, G., et al., *Contribution of the androgen receptor to prostate cancer predisposition and progression.* Prostate Cancer: New Horizons in Research and Treatment, 2002: p. 71-87.

142. Balk, S.P. and K.E. Knudsen, *AR, the cell cycle, and prostate cancer.* Nuclear receptor signaling, 2008. **6**(1): p. nrs. 06001.

143. Jenster, G. *The role of the androgen receptor in the development and progression of prostate cancer*. in *Seminars in oncology*. 1999.

144. Knudsen, K.E. and T.M. Penning, *Partners in crime: deregulation of AR activity and androgen synthesis in prostate cancer.* Trends in Endocrinology & Metabolism, 2010. **21**(5): p. 315-324.

145. Freedland, S.J., et al., *Death in patients with recurrent prostate cancer after radical prostatectomy: prostate-specific antigen doubling time subgroups and their associated contributions to all-cause mortality.* Journal Of Clinical Oncology: Official Journal Of The American Society Of Clinical Oncology, 2007. **25**(13): p. 1765-1771.

146. Magnan, S., et al., *Intermittent vs continuous androgen deprivation therapy for prostate cancer: a systematic review and meta-analysis.* JAMA oncology, 2015. **1**(9): p. 1261-1269.

147. Miyamoto, H., E.M. Messing, and C. Chang, *Androgen deprivation therapy for prostate cancer: current status and future prospects.* The Prostate, 2004. **61**(4): p. 332-353.

148. Taplin, M.-E., et al., *Androgen receptor mutations in androgen-independent prostate cancer: Cancer and Leukemia Group B Study 9663.* Journal of clinical oncology, 2003. **21**(14): p. 2673-2678.

149. Tran, C., et al., *Development of a second-generation antiandrogen for treatment of advanced prostate cancer.* Science, 2009. **324**(5928): p. 787-790.

150. Waltering, K.K., A. Urbanucci, and T. Visakorpi, *Androgen receptor (AR) aberrations in castration-resistant prostate cancer.* Molecular and cellular endocrinology, 2012. **360**(1-2): p. 38-43.

151. Huggins, C. and C.V. Hodges, *Studies on prostatic cancer. I. The effect of castration, of estrogen and of androgen injection on serum phosphatases in metastatic carcinoma of the prostate.* Cancer research, 1941. **1**(4): p. 293-297.

152. Robinson, D., et al., *Integrative clinical genomics of advanced prostate cancer.* Cell, 2015. **161**(5): p. 1215-1228.

153. Ross, R.W., et al., *Efficacy of androgen deprivation therapy (ADT) in patients with advanced prostate cancer: association between Gleason score, prostate-specific antigen level, and prior ADT exposure with duration of ADT effect.* Cancer: Interdisciplinary International Journal of the American Cancer Society, 2008. **112**(6): p. 1247-1253.

154. Kuiper, G., et al., *Structural organization of the human androgen receptor gene.* Journal of Molecular Endocrinology, 1989. **2**(3): p. R1-R4.

155. Attard, G., et al., *Characterization of ERG, AR and PTEN gene status in circulating tumor cells from patients with castration-resistant prostate cancer.* Cancer research, 2009. **69**(7): p. 2912-2918.

156. Griffiths, K., *The regulation of prostatic growth.* Molecular Biology of Prostate Cancer. Berlin, New York, NY: Walter de Gruyter, 1998: p. 9-22.

157. Harris, W.P., et al., *Androgen deprivation therapy: progress in understanding mechanisms of resistance and optimizing androgen depletion.* Nature clinical practice Urology, 2009. **6**(2): p. 76-85.

158. Tsao, C.K., et al., *Targeting the androgen receptor signalling axis in castration-resistant prostate cancer (CRPC).* BJU international, 2012. **110**(11): p. 1580-1588.

159. Bubendorf, L., et al., *Survey of gene amplifications during prostate cancer progression by high-throughput fluorescence in situ hybridization on tissue microarrays.* Cancer research, 1999. **59**(4): p. 803-806.

160. Chen, C.D., et al., *Molecular determinants of resistance to antiandrogen therapy.* Nature medicine, 2004. **10**(1): p. 33-39.

161. Visakorpi, T., et al., *In vivo amplification of the androgen receptor gene and progression of human prostate cancer.* Nature genetics, 1995. **9**(4): p. 401-406.

162. Taylor, B.S., et al., *Integrative genomic profiling of human prostate cancer.* Cancer cell, 2010. **18**(1): p. 11-22.

163. Leversha, M.A., et al., *Fluorescence in situ hybridization analysis of circulating tumor cells in metastatic prostate cancer.* Clinical cancer research, 2009. **15**(6): p. 2091-2097.

164. McDonnel, T.J., et al., *Expression of bcl-2 oncoprotein and p53 protein accumulation in bone marrow metastases of androgen independent prostate cancer.* The Journal of urology, 1997. **157**(2): p. 569-574.

165. Gleave, M., et al., *Progression to androgen independence is delayed by adjuvant treatment with antisense Bcl-2 oligodeoxynucleotides after castration in the LNCaP prostate tumor model.* Clinical Cancer Research, 1999. **5**(10): p. 2891-2898.

166. Cohen, M.B. and O.W. Rokhlin, *Mechanisms of prostate cancer cell survival after inhibition of AR expression.* Journal of cellular biochemistry, 2009. **106**(3): p. 363-371.

167. Bitting, R.L. and A.J. Armstrong, *Targeting the PI3K/Akt/mTOR pathway in castration-resistant prostate cancer.* Endocrine-related cancer, 2013. **20**(3): p. R83-R99.

168. Bao, Z., et al., *A novel cutaneous fatty acid–binding protein-related signaling pathway leading to malignant progression in prostate cancer cells.* Genes & cancer, 2013. **4**(7-8): p. 297-314.

169. Randle, P., et al., *The glucose fatty-acid cycle its role in insulin sensitivity and the metabolic disturbances of diabetes mellitus.* The Lancet, 1963. **281**(7285): p. 785-789.

170. Furuhashi, M. and G.S. Hotamisligil, *Fatty acid-binding proteins: role in metabolic diseases and potential as drug targets.* Nature reviews Drug discovery, 2008. **7**(6): p. 489-503.

171. Di Sebastiano, K.M. and M. Mourtzakis, *The role of dietary fat throughout the prostate cancer trajectory.* Nutrients, 2014. **6**(12): p. 6095-6109.

172. McArthur, M.J., et al., *Cellular uptake and intracellular trafficking of long chain fatty acids.* Journal of lipid research, 1999. **40**(8): p. 1371-1383.

173. Chmurzyńska, A., *The multigene family of fatty acid-binding proteins (FABPs): function, structure and polymorphism.* Journal of applied genetics, 2006. **47**(1): p. 39-48.

174. Ockner, R.K., et al., *A binding protein for fatty acids in cytosol of intestinal mucosa, liver, myocardium, and other tissues.* Science, 1972. **177**(4043): p. 56-58.

175. Smathers, R.L. and D.R. Petersen, *The human fatty acid-binding protein family: evolutionary divergences and functions.* Human genomics, 2011. **5**(3): p. 1-22.

176. Haunerland, N.H. and F. Spener, *Fatty acid-binding proteins–insights from genetic manipulations.* Progress in lipid research, 2004. **43**(4): p. 328-349.

177. Storch, J. and A.E. Thumser, *The fatty acid transport function of fatty acid-binding proteins.* Biochimica et Biophysica Acta (BBA)-Molecular and Cell Biology of Lipids, 2000. **1486**(1): p. 28-44.

178. Storch, J. and L. McDermott, *Structural and functional analysis of fatty acid-binding proteins.* Journal of lipid research, 2009. **50**: p. S126-S131.

179. Schachtrup, C., et al., *Functional analysis of peroxisome-proliferator-responsive element motifs in genes of fatty acid-binding proteins.* Biochemical journal, 2004. **382**(1): p. 239-245.

180. Tan, N.-S., et al., *Selective cooperation between fatty acid binding proteins and peroxisome proliferator-activated receptors in regulating transcription.* Molecular and cellular biology, 2002. **22**(14): p. 5114-5127.

181. Michalik, L. and W. Wahli, *PPARs mediate lipid signaling in inflammation and cancer.* PPAR research, 2008. **2008**.

182. Forootan, F.S., et al., *The expression of C-FABP and PPAR gamma and their prognostic significance in prostate cancer.* International Journal of Oncology, 2014. **44**(1): p. 265-275.

183. Hashimoto, T., et al., *Expression of heart-type fatty acid-binding protein in human gastric carcinoma and its association with tumor aggressiveness, metastasis and poor prognosis.* Pathobiology, 2004. **71**(5): p. 267-273.

184. Zhao, G., et al., *Effect of FABP5 gene silencing on the proliferation, apoptosis and invasion of human gastric SGC-7901 cancer cells.* Oncology Letters, 2017. **14**(4): p. 4772-4778.

185. Levi, L., et al., *Genetic ablation of the fatty acid–binding protein FABP5 suppresses HER2-induced mammary tumorigenesis.* Cancer research, 2013. **73**(15): p. 4770-4780.

186. Wang, W., et al., *FABP5 correlates with poor prognosis and promotes tumor cell growth and metastasis in cervical cancer.* Tumor Biology, 2016. **37**(11): p. 14873-14883.

187. Powell, C.A., et al., *Fatty acid binding protein 5 promotes metastatic potential of triple negative breast cancer cells through enhancing epidermal growth factor receptor stability.* Oncotarget, 2015. **6**(8): p. 6373.

188. Kawaguchi, K., et al., *The cancer-promoting gene fatty acid-binding protein 5 (FABP5) is epigenetically regulated during human prostate carcinogenesis.* Biochemical Journal, 2016. **473**(4): p. 449-461.

189. Myers, J.S., A.K. von Lersner, and Q.-X.A. Sang, *Proteomic upregulation of fatty acid synthase and fatty acid binding protein 5 and identification of cancer-and race-specific pathway associations in human prostate cancer tissues.* Journal of Cancer, 2016. **7**(11): p. 1452.

190. Al-Jameel, W., et al., *Inactivated FABP5 suppresses malignant progression of prostate cancer cells by inhibiting the activation of nuclear fatty acid receptor PPARγ.* Genes & cancer, 2019. **10**(3-4): p. 80.

191. Jeong, C.-Y., et al., *Fatty acid-binding protein 5 promotes cell proliferation and invasion in human intrahepatic cholangiocarcinoma.* Oncology reports, 2012. **28**(4): p. 1283-1292.

192. Fang, L.Y., et al., *Fatty-acid-binding protein 5 promotes cell proliferation and invasion in oral squamous cell carcinoma.* Journal of oral pathology & medicine, 2010. **39**(4): p. 342-348.

193. McKillop, I.H., C.A. Girardi, and K.J. Thompson, *Role of fatty acid binding proteins (FABPs) in cancer development and progression.* Cellular Signalling, 2019. **62**: p. 109336.

194. Morgan, E.A., et al., *Expression of cutaneous fatty acid-binding protein (C-FABP) in prostate cancer: potential prognostic marker and target for tumourigenicity-suppression.* International journal of oncology, 2008. **32**(4): p. 767-775.

195. Forootan, F.S., et al., *Fatty acid activated PPARγ promotes tumorigenicity of prostate cancer cells by up regulating VEGF via PPAR responsive elements of the promoter.* Oncotarget, 2016. **7**(8): p. 9322.

196. Forootan, S.S., et al., *Atelocollagen-delivered siRNA targeting the FABP5 gene as an experimental therapy for prostate cancer in mouse xenografts.* International journal of oncology, 2010. **36**(1): p. 69-76.

197. Wang, M.-L., et al., *Antinociceptive effects of incarvillateine, a monoterpene alkaloid from Incarvillea sinensis and possible involvement of the adenosine system.* Scientific reports, 2015. **5**(1): p. 1-11.

198. Al-Jameel, W., et al., *Inhibitor SBFI26 suppresses the malignant progression of castration-resistant PC3-M cells by competitively binding to oncogenic FABP5.* Oncotarget, 2017. **8**(19): p. 31041.

199. Rosen, E.D. and B.M. Spiegelman, *PPARgamma : a nuclear regulator of metabolism, differentiation, and cell growth.* J Biol Chem, 2001. **276**(41): p. 37731-4.

200. Gouda, H.N., et al., *The association between the peroxisome proliferator-activated receptor-γ2 (PPARG2) Pro12Ala gene variant and type 2 diabetes mellitus: a HuGE review and meta-analysis.* American journal of epidemiology, 2010. **171**(6): p. 645-655.

201. Ahmadian, M., et al., *PPARγ signaling and metabolism: the good, the bad and the future.* Nature medicine, 2013. **19**(5): p. 557-566.

202. Bermudez, V., et al., *PPAR-gamma agonists and their role in type 2 diabetes mellitus management.* Am J Ther, 2010. **17**(3): p. 274-83.

203. Elix, C., S.K. Pal, and J.O. Jones, *The role of peroxisome proliferator-activated receptor gamma in prostate cancer.* Asian journal of andrology, 2018. **20**(3): p. 238.

204. Yang, C.-C., et al., *Peroxisome Proliferator-Activated Receptor γ–Independent Suppression of Androgen Receptor Expression by Troglitazone Mechanism and Pharmacologic Exploitation.* Cancer research, 2007. **67**(7): p. 3229-3238.

205. Shiau, C.-W., et al., *Thiazolidenediones mediate apoptosis in prostate cancer cells in part through inhibition of Bcl-xL/Bcl-2 functions independently of PPARγ.* Cancer research, 2005. **65**(4): p. 1561-1569.

206. Qin, L., et al., *Peroxisome proliferator-activated receptor γ agonist rosiglitazone inhibits migration and invasion of prostate cancer cells through inhibition of the CXCR4/CXCL12 axis.* Molecular medicine reports, 2014. **10**(2): p. 695-700.

207. Moss, P.E., B.E. Lyles, and L.V. Stewart, *The PPARgamma ligand ciglitazone regulates androgen receptor activation differently in androgen-dependent versus androgen-independent human prostate cancer cells.* Exp Cell Res, 2010. **316**(20): p. 3478-88.

208. Ahmad, I., et al., *Sleeping Beauty screen reveals Pparg activation in metastatic prostate cancer.* Proceedings of the National Academy of Sciences, 2016. **113**(29): p. 8290-8295.

209. Rogenhofer, S., et al., *Enhanced expression of peroxisome proliferate-activated receptor gamma (PPAR-γ) in advanced prostate cancer.* Anticancer research, 2012. **32**(8): p. 3479-3483.

210. Segawa, Y., et al., *Expression of peroxisome proliferator-activated receptor (PPAR) in human prostate cancer.* The Prostate, 2002. **51**(2): p. 108-116.

211. Matsuyama, M. and R. Yoshimura, *Peroxisome Proliferator-Activated Receptor-gamma Is a Potent Target for Prevention and Treatment in Human Prostate and Testicular Cancer.* PPAR Res, 2008. **2008**: p. 249849.

212. Nakamura, Y., et al., *Peroxisome proliferator-activated receptor gamma in human prostate carcinoma.* Pathology international, 2009. **59**(5): p. 288-293.

213. Forman, B.M., et al., *15-deoxy-Δ12, 14-prostaglandin J2 is a ligand for the adipocyte determination factor PPARγ.* Cell, 1995. **83**(5): p. 803-812.

214. Butler, R., et al., *Nonapoptotic cell death associated with S-phase arrest of prostate cancer cells via the peroxisome proliferator-activated receptor gamma ligand, 15-deoxy-delta12,14-prostaglandin J2.* Cell Growth Differ, 2000. **11**(1): p. 49-61.

215. Kubota, T., et al., *Ligand for peroxisome proliferator-activated receptor γ (troglitazone) has potent antitumor effect against human prostate cancer both in vitro and in vivo.* Cancer research, 1998. **58**(15): p. 3344-3352.

216. Mueller, E., et al., *Effects of ligand activation of peroxisome proliferator-activated receptor γ in human prostate cancer.* Proceedings of the National Academy of Sciences, 2000. **97**(20): p. 10990-10995.

217. Qin, L., et al., *Peroxisome proliferator-activated receptor γ ligands inhibit VEGF-mediated vasculogenic mimicry of prostate cancer through the AKT signaling pathway.* Molecular medicine reports, 2014. **10**(1): p. 276-282.

218. Moss, P.E., B.E. Lyles, and L.V. Stewart, *The PPARγ ligand ciglitazone regulates androgen receptor activation differently in androgen-dependent versus androgen-independent human prostate cancer cells.* Experimental cell research, 2010. **316**(20): p. 3478-3488.

219. Zhengzheng, B., et al., *A Novel Cutaneous Fatty Acid–Binding Protein-Related Signaling Pathway Leading to Malignant Progression in Prostate Cancer Cells*. 2013.

220. Tontonoz, P., et al., *mPPAR gamma 2: tissue-specific regulator of an adipocyte enhancer.* Genes & development, 1994. **8**(10): p. 1224-1234.

221. Tontonoz, P., E. Hu, and B.M. Spiegelman, *Stimulation of adipogenesis in fibroblasts by PPARγ2, a lipid-activated transcription factor.* Cell, 1994. **79**(7): p. 1147-1156.

222. Strand, D., et al., *PPARγ isoforms differentially regulate metabolic networks to mediate mouse prostatic epithelial differentiation.* Cell death & disease, 2012. **3**(8): p. e361-e361.

223. Small, M.B., Y. Gluzman, and H.L. Ozer, *Enhanced transformation of human fibroblasts by origin-defective simian virus 40.* Nature, 1982. **296**(5858): p. 671-672.

224. He, F., *Bradford protein assay.* Bio-protocol, 2011: p. e45-e45.

225. Mishra, P., et al., *Application of student's t-test, analysis of variance, and covariance.* Annals of cardiac anaesthesia, 2019. **22**(4): p. 407.

226. Justus, C.R., et al., *In vitro cell migration and invasion assays.* JoVE (Journal of Visualized Experiments), 2014(88): p. e51046.

227. Unniyampurath, U., R. Pilankatta, and M.N. Krishnan, *RNA interference in the age of CRISPR: will CRISPR interfere with RNAi?* International journal of molecular sciences, 2016. **17**(3): p. 291.

228. Pushparaj, P.N., et al., *RNAi and RNAa-the yin and yang of RNAome.* Bioinformation, 2008. **2**(6): p. 235.

229. Salgia, M.M., et al., *Different roles of peroxisome proliferator-activated receptor gamma isoforms in prostate cancer.* American journal of clinical and experimental urology, 2019. **7**(3): p. 98.

230. Al-Bayati, A., *Increased FABP12 expression in prostate cancer and its possible promoting role in tumorigenicity*. 2021, University of Liverpool.

231. Saez, E., P. Olson, and R.M. Evans, *Genetic deficiency in Pparg does not alter development of experimental prostate cancer.* Nature Medicine, 2003. **9**(10): p. 1265-1266.

232. Zhen, S., et al., *Targeted delivery of CRISPR/Cas9 to prostate cancer by modified gRNA using a flexible aptamer-cationic liposome.* Oncotarget, 2017. **8**(6): p. 9375.

Appendix. A

1.Equipment

BD BioCoatTM Growth Factor Reduced (GFR) Matrigel TM Invasion Chamber Carbon Steel

BD Biosciences, USA

CO2 incubator Model TC2323

Borolabs, Basingstoke, UK

Cell culture filter cap flasks

Cell culture plates Cryogenic vial Nunc, Denmark

Carbon steel surgical blades

Swann-Morton, Sheffield, UK

Falcon 2059 tube

Becton Dikinson, USA

Gel electrophoresis

Bio-Rad, UK

GelCount

OXFORD OPTRONIX, Oxford, UK

Haemocytometer slide

Weber scientific International, NJ, USA

Hot plate (Ori-Block 08-3)

Techne, England, UK

Haemocytometer

SLS Ltd., Nottingham, UK

Immobilon, Transfer membrane

Millipore, UK

Microtubes

Starlab, Milton Keynes, UK

Multiskan MS plate reader

Labsystem, Finland

Microcentrifuge

Beckman coulter, UK

Needle

BD Microlance, Ireland

NanoDrop spectrophotometer

Labtech International, Ringmer, UK

Pipette tips

QIAGEN, Crawley, UK

Syringes

BD Microlance, Ireland

Spectrophotometer

BioTec, Brigend, UK

Cell culture pipettes 5-50 ml

Greiner Bio-One bio-one, UK

Universal tube

Greiner Bio-One, UK

Water bath

Grant Instruments, UK

Whatman filter paper

Whatman, England, UK

2.Reagents

Reagents for cell culture

DMSO	Sigma-Aldrich, Germany
Foetal calf serum	Gibco, Invitrogen, Paisley, UK

L-Glutamine	Lonza, Belgium
Opti-MEM I medium	Gibco, Invitrogen, Paisley, UK
Penicillin/ Streptomycin	Lonza, Belgium
Phosphate buffered saline (tablet)	Gibco, Invitrogen, Paisley, UK
RPMI 1640	Gibco, Invitrogen, Paisley, UK
Sodium pyruvate	Sigma, USA
Trypsin	Gibco, Invitrogen, Paisley, UK
Versene	Gibco, Invitrogen, Paisley, UK
Zeocin	Invitrogen, CA, USA

Reagents for Western blot

β-mercaptoethanol	Sigma, USA
Ammonium persulfate (APS)	Sigma, USA
Bradford reagent	Sigma, USA
Bromophenol blue	Sigma, USA
CelLytic-M	Sigma, USA
Coomassie blue	Bio-Rad GmbH,UK
ECL detection kit	GE Healthcare, buckinghamshire, UK
Glycine	Melford, UK
Methanol	Fisher scientific, Loughborough, UK

Reagents for general molecular biology

Ampicillin	Sigma, USA
Agarose	Genflow, Fradley, UK

Glucose	Sigma, USA
Glycerol	Sigma, USA
Isopropanol	BDH, England, UK
LB agar	Sigma, USA
LB broth	Sigma, USA
Magnesium chloride	Sigma, USA
Magnesium sulphate	Sigma, USA
Zeocin	Invitrogen, CA, USA

Reagents for cell invasion assay

Crystal violet	Sigma, USA

Reagents for soft agar assay

Cell Transformation Assay Kit	Abcam, UK

---

3. Buffers

Cell Culture

Routine cell culture medium

RPMI medium 1640…….500ml

Foetal calf serum……. 10% (v/v)

Pen-Strep (5000 U/ml) ….. 5ml

L-Glutamine (20mM) …… 5ml

Sodium pyruvate (100mM) ... 5ml

Selective medium

Routine medium with ZeocinTM… (100µg/ml)

Trypsin/EDTA solution (T/E) (2.5%)

1 × Versene……. 100ml

Trypsin……2.5ml

MTT solution (5mg/ml)

MTT……..50mg

PBS……...10ml

PBS

PBS……1 tablet

dH2O…… 500ml

Autoclaved

Western Blot

M Tris pH 6.8

Tris base……...12.1gr

dH2O……. 100ml

pH adjusted with HCl

10% (w/v) SDS solution

Sodium Dodecyl Sulfate…10gr

dH2O……100ml

(w/v) APS solution 10 %

Ammonium persulfate...100mg

dH2O……...1ml

SDS-PAGE sample loading buffer (SLB X 2)

M Tris-HCl (pH 6.8) …2.5ml

Glycerol 40% (v/v) ….. 4ml

Bromophenol blue 0.5% (w/v) …...0.8ml

SDS 10%.....2ml

β-mercaptoethanol…….0.5ml

dH2O……. 4.7ml

SDS-PAGE sample loading buffer (SLB X5)

M Tris-HCl (pH 6.8) …1.25ml

Glycerol 40% (v/v) …….15ml

Bromophenol blue 0.5% (w/v) …2.5ml

SDS 10% …….5ml

β-mercaptoethanol …….1.25ml

Transfer buffer (pH 8.3)

Glycine …….14.4g (192mM)

Methanol …… 20% (v/v)

Tris base ……. 3.03g (25mM) 173

dH2O ……. up to 1Lit

pH adjusted with HCl

TBS buffer (pH 7.6 X 10)

Sodium chloride ……... 87.66gr (1500mM)

Tris base ……... 60.58gr (500mM)

dH2O …… up to 1 Lit

pH adjusted with HCl

Autoclaved

TBS-Tween 1% x1

TBS buffer …… 100ml x10

Tween 20 ……. 1ml

dH2O ……..…. up to 1 Lit

TBS-T-milk 5%

Dried milk ……. 5gr

TBS-T ……... 100ml x1

Molecular Biology

LB medium

LB broth ……20gr

dH2O …… 1 Lit

Autoclaved

LB agar

LB agar …….35gr

dH2O …… 1 Lit

Autoclaved

Glycerol …… 5ml

LB medium ……. 4ml

Bacteria culture ……... 3ml

10 × TBE stock solution

Tris base ……. 108gr (890mM)

Boric acid ……... 55gr (890mM)

EDTA 0.5M, pH 8 ……. 40ml (20mM)

dH2O ……. up to 1 Lit

Adjust the pH and sterilized by autoclave

50x TBE stock solution

Tris base …… 242gr

Glacial Acetic Acid ….. 57.1gr

EDTA 0.5M, pH 8 …… 100ml

dH2O ……. up to 1 Lit

Adjust the pH and sterilized by autoclave

TE buffer (pH 7.6)

Tris-HCl …… 1.21gr (10mM

EDTA …… 0.3722gr (1mM

dH2O ……. up to 1 Lit

Adjust the pH and sterilized by autoclave

Reagents for tumorigenicity *in vivo*

Isofluorane ..... Hoechst, German

Novalgin ..... Hoechst, Germany

Potassium ..... D-luciferin Promega, USA

Appendix. B

S A B

SCOTTISH ACCREDITATION BOARD

This is to certify that

Bandar Theyab Alenezi

has successfully achieved the learning outcomes of the following modules as required under UK and EU training frameworks.

MODULES: L (EU1 Legislation), E1 (EU2 Ethics)

PILA (EU3.1 Basic Biology (theory), EU4 Animal Care, Health & Management (theory), EU5 Recognition of PSD, EU7 Minimally Invasive Procedures (theory), EU3.2 Basic Biology (practical), EU8 Minimally Invasive Procedures (skills))

K (EU6.1 Humane Killing (theory), EU6.2 (skills))

PILB (EU20 Anaesthesia – Minor Procedures)

PILC (EU21 Advanced Anaesthesia, EU22 Principles of Surgery)

TRAINING IN (list animal/types species of PILA):

Mouse

Training organised by: CHARLES RIVER UK LTD

Certificate Number: BE3752

Date: 3rd September 2018

Signature 1
For Course Organiser

Jean Wilson

Signature 2
For Scottish Accreditation Board

Please note, this Certificate allows you to apply for a Licence, but it is not a licence to perform procedures under the Animals (Scientific Procedures) Act 1986.
References to EU Modules relates to requires arising from Directive 2010/63/EU – further information can be obtained at:
http://ec.europa.eu/environment/chemicals/lab_animals/pdf/Endorsed_E-T.pdf

Figure B.1: Animal work accreditation.

Home Office

No. IC697202C

ANIMALS (SCIENTIFIC PROCEDURES) ACT 1986

PERSONAL LICENCE

to

carry out regulated procedures on living animals.

In pursuance of the powers vested in him by the above Act, the Secretary of State hereby licenses

Mr Bandar Alenezi
The University of Liverpool
Foundation Building Brownlow Hill Liverpool L69 7ZX

to apply regulated procedures of the category or categories specified below to animals of the species or groups specified below at places specified in authorised project licences subject to the restrictions and provisions contained in the Act, and subject also to the limitations and conditions contained in this licence and to such other conditions as the Secretary of State may from time to time prescribe:

Description of animal(s)

- Mice

Categories of regulated procedure:

A. Minor/minimally invasive procedures not requiring sedation, analgesia or general anaesthesia
B. Minor/minimally invasive procedures involving sedation, analgesia or brief general anaesthesia. Plus surgical procedures conducted under brief non-recovery general anaesthesia
C. Surgical procedures involving general anaesthesia. Plus administration and maintenance of balanced or prolonged general anaesthesia

This licence shall be in force until revoked by the Secretary of State and shall be periodically reviewed by him.

Figure B.2: Page 1 of personal licence.

Home Office
2 Marsham Street
London SW1P 4DF

For the Secretary
of State

15 January 2019

NB. This licence does not authorise the licensee to perform a regulated procedure to an animal unless the procedure is applied as part of a programme of work specified in a project licence authorising the application, as part of that programme, of a regulated procedure of that description to an animal of that description.

Figure B.3: Page 2 of personal animal licence.

Published papers

LUPINE PUBLISHERS

ISSN: 2638-5945

Open Access Journal of Oncology and Medicine

DOI: 10.32474/OAJOM.2021.05.000206

Review Article

Peroxisome Proliferator-Activated Receptor Gamma (Pparγ) and Prostate Cancer

Xi Jin[1#], Bandar A. Alenezi[2#], Gang He[3], Hongwen Ma[1], Qiang Wei[1], and Youqiang Ke[1, 2, 3*]

[1]*Department of Urology, Institute of Urology, West China Hospital, Sichuan University, China*

[2]*Department of Molecular & Clinical Cancer Medicine, Liverpool University, Liverpool, United Kingdom.*

[3]*Sichuan Antibiotics Industrial Institute, Chengdu University, China*

[#]*These authors contributed equally to this work.*

***Corresponding author:** Professor Youqiang Ke, Department of Molecular & Clinical Cancer Medicine, Liverpool University, United Kingdom.

Received: November 25, 2021 **Published:** December 6, 2021

Abstract

The fatty acid receptor peroxisome proliferator-activated receptor gamma (PPARγ) is a transcription factor, which includes two isoforms named PPARγ1 and PPARγ2 respectively. In human body, PPARγ involves in metabolic disorder, neurodegenerative disease and inflammation. Recent advance in PPARγ study has led to the discoveries of several genes that are regulated by PPARγ in prostate cancer cells. Evidence showed that PPARγ plays important roles in development and in malignant progression of prostate cancer. In this mini-review, we described the PPARγ structure and summarized their involvement in different diseases. Our focus is on the roles of PPARγ isoforms in prostate cancer.

Peroxisome Proliferator-Activated Receptor Gamma

Peroxisome Proliferator-Activated Receptor Gamma (PPARγ) is a transcription factor that is ligand dependent and is a member of the nuclear hormone receptor superfamily. PPARγ is expressed in two isoforms: PPARγ1 and PPARγ2, the latter contains thirty extra amino acids (Figure 1). Both synthetic and endogenous ligands can band to and activate PPARγ [1]. When activated, PPARγ is translocated into the nucleus and forms a heterodimer with the retinoid X receptor (RXR), where it serves as a transcriptional regulator of genes via DNA binding [2]. It is well established that PPARγ plays a critical role in adipocyte differentiation, the inflammatory response, and peripheral glucose consumption. PPARγ agonists are frequently utilised to treat type II diabetes [1]. Diabetes type II is the most prevalent endocrine-metabolic condition worldwide, characterised by insulin resistance and insulin secretion abnormalities. PPARγ agonists were utilised to sensitise tissues (muscle, adipose tissue, and liver) to insulin stimulation. However, these PPARγ agonist medicines were associated with significant side effects such as increased weight, oedema, heart failure, and an increased risk of myocardial infarction [3]. The role of PPARγ in prostate cancer (PCa) has been controversial. Initially, it was believed that PPARγ functioned as a tumour suppressor in prostate cells since agonist ligands suppressed the proliferation of PCa cells. However, further investigations revealed that these agonists suppressed cell growth in a manner independent of PPARγ [4-8]. Furthermore, PPARγ expression rises with the grade/stage of cancer cases [9-11]. These results suggested that it is not a tumour suppressor. In the contrary, studies also find PPARγ activity may contribute to the development and the progression of the prostate cancer. While a tumour suppressor expression level frequently reduced as the develop and progress of the malignancies, PPARγ expression level appeared to be significantly increased with elevated PCa stage and grade, strongly implying that it is cancer-promoter or oncogene. For example, it was discovered by immunohistochemical staining that PPARγ expression was significantly greater and more intense in prostate cancer and prostatic intraepithelial neoplasia (PIN) tissues than in benign prostatic hyperplasia (BPH) and normal prostate tissues samples [11]. Similarly, utilising more tissue samples in a separate investigation by a different group, it was discovered that PPARγ expression was substantially higher in advanced PCa tissues than in low-risk PCa and BPH specimens ($P < 0.001$) [10]. In addition, two smaller investigations found higher

Global Development on Causes, Epidemiology, Aetiology, and Risk Factors of Prostate Cancer: An Advanced Study

Bandar T. Alenezi[1], Mohammed H. Alsubhi[1], Xi Jin[2], Gang He[3], Qiang Wei[2*] and Youqiang Ke[1*]

DOI:

ABSTRACT

As the second most recurring cancer in men globally, prostate cancer is a major concern to men's health. It is estimated that approximately 1.3 million new cases are diagnosed every year, those cases are leading to the casualties of nearly 360,000 men during 2018, which represents about 3.8% of all male cancer related deaths. Increasing of age among men can be correlated with global prostate cancer incidence and mortality, with the average age of diagnosis is 66 years old. Prostate cancer is usually asymptomatic or with minimal symptoms in the early stages of the disease, during this period there is minimal to no need of treatment. At early stage, the symptoms of prostate cancer are similar to those observed in prostatic hypertrophy. But in more advanced stages of prostate cancer, more painful symptoms may appear. Elevated levels of Prostate Specific Antigen (PSA) are the main marker used to detect prostate cancer. The disease can be confirmed with a biopsy of the prostate gland. In this work, we try to review the prostate cancer's causes, epidemiology, aetiology, and risk factors globally, as we think that it is a pivotal way to keep update our understanding on this increasingly important health threat to men.

Keywords: Prostate Cancer; statistics; Epidemiology; mortality; risk factors and prevention.

1. INTRODUCTION

Prostate cancer is considered to be the second most recurring cancer in men globally, with estimated 1,276,106 new cases and a leading to 358,989 casualties (3.8% of all casualties by cancer in men) during 2018 [1,2]. Global Prostate Cancer incidence and mortality is correlated with increasing age, 66 years is the average age when diagnosed. To be noted, the incidence rate is higher in African-American men when compared to white men, with almost 159 new cases diagnosed per 100,000 men and with a mortality rate of almost double than White men [3]. This variation is hypothetically attributed to the differences in social, environmental and genetic aspects. while 2,293,818 new cases are expected until 2040, there will be a small variation in mortality with an increase of 1.05% [4]. Globally prostate cancer is the second most familiar and fifth-most hostile neoplasm among male individuals. One of the emerging issues in men is prostate cancer. The Prostate is a ductal small walnut-shaped gland situated in men below the urinary bladder that produces the seminal fluid for sperms provision and transportation. The risk of emerging prostate cancer during the man's lifetime is one out of seven. According to the epidemiological studies, different environmental and genetic factors are associated with the progression of abnormal prostate cell growth which ultimately causes the development of cancerous cells [210,211]. Many risk factors have been implicated in the etiology of cancer including; tobacco and alcohol consumption, unhealthy diet, physical inactivity, viral infection, bacterial infection, urban air pollution, ionizing radiation and indoor smoke [212].

[1]*Department of Molecular & Clinical Cancer Medicine, Liverpool University, Liverpool, L69 3GA, United Kingdom.*
[2]*Institute of Urology, West China Hospital, Sichuan University, No.37 Guo Xue Xiang, Chengdu, Sichuan, 610041, China.*
[3]*Sichuan Antibiotics Industrial Institute, Chengdu University, Chengdu 610081, China.*
**Corresponding author: E-mail: yqk@liverpool.ac.uk;*

Molecular mechanisms on how FABP5 inhibitors promote apoptosis-induction sensitivity of prostate cancer cells

Jiacheng Zhang, Gang He, Xi Jin, Qiang Wei, **Bandar T. Alenezi,** Abdulghani A. Naeem, Saud A. Abdulsamad, Mohammed I. Malki, Philip S. Rudland, and Youqiang Ke

ABSTRACT

The increased level of FABP5 promotes malignant progression partially by suppressing apoptosis of prostate cancer cells. Thus targeting FABP5 with its inhibitors to promote apoptosis could be a novel strategy for treatment of prostate cancer. In this work, we first treated an androgen-responsive cell line (22Rv1) and a highly malignant androgen-independent cell line (PC3) with the apoptosis-inducer camptothecin and then with a chemical- (SB-FI-26) or a bio- (dmrFABP5) FABP5 inhibitor. Our results showed that SB-FI-26 produced significant increases in the percentages of apoptotic cells in 22Rv1 and PC3 by 18.8% (±4.1) and 4.6% (±1.1), respectively. DmrFABP5 also produced significant increases in apoptosis by 23.1% (±2.4) and 15.8% (±3.0), respectively, in these two cell lines. Both FABP5 inhibitors significantly reduced the levels of the phosphorylated (presumably, biologically active form) nuclear fatty acid receptor PPARγ, indicating that these inhibitors promoted apoptosis-induction sensitivity of the cancer cells by suppressing the biological activity of PPARγ. Thus, the phosphorylated PPARγ levels were reduced by FABP5 inhibitors, the levels of the phosphorylated AKT and activated NFκB were coordinately altered by additions of the inhibitors. These changes eventually led to the increased levels of cleaved caspase-9 and cleaved caspase-3; and thus, increase in the percentage of cells undergoing apoptosis. In untreated prostate cancer cells, increased FABP5 suppressed the apoptosis by increasing the biological activity of PPARγ, which, in turn, led to a reduced apoptosis by interfering with the AKT- or NFκB signaling pathway. Thus our results suggested that the FABP5 inhibitors enhanced the apoptosis-induction of prostate cancer cells by reversing the biological effect of FABP5 and its related pathway.